ELUCIDATING THE ANTI-INFLAMMATORY AND ANTI-DIABETIC PROPERTIES OF UROLITHIN BIOACTIVE METABOLITES FROM PECAN

A Dissertation

by

PRERNA BHARGAVA

Submitted to the Office of Graduate and Professional Studies of
Texas A&M University
in partial fulfillment of the requirements for the degree of

DOCTOR OF PHILOSOPHY

Chair of Committee,	Luis Cisneros-Zevallos
Committee Members,	Joseph Awika
	Chaodong Wu
	Leo Lombardini
Head of Department,	Stephen Searcy

May 2019

Major Subject: Food Science and Technology

ABSTRACT

Pecans are a rich source of ellagitannins which are not absorbed by humans, rather they are catabolized into urolithins by human gut microbiota and enterohepatic circulation. Urolithin A and B have been studied for their antioxidant, antimicrobial, anti-inflammatory, anticancer, and antihyperglycemic properties. This project combined a holistic approach of traditional medicine with scientific evidences. A diseased state, with proper human diet, could potentially be reversed by a combination of bioactive compounds. Polyphenols mitigate insulin resistance, obesity, inflammation, cardiovascular diseases and many others. The challenge is poor systemic bioavailability of these secondary metabolites. However, biotransformation of polyphenols by intestinal microflora conserves their functions and makes them bioavailable.

The aim of this investigation was to elucidate role of oxidative stresses in anti-inflammatory effect of urolithin A and B and understand their role in a diabetic model. Urolithin A and B exerted anti-inflammatory properties in inflamed colon Caco-2 and endothelial HUVEC cells by suppressing ROS and upregulating LXRα. α. In presence of LPS and PA and TNF α urolithin A suppressed increased levels of intracellular ROS and downregulated the pathways such as inflammation and insulin signaling in cell models. Whereas urolithin B, in a ROS independent mechanism worked in HUVEC, Caco-2 and C2C12 cells. Urolithin A and B suppressed insulin resistance induced by palmitic acid in muscle C2C12 cells and AML 12 by upregulating protein expression of pIRS and pAKT. They also downregulated the glucose production in insulin resistant hepatic AML 12 cells.

. Thereby, this study successfully demonstrated the multifaceted nature of urolithin A and B to ameliorate inflammation and insulin resistance in *in-vitro* model, key events in the scenario of the metabolic syndrome.

DEDICATION

To my family for their unconditional love and support

ACKNOWLEDGEMENTS

I would like to take this opportunity to express my sincere gratitude to my adviser Dr. Luis Cisneros-Zevallos, for his mentoring, patience, enthusiasm and motivation that have been instrumental in completion of this dissertation. Without his valuable guidance this project would not have materialized. I would also like to thank my committee members, Dr. Peter Murano, Dr. Joseph Awika, Dr. Chaodong Wu and Dr. Leo Lombardini for their constant encouragement, support and valuable time- to-time inputs.

Additionally, I would like to show my gratitude towards Dr. Shareena Sreedharan, for her guidance and cooperation throughout this journey. I would like to thank Dr. Vimal Nair, for guiding me through chemical analysis and the chemistry involved in this project. Besides, I really appreciate the support from my fellow lab friends Dr. Elisa Schreckinger, Dr. Woo Young Bang and Alejandra Torres for stimulating discussions and motivation. I am grateful to them for their continuous support and help.

This research project imprints support and guidance of many people including Dr. Charlie Hall and Dr. Rebecca Creasy for giving me the opportunity to work as their teaching assistant. Also, would like to extend my gratitude to Dr. Dan Lineberger, Dr. Patricia Klein and Dr. Stephen Talcott for their guidance and help in the difficult times.

I would also like to acknowledge and give a special thanks for their unconditional trust, care to my parents Anuraag Bhargava and Richa Bhargava, my sister-in-law Ritika Bhargava and most importantly my grandmother Pushpa Bhargava. A special note of gratitude towards my brother Prateek Bhargava for being my emotional support, his

edifying counseling sessions that helped me stay motivated. This acknowledgement will be incomplete if I do not mention my friends who stood by me like family to help me accomplish this research project.

CONTRIBUTORS AND FUNDING SOURCES

Contributors

This work was supported by a dissertation committee consisting of Professors Dr. Luis Cisneros-Zevallos [adviser], Dr. Joseph Awika, Dr. Chaodong Wu and Dr. Peter Murano of the Department of Nutrition and Food Science, and Dr. Leo Lombardini of the Department of Horticulture.

Funding Sources

This project was supported by Texas Pecan Board.

TABLE OF CONTENTS

Page

LIST OF FIGURES

Page

LIST OF TABLES

Page

CHAPTER I

INTRODUCTION- THE HOLISTIC ROLE OF PECAN METABOLITES IN THE PREVENTION AND THERAPEUTIC AMELIORATION OF THE METABOLIC SYNDROME

Summary:

The role of inflammation and its connection with metabolic disorders has always been an ambiguous topic for research. Inflammation has been correlated to be the onset of many diseases. Recently, the connection with gut microbiota and many disorders has been an area research of interest. Low grade inflammation signals to defend the body, by inducting cascade of responses. However, unattended inflammation could play a pivotal role by culminating in a loop or a vicious cycle in perpetuating the disease. Various stimuli can demote healthy individuals into pre-diseased state and finally transition into diseased state. This chapter includes some disease models and an approach to delineate a rational strategy to address chronic diseases. The objective of this chapter is to introduce the diseased models and literature about pecan and urolithins.

Introduction:

The prevalence of chronic disease in the United States is continuously rising and is projected to affect approximately 48% of the US population by 2020 [1]. The majority of mortalities is caused by cardiovascular diseases, followed by cancer, chronic lung disease and diabetes mellitus [2]. It is estimated that ischemic heart disease and stroke will be the leading causes of death by 2030 [2-3]. Diabetes was estimated to affect 6.4% of the world population in 2010 (285 million adults), this number is projected to rise to 7.7% (439 million)

in 2030 [4]. Between 2010 and 2030, there will be a drastic increase in the individuals suffering from diabetes, with estimate to be around 69% in developing and 20% in developed countries [4]. Thus, there is a major need to control the progression of chronic diseases such as metabolic syndrome.

Metabolic syndrome (MetS) is characterized by dyslipidemia, arterial hypertension, type 2 diabetes mellitus (T2DM) and cardiovascular diseases (CVD) [3, 5]. It is a global phenomenon favored by an obesogenic environment which promotes consumption of energy-dense foods and discourages energy expenditure, resulting in weight gain. In recent years there has been an increase in obesity in young people, indicating that T2DM and metabolic syndrome is not exclusive to adulthood but are also evident in childhood [3, 6]. Cameron et al. (2004) have concluded that the differences in genetic background, the diet rich in saturated fats, refined carbohydrates, levels of physical activity, smoking, sedentary lifestyle and high body mass index (BMI), family history are the plausible causes of metabolic syndrome [6-7].

Dietary modification and pharmaceutical intervention are common avenues to treat risk factors associated with both MetS and CVD. The advancing and fast running society has procured a lifestyle resulting in an increased prevalence of metabolic diseases among people. The aims of this dissertation are to highlight the potential dietary preventive and therapeutic measures which will connect the missing pieces of how to lead a healthy life focusing on identifying natural treatments to treat metabolic dysregulation [8].

Pecan (*Carya illinoinensis*) is a native tree from North America and belongs to the Juglandaceae family. It is a deciduous tree that can live for hundreds of years and can reach very big dimensions. The fruit is a drupe consisting of a nut enclosed in a pod which becomes

dry on maturing and splits into four valves [9]. Geographically, in the US, pecan domesticates in Ohio, Indiana, Illinois, Kentucky, Tennessee, Mississippi, Louisiana, Texas and Georgia. The United States is the world's biggest producer, contributing to about 55% of the world's production, with a net value of $684 million. New Mexico was the highest producer of pecan in 2017 (USDA 2018). Commercially pecan is also grown in Brazil, Israel, Australia, Peru, South Africa, China, and Argentina[10-11]. These nuts are often consumed raw, as a part of cereals, energy bars, chocolate bars and pies[10]. They are a rich source of protein, fat, dietary fibers, micronutrients such as manganese and vitamin E [12]. They contain about 65-75% lipids, which is higher than peanuts (48-52%) and almonds (51%) [12]. Pecans consist of 57.28 g/100g of oleic acid, 31.50 g/100g of linoleic acid, 6.66 g/100g of palmitic acid, 2.38 g/100g of steric acid and 1.73 g/100g of linolenic acid [10].

Recent studies have demonstrated that extracts from different parts of the pecan tree, such as kernel, leaves, shell and bark, have shown to placate chronic diseases. Pecans have also shown to have antimicrobial [13-14], anthelmintic, astringent, antidiarrheal, anti-hyperglycemic [15], anti-diabetic [15-16], anti-inflammatory [17] and anti-obesity properties. These properties have been attributed due to the presence of polyphenols. Phenolic profiles of pecan kernels include gallic acid (138 µg/g), proanthocyanidins (494.1 ± 86.2 mg/100 g FW), prodelphinidins (3-O-gallates) including epigallocatechin, epicatechin-3-O-gallate, and the more common flavan-3-ols, catechin, epicatechin and ellagitannins (20.96-86.20 $mg \cdot g^{-1}$)[18-22]. The quantity of phytochemical is also influenced by the cultivar, cultivation procedures, location, climatic condition, horticultural practices, maturity and environment [23]. A study on pecan (cv. Pawnee) reported a composition of 2.13 ± 0.05 g/100g of moisture, 78.07 ± 0.72 g/100g of lipid, 6.00 ± 0.04 g/100g protein, 1.25 ± 0.00 g/100g ash, 3.67 ±0.06

g/100 g/ml sugar and 0.80 ± 0.01 g/100g tannin [24]. Additionally, 2.85 g/100g of dietary fibers, and 0.90 mg/100 g Vitamin C [10]. Polyphenols from pecan nut shells have shown to reduce breast cancer by having a cytotoxic effect against MCF-7 cells and 52% inhibition on Ehrlich ascites tumor growth and thereby increasing the life expectancy of mice by 67% [25]. In another study, low molecular weight polyphenols of pecan (ellagic acid pentose, digalloyl ellagic acid, ellagic acid, valoneic acid dilactone hydrate, methyl ellagic acid hexoside, ellagic acid galloyl pentose and ellagic acid HHDP glucose) showed suppression of nitric oxide and intracellular ROS production in LPS challenged Raw 264.7 macrophages [17]. Polyphenols from shell and bark have shown to have anti-diabetic properties [15-16]. Additionally, an intake of whole pecans as a part of human diet it reduced VLDL (very low density lipoprotein) and enhance human serum lipid profile [13, 17, 23, 26-28].

The challenge is poor systemic bioavailability of these secondary metabolites. However, biotransformation of polyphenols by intestinal microflora conserves their function and makes them bioavailable [29]. Pecans are a rich source of ellagitannins which are not absorbed by humans, rather they are metabolized into urolithins by human gut microbiota and enterohepatic circulation. Human studies have demonstrated that intake of fruits rich in ellagitannins, such as walnut and pomegranate, by humans were converted into urolithins by the action of the gut micro-organisms and traces of urolithins were identified in urine, feces and plasma [22, 30-32].

Urolithins undergo phase I and phase II modifications inside the body. Studies have shown that these glycones and aglycones have ameliorating biological activity against chronic diseases [30]. Methylated and unmethylated derivatives of urolithin A and B have shown to inhibit neuroinflammation because these metabolites could potentially cross the

blood brain barrier. In murine microglia cells, urolithins suppressed levels of nitric oxide, IL-6 and TNF α, thus suppressing the inflammation [33]. Urolithins A and B have also shown to suppress adhesion molecules in aortic and vascular stimulated cells, thus ameliorating endothelial dysfunction [34]. Urolithin B has also shown to improve cardiomyocyte contractile function in Trimethylamine-N-oxide (TMAO) stimulated cells, suggesting a potential role of urolithin B against cardiovascular diseases [35]. However, studies relating to the mechanistic mode of action of urolithins in abating palmitic acid-induced oxidative stress and its link to inflammation and the metabolic syndrome is not well studied.

Model of disease:

According to Liu et al., 2012, disease model progression is divided into three different stages, a normal state, a pre-disease state (or critical state) and the disease state. The normal state is a representation of disease under control or healthy state, a pre-disease state is an acute reversible point just before a disease progresses to the chronic stage. However, after reaching chronic state, the disease cannot be reversed [36]. Osorio et al., 2015, adapted the model and described it in two stages, preventive (pre-disease state to normal state) and therapeutic (pre-diseased stage to disease stage). They suggested that progression of disease with proper healthy nutritional diet and life style could potentially reverse from disease state to heathy state [37-38].

We adapted this model and explain metabolic syndrome, as represented in Figure 1, body undergoes systemic low-grade inflammation (basal inflammation) which could be triggered by external or internal stimuli such as genetic, environmental changes, visceral adiposity, hypertension, dyslipidemia, circadian cycle which causes energy imbalance in human body, this predisposes the body to chronic diseases [39-43]. Inflammation is the first

stage. It is an immune response classified by increase in temperature (fever), redness due to accumulation of blood, pain and swelling at the site of trigger. If this inflammation prolongs, antigen-presenting cells (APC) and B- and T lymphocytes switches to adaptive immunity. This inflammation perpetuates a low-grade inflammatory state as localized response, coordinated by accumulation of plasma and leukocytes. After all the immune responses are exhausted and body is unable to prevent the disease, the body requires external approaches (such as medication) to restore homeostasis [40]. At this stage, low grade inflammation proceeds to pre-diseased state where unfavorable stimuluses such as excessive nutrients (saturated fatty acid and/or carbohydrates rich diet), perpetuates immune cells to secrete cytokines and chemokines to sustain the disease. Obesity is a pre-disease state which can be defined as a continuous episode of low-grade acute inflammation which formulates in a vicious loop. It continues to increase the leukocytes, cytokines and chemokines. These leukocytes circulate in the body and targets various organs leading β pancreatic cells to undergo glucose insensitivity which advances the body towards insulin resistance. Insulin resistance is inability of insulin to stimulate glucose uptake in muscle and liver cells leading to hyperglycemia. Insulin resistance initiates dysfunction in various organs such as liver, muscle. In this situation if body does not restore the pre-disease state, then the loop perpetuates in to a bigger loop, self-fed by the increased cytokine production culminating into metabolic syndrome.

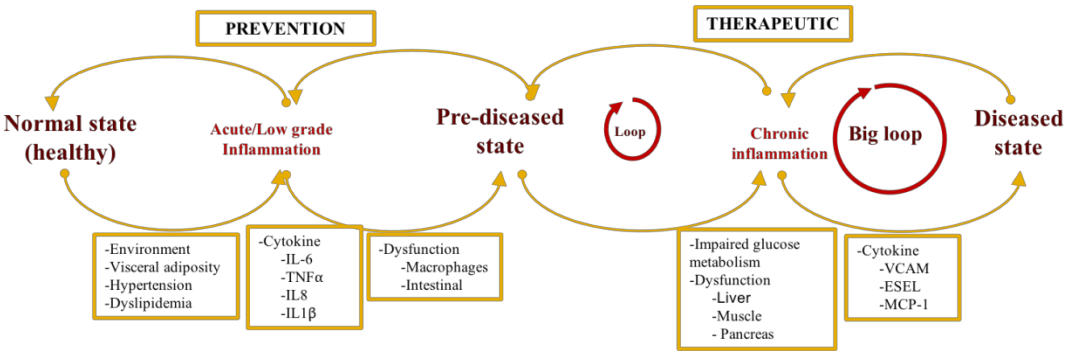

Figure 1: Relationship between normal state, pre-disease state and chronic disease state in human health

A proposed disease model progression is divided into preventive (normal state to pre-disease state) and therapeutic (pre-diseased stage to disease stage) and progression of disease with proper healthy nutritional diet and life style could potentially reverse from disease state to heathy state. Body undergoes systemic low-grade inflammation (basal inflammation) which could be triggered by external or internal stimuluses such as genetic, environmental changes, diet, visceral adiposity, hypertension, dyslipidemia, circadian cycle which causes energy imbalance in human body, this predisposes the body to chronic diseases which progresses to dysfunction in leukocytes, intestinal and adipocytes and increases the expression of pro-inflammatory genes. This transitions the body to Pre-diseased stage due to continuous episode of systemic inflammation leading to insulin resistance, glucose insensitivity and chronic inflammation. At this point there is dysfunction in pancreatic-Bcell, liver, muscle and endothelium. Perpetuation of this state culminates into a bigger loop leading to development of metabolic syndrome. figure adapted from [36-37]

Understanding the disease pathology:

Poor dietary habits and lack of proper balance and physical activity could lead to obesity and chronic inflammation. Chronic inflammation has been implicated in instigating chronic diseases such as cardiovascular disease, cancer, and diabetes. They are the leading cause of death in developing as well as more developed countries [1, 4, 44]. Several nutrition-based strategies such as plant-based polyphenols have shown to mitigate chronic inflammation and diseases[45-47]. However, their mechanisms are inadequately studied.

One mechanism to the progression of diseases could potentially begin from impairment of gut microbiota. Intestinal system has been studied for releasing unwanted substances such as lipopolysaccharide (LPS) in to the blood stream causing defective shift in the homeostatic functionality of human body, as shown in Figure 2. Studies have shown that such shifts are also caused by dietary habits. Microbiota regulates the architecture of intestines by altering the permeability of gut and epithelial cells form the first physical barrier of defense against the gut milieu [48-53]. This distinct microflora community in the human body participates in nutrient absorption, regulation, digestion and metabolism of multiple metabolic pathways. These highly complex symbiotic network of host-microbiome signaling systems influence many human diseases [1, 54-55]. These epithelial cells respond to various inflammatory stimuli such as bacterial and viral infection, cytokines and many more. Imbalanced diet such as high fat diet containing Palmitic Acid (PA) influences the gut microbiome. It has been observed that high fat diet facilitates increase in gram negative bacteria which increases leakages of LPS through the intestinal barriers [56].

LPS stimulates the inflammatory response by binding to Toll Like Receptor-4 (TLR4) and triggers production of intracellular Reactive Oxygen Species (ROS) via NADPH oxidase and the mitochondria. ROS such as superoxide anion (O_2^-), hydroxyl radical (OH^-) and hydrogen peroxide (H_2O_2) are generated as byproducts of mitochondria metabolism or by the enzymatic reaction of NADPH oxidase. ROS arbitrates the activation of NF-κB via a redox (reduction/oxidation) mechanisms [57-58]. Then ROS-dependent NF-κB activation mediates the LPS-induced gene expressions such as COX-2, IFN-β, TNF- α and iNOS [59-61].

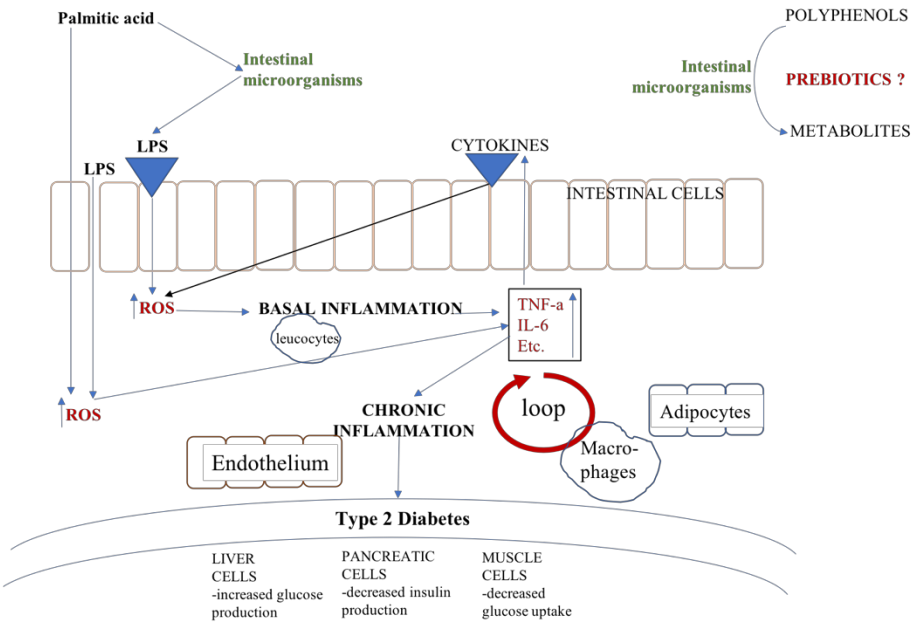

Figure 2: Relationship between microbiota, oxidative stress, inflammation and individual tissues playing a role in causing chronic diseases such as diabetes

Figure 1 is explained further. Palmitic acid (PA) shifts the equilibrium of intestinal micro-organism leading to release of Lipopolysaccharide (LPS) into the body. Both LPS and PA induces oxidative stresses in the body which stimulates low grade/basal inflammation. This leads to increase in expression of cytokines. Cytokines also increases Reactive Oxygen Species (ROS) culminating a vicious loop. This inflammation affects the intestinal, adipocytes, macrophages and endothelium. Continuation of this low-grade inflammation progresses into chronic inflammation, affecting the liver, muscle and pancreatic cells perpetuating the body to progress to diabetes.

Reactive oxygen species has been known to have dual mechanisms in the body. In low or basal concentrations, they mitigate diseases by regulating cell growth, the adhesion among cells and their differentiation At high levels, they activate inflammatory responses causing chronic diseases because they oxidize and damage cellular constituents such as proteins, lipids and DNA [62-63]. These oxidative stresses instigate metabolic disturbances leading to conditions such as dyslipidemia, hyperglycemia and hypertension causing obesity

(the pre-disease state). Diseases including CVD, pulmonary diseases, cancer, and type II diabetes mellitus are the predisposed conditions due to obesity [64-65].

After low grade inflammation, the second stage is obesity, which has also often been associated to dysbiosis, where the changes in the distribution of microbiota or a shift in the distribution of the microorganisms causes increase in biomarkers and ROS [66]. Adipose tissue is an endocrine system majorly involved in obesity; adipocytes are known to produce a variety of biologically active cytokines such as adipokines (e.g., plasminogen activator inhibitor (PAI)-1, visfatin, resistin, leptin, and adiponectin), TNF-α, IL-6/8, monocyte chemoattractant protein 1 (MCP-1), CRP, and osteopotin. Obesity instigates macrophages to switches into M1 polarization by inducible nitric oxide synthase (NOS) and further produces TNF-α, IL-1 β, IL-6, MCP-1, and superoxide anion (O_2^-) [63, 67]. Compositional changes in the microorganisms alter the intestinal monosaccharide absorption and energy withdrawal from indigestible food components (principally carbohydrates) via short chain fatty acid (SCFA) production and de novo hepatic lipogenesis[50, 68]. Influx of excess FFAs and secretion of inflammatory cytokines from adipose tissue stimulates inflammatory responses causing an oxidative stress with elevated ROS. This promotes JNK and IKB complex activating NF κB pathway leading to secretion of cytokines such as TNF- α, IL1β, IL6 etc. cytokines [63]. These cytokines in obesity constructs a loop of uncontrolled inflammation triggering a bigger loop as shown in Figure 1 leading to inflammatory responses in brain, muscle, liver and many other organs. In obese individuals, lipid accumulation takes place in muscle, adipose tissue and liver [66, 69]. The exacerbation of cytokine and cellular inflammation due to obesity progresses to insulin resistance followed by diabetes. In adipose tissue, insulin resistance with lipid storage dysfunction are key events

in obesity, which promotes macrophage infiltration triggering a cascade of inflammatory responses such as hypoxia, oxidative stress and often necrosis. These events fuels the progression of the loop [40, 64].

Insulin resistance primarily affects liver, muscle and adipocytes. Pancreas secrete insulin (from β-cells), glucagon (from α-cells) and somatostatin (from δ-cells). Pancreas senses the glucose in the body and secretes insulin, as shown in Figure 3. This insulin activates pathways in different organs such as muscle and liver for glucose metabolism [38, 70-71]. During hypoglycemia, glucagon stimulates liver to convert glycogen reserves to release glucose in the blood. It also promotes the formation of new glucose from other substrates (lactic acid from muscle and glycerol from adipocytes) by a process called gluconeogenesis. Somatostatin works in regulating glucagon [72-73]. During a dysfunction like increased lipid and glucose content such as dyslipidemia and hyperglycemia respectively, causes oxidative stress which circumvents insulin perception and secretion in different organs such as liver and muscles [69]. Insulin stimulates glucose uptake by activating cascade of pathways such as glycolysis (glucose is converted into substrate pyruvate which is utilized by other processes to produce energy in the form of ATP), glycogenolysis (converting glucose into glycogen) and lipogenesis (accumulation of lipids) [69, 73-75]. During postprandial state, glucose is condensed into glycogen and converted into fatty acids or amino acids. Insulin activates Akt which regulates glucokinase (an enzyme used for conversion of glucose to glucos6-phosphate) for metabolism of glucose [69, 74-75]. During a dysfunction, insulin resistance occurs to diet (PA) or there is increase in cytokines levels causing oxidative stress on the liver which stimulates glucose production by gluconeogenesis and exacerbates hyperglycemia in the body. Non-alcoholic fatty liver disease and dyslipidemia are also associated with infiltration

of Kupffer cells (specialized macrophages in liver) which triggers oxidative stress mediated pathways [40, 69].

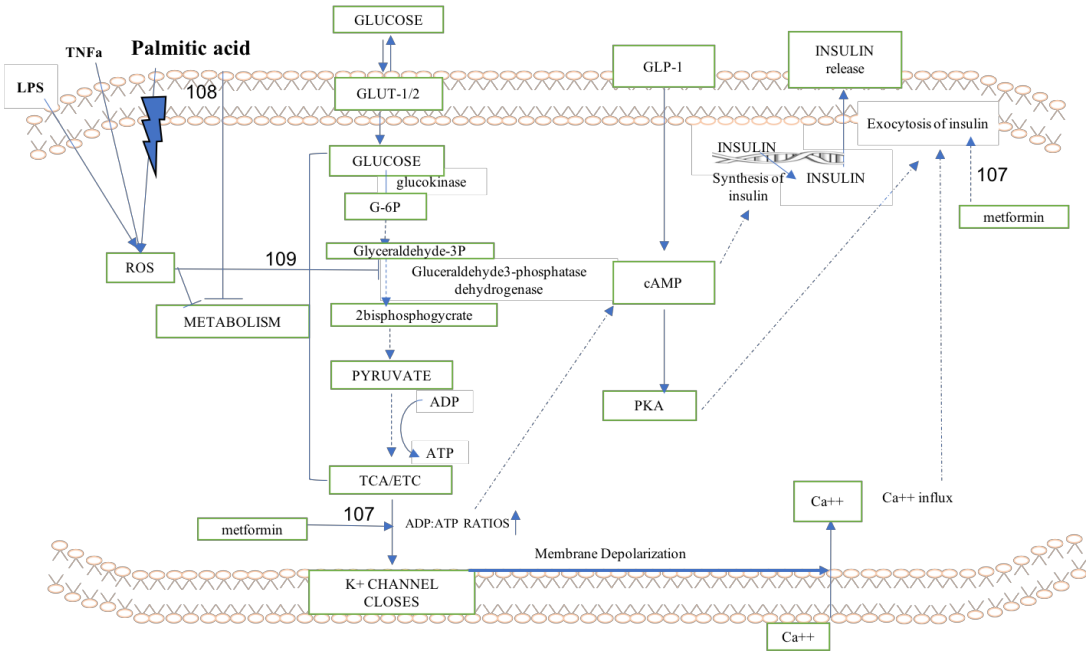

Figure 3: Schematic representation of glucose mediated insulin production of a pancreatic B-cell model challenged by palmitic acid, LPS and TNF-α

Palmitic acid binds to FFA receptor and increases oxidative stresses by increasing reactive oxygen species. Oxidative stresses can be produced by LPS and TNFa also binding to their corresponding receptors. ROS inhibits the glucose metabolism pathway affecting the glucose sensitivity of B-cells. In a normal cell, glucose is transported inside the pancreas by GLUT-2, it undergoes glycolysis, oxidative metabolism which generates adenosine triphosphate (ATP). Production of ATP increases the ATP/ADP ratio. This increased ratio leads to closure of ATP-sensitive K+-channels ($K_{ATP\text{-}channels}$). Allowing the calcium ions to seep inside the cell which facilitate insulin release. Elevated Ca^{2+} triggers exocytotic release of insulin granules. GLP-1 and ATP promotes formation of cAMP, amplifying secretion via protein kinase A (PKA) and metformin upregulates the insulin release and restores ADP:ATP ratio in fatty acid stimulated glucose insensitivity. Patane et al. (2000)[107], Gehrmann et al., (2010)[108], Munhoz et al. (2016)[109].
ROS, Reactive oxygen species; PKA, protein kinase A; cAMP, cyclic AMP; GLP, glucagon like peptide, TCA/ETC, Tricitric acetate and electron transport chain pathways;

Skeletal muscles are responsible for 75-80% of glucose metabolism. Insulin from the pancreatic cells trigger glucose transporter (GLUT-4) to uptake glucose and convert it into glycogen which serves as an energy reserve for the body [76]. As shown in figure 4 and 5, during a dysfunction such increased intake of PA causes elevated levels of ROS which downregulates phosphorylation of insulin receptor substrate/ PI3K and curtails translocation of GLUT-4 (transporter of glucose) to the cell membrane. Studies have demonstrated that consumption of saturated fatty acids like palmitic acid alters the insulin signaling pathway owing to which IRS/PI3K/AKT is unable to initiate glucose uptake properly [69, 77-79]. This leads to skeletal muscles to undergo anaerobic glycolysis producing lactate from pyruvate which is transported to the liver. The liver converts lactate (from skeletal muscle), glycerol (from adipocytes) to glucose. These gluconeogenic precursors are transported to liver which are utilized for synthesis of glucose [80-82]. GLUT 2 (transporter of glucose) releases glucose in the blood circulation. Consequences are perturbation in adipocytes resulting in increased secretion of free fatty acids (FFA) into the blood stream which impairs the muscle insulin signaling. All these dysfunctions facilitate obesity and insulin resistance which causes diabetes. Diabetes mellitus (is the stage 3 in the diseased model) is a disease that is delineated by chronic hyperglycemia driven by dysfunction in insulin secretion, insulin action or both [83]. Obesity related chronic inflammation is a pre-disease state which translates in to a disease state such as diabetes, hypertension, cardiovascular diseases [69, 77-79].

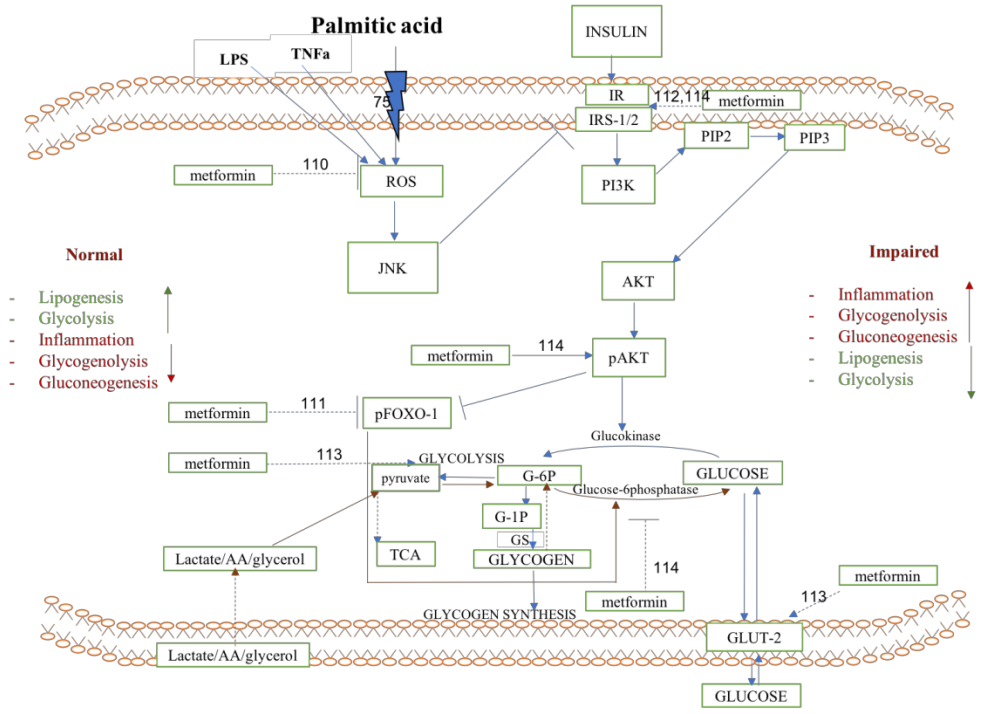

Figure 4: Schematic representation of insulin mediated glucose uptake and release in a hepatic cell model challenged by palmitic acid, LPS and TNF-α

Palmitic acid binds to FFA receptor and increases oxidative stresses by upregulating reactive oxygen species. Oxidative stresses can be produced by LPS and TNFa also binding to their corresponding receptors. These oxidative stress leads to activate JNK. JNK inhibits insulin receptor substrate (IRS-1). Thus, it downregulates PI3K activity of initiating conversion of PIP2 to PIP3. Thereby, it downregulates phosphorylation of Akt and increases gluconeogenesis since Akt cannot inhibit FOXO. FOXO initiates gluconeogenesis (converts glucose-6-P to glucose in presence of glucose 6 phosphatase). Thereby there is an increase in the glucose production inside the cell. Glucose 6-P is a substrate utilized for glycolysis and synthesis of glycogen. Akt regulates glucokinase which is a key enzyme in glycolysis. Fatty acids like palmitic acid alters the insulin signaling pathway leading to skeletal muscles to undergo anaerobic glycolysis producing lactate from pyruvate which is transported to the liver. The liver converts lactate (from skeletal muscle), glycerol (from adipocytes) and gluconeogenic amino acids are transported to the liver which are used as the precursors for the synthesis of glucose. Metformin is a pharmaceutical drug known to suppress ROS and increase activity of IRS and GLUT-2. GLUT-2 is a transporter of glucose, it facilitates glucose uptake and release from liver cell by gradient diffusion process. Viollet et al. (2012)[110], Valenti et al. (2008)[111], Guton et al. (2003)[112], Gao et al. (2010)[75], Zheng et al. (2015)[113], Xu et al. (2016)[114].
IR, Insulin receptor; IRS, insulin receptor substrate; PI-3K, phosphatidylinositol 3-kinase; PIP2, phosphatidylinositol 4,5-bisphosphate; PIP3, phosphatidylinositol (3,4,5)-trisphosphate; Akt, protein kinase B; GLUT, glucose transporter; ROS, reactive oxygen species; FOXO, Forkhead box protein.

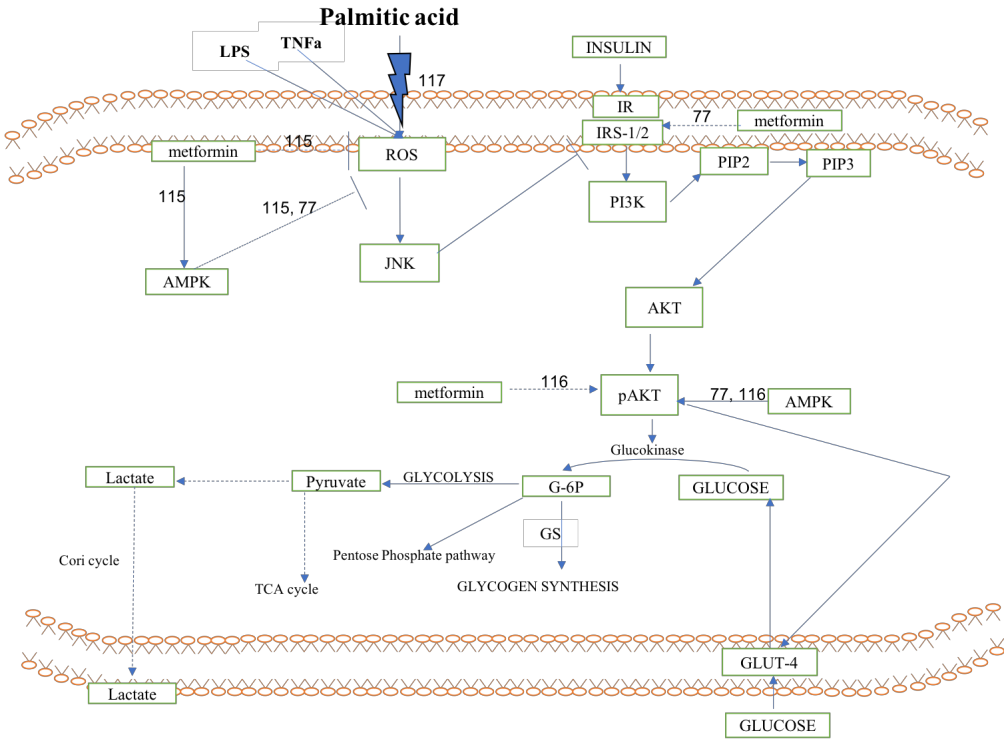

Figure 5: Schematic representation of insulin mediated glucose uptake in a skeletal muscle cell model challenged by palmitic acid, LPS and TNF-α

Palmitic acid binds to FFA (free fatty acid) receptor and increases oxidative stresses by upregulating reactive oxygen species. Oxidative stresses can be produced by LPS and TNF-α also binding to their corresponding receptors. These oxidative stress leads activation of JNK. JNK inhibits insulin receptor substrate (IRS-1). Thus, downregulates PI3K activity of initiating conversion of PIP2 to PIP3. Thereby, it downregulates phosphorylation of Akt and thus preventing GLUT-4 translocation to the cell membrane to facilitate glucose uptake. pAkt also regulates glucokinase which is a key enzyme in glycolysis. Fatty acids like palmitic acid alters the insulin signaling pathway leading to skeletal muscles to undergo anaerobic glycolysis producing lactate from pyruvate which is transported to the liver. Metformin is a pharmaceutical drug known to suppress ROS and increase activity of IRS and stimulates phosphorylation of Akt. GLUT-4 is a transporter of glucose, it facilitates glucose uptake Kumar et al. (2002)[115], Kim et al. (2013)[77], Park et al. (2014)[116], Lee et al. (2017)[117]. Insulin receptor; IRS, insulin receptor substrate; PI-3K, phosphatidylinositol 3-kinase; PIP2, phosphatidylinositol 4,5-bisphosphate; PIP3, phosphatidylinositol (3,4,5)-trisphosphate; Akt, protein kinase B; GLUT, glucose transporter; AMPK, AMP-activated protein kinase; ROS, reactive oxygen species;

Mode of action and reversibility:

The dietary habits of individuals attributed to the different geographical regions influences the consumption of polyphenols. Polyphenols are classified as the group of phytochemicals containing phenol rings and are categorized into flavonoids, phenolic acids (virgin olive oil, red wine, walnuts, red raspberry), resveratrol (grapes, red wine and nuts) and lignans (virgin olive oil, rye flour and sesame seed oil) [84]. Polyphenols are characterized by the presence of one or several phenolic groups in their structure which are capable of reducing reactive oxygen species and various metabolic pathways. This uniqueness in structural property is taken into consideration while studying the bioavailability, biological properties and health bestowing effects. Fruits such as apple, grapes, pears and berries contain 200-300 mg/100 g, cloves contain 15 mg/100g, rosé wine contains 10 mg/100 ml [85-86].

Polyphenols mitigate insulin resistance, obesity, inflammation, CVD and many diseases. They promote glycolysis by activating AMPK (AMP- activated protein kinase) like observed with capsaicin where blood glucose levels were regulated and AMPK was activated in C2C12 muscle cells, thus ameliorating insulin resistance [77]. Capsaicin suppressed inflammation in macrophages by inhibiting NFκB and production of cytokines (e.g., TNF-α, IL-6, iNOS, COX-2 and MCP-1), thus ameliorating inflammation [87-88]. Resveratrol, another polyphenolic compound found in wine has shown to significantly induce glucose uptake in C2C12 cells, via AMPK activation [89].

Some more examples such as epigallocatechin gallate (EGCG) compound found in tea has shown to increase muscle insulin sensitivity in C2C12 cells, insulin release in pancreatic cells [90]. EGCG, epicatechin gallate (ECG) and curcumin reduces insulin receptor

substrate-1 (IRS-1) Ser307 phosphorylation [91], increases Akt phosphorylation via ERK1/2, p38 MAPK, and AMP-activated protein kinase, thus resulting in attenuation of insulin resistance [91]. Similarly, polyphenols such as gingerol and anthocyanins lower insulin resistance by inhibiting PI3K/AKT and JNK of activation of the AMPK-SirT1-PGC1α axis to protect from diabetes [92-93]. In addition, condensed tannins attenuates glucose production from carbohydrates by inhibiting α-glucosidase [94]. Genistein and quercetin have shown to decrease inflammation in macrophages by suppressing the inflammatory markers (TNF-α, IL-1β, and IL-6), followed by inhibiting the JNK- and ERK- phosphorylation, NFκB activation followed by AMPK activation [95-96]. Quercetin has shown to inhibit the production of TNF-α and NO while attenuating IL-6, IL-1β, IL-8, and MCP-1 expression [96-97]. Curcumin downregulates transcription factors (e.g., NFκB, AP-1, STAT) and enzymes (e.g., COX-2, LOX, MMP9, MAPK, mTOR, Akt, IKK, c-Jun/fos), upregulates PPAR**γ**[98-99], and reduces the expression of inflammatory mediators, cytokines (e.g., TNF α), and adhesion molecules (e.g. ICAM-1, VCAM- 1) [100]. These examples portray how polyphenols have such diverse mode of action in mitigating chronic diseases.

Bioactive compounds such as flavonoids have demonstrated to protect cardiovascular diseases at specific phases. In pre-diseased phase, flavonols prevent platelet aggregation and thrombosis, inhibit oxidative stress, improve blood flow and protect endothelial function by minimizing inflammation [101-103]. At diseased phase, flavanols are known to interfere ischemia-induced cell death mechanisms, apoptosis and necrosis [102-105]. Meta-analysis of cohort studies concluded that consumption of anthocyanins, proanthocyanins, flavones, flavanones and flavan-3-ols were inversely correlated with CVD. The dose–response analysis indicates that an average increase of 10 mg of flavonol intake

per day could be associated with a 5 % decrease in CVD [106]. These studies demonstrate that polyphenolic compounds have the capability to attack at different stages, which could illustrate that these compounds are suppressing the vicious loop and thereby ameliorating the diseases.

In another study, mice were induced with severe hyperglycemia and insulinemia induced by streptozotocin in mice caused sever deficiency in pancreatic β cell. When the mice were fed with a low-calorie, low-protein and low-carbohydrate high-fat 4-day fasting mimicking diet (FMD). It stimulated progenitor or other cells to regenerate β cells and also reversed the expression of genes involved in diabetes [38]. Suggesting that diet plays a pivotal role and has the potential to revert chronic diseases. Another observation could be made there is probability that this diet was able to suppress the loop and therefore the disease was reversed.

Evidences and intervention studies have illustrated that incorporation of polyphenols from olive oil, wine, curcumin, grapes rich polyphenols have the potential to alleviate MetS. Bioactive compounds have shown to decrease body weight, blood pressure, and blood glucose and improve lipid metabolism. These polyphenols have shown to have synergistic, agonistic and additive properties. The antioxidant nature of these bioactive compounds such as nuts, fruits, vegetables, seasoning with aromatic plants, spices, begins by mitigating the early symptoms of inflammation followed by placating pre-diseased molecular markers and thus preventing the development and progression of MetS.

The progression of medicine began with the Greek physician Hippocrates, who redefined the treatments based on scientific observations. Back in the ancient era, treatment of all sort of diseases were done on the basis of scared and spiritual beliefs, prayers, magical

practices and herbal mixtures. The advent of conventional unorthodox medicinal practices was followed in African, Arab, Chinese, Indian, Japanese cultures employed mixing the herbs and they claimed reversing chronic diseases. With industrial revolution and advancement of technology the approach towards curing pathology of disease has taken a different perspective. However, the role of these mixtures and the science of how they work are still an area of interest. Combining traditional herbal mixtures with scientific justifications should be the approach thenceforth [1, 54-55].

As represented in Figures 1 and 2, we hypothesize that in metabolic syndrome stimulated by unhealthy diet, low-grade inflammation begins at intestinal cells, which progresses to obesity which advances to endothelial, liver, pancreatic and muscle cells. The purpose of this investigation is to determine specific role of urolithin A and B in this model of disease and unfolding its therapeutic and preventive properties. To discern this objective, we use different cell models including Caco-2 (mimics intestinal cells), HUV-EC (endothelial cells), AML 12 (hepatocytes), β TC-6 (pancreatic β cells), C2C12 (skeletal myocytes) to demonstrate specific role of urolithins mode of action and how oxidative stresses play a vital role in each pathway.

Overall Objective:

The aim of this project is quantification of urolithins from pecans after microbial fermentation and exploring the mechanism of urolithins in abating oxidative stresses induced by palmitic acid- in pancreatic cells, hepatic and muscle cells and inflammation in colon cells and endothelial cells under the scenario of a holistic model of metabolic syndrome.

Central hypothesis:

Pecan produces urolithins on exposure to fecal microorganisms, which contributes in suppression of inflammation in an *in-vitro* model using Caco-2 (colon cells) and HUVEC (endothelial cells) and palmitic acid induced diabetes in AML-12 (hepatocytes), C2C12 (myocytes) and ß-TC6 (pancreatic ß-cells) cells.

Specific aims:

Aim I (Chapter II):

To quantify and identify the metabolite from pecan and investigate its anti-inflammatory properties in Caco-2 cells

Hypothesis:

Ellagitannin-rich pecan will produce urolithin A and B when exposed to fecal microbiome and urolithin will suppress inflammation in Caco-2 cells.

Objectives

1. To identify phenolic compounds produced from pecan upon acid hydrolysis and exposure to fecal organisms to characterize specific metabolite
2. To identify the role of urolithin against inflammation in intestinal cell model system- Caco-2.
3. To determine the mechanism of action by which urolithin A and B will exert their anti-inflammatory properties in Caco-2 cells.

Aim 2 (Chapter III):

To investigate the anti-diabetic properties of urolithin A and B in C2C12, AML 12 and ßTC6 cell model system.

Hypothesis:

Urolithin A and B will restore the glucose uptake in C2C12 and AML12 and insulin secretion in ßTC6 by suppressing the ROS levels and reinstate PI3K/Akt pathway.

Objectives

1. To identify the role of urolithins against diabetic cell model system using C2C12, AML 12 and ßTC6.
2. To determine the mechanism of action by which urolithin A and B will exert their anti-diabetic properties in C2C12, AML 12 and ßTC6 cells.

Aim 3 (Chapter IV):

To investigate the anti-inflammatory properties of urolithin A and B in HUV-EC cell model system.

Hypothesis:

Urolithin A and B will ameliorate LPS and TNF α induced inflammation in HUV-EC.

Objectives

1. To identify the role of urolithin against inflammation in endothelial cell model system.
2. To determine the mechanism of action by which urolithin A and B potentially exert their anti-inflammatory mechanism.

CHAPTER II

FERMENTATIVE GUT MICROBIAL METABOLITES FROM PECAN AND THE MODE OF ACTION OF UROLITHINS A AND B AGAINST INFLAMMATION IN LPS STIMULATED COLON CACO-2 CELLS

Summary:

First part of the investigation deals with identification and quantification of the various phytochemicals in pecans using liquid chromatography-mass spectrometry (LC-MS). Isolation and identification of different secondary metabolites in a plant is an essential step in elucidating the mechanism of action in biological systems. The second step includes understanding the metabolism of these phytochemicals by the intestinal microbial milieu. For this acid hydrolyzed pecan is exposed to mice feces. Subsequently, the quantification of pecan metabolites was performed using LCMS. Urolithin A and Urolithin B glucuronide were identified.

The progression of diseases initiates with an inflammation in the intestinal cells, which culminates into chronic diseases. To elucidate the role of urolithins in a diseased model system, second part of the investigation involves explicating anti-inflammatory effect of urolithins on intestinal epithelial cell, Caco-2 by measuring ROS and gene expression of pro-inflammatory genes. The cells were inflamed with LPS (lipopolysaccharide) and urolithin A was more effective than urolithin B in suppressing ROS and proinflammatory cytokines. The study also highlights that the possible mode of action of urolithins in suppressing inflammation is via upregulating LXR α as well as through ROS suppression.

Thus, the study confirms that urolithin metabolites have anti-inflammatory properties in colon cells.

Introduction:

The role of inflammation and its connection with metabolic disorder has always been an ambiguous topic of research. As described earlier, inflammation has been correlated to many chronic diseases and its connection with gut microbiota initiating many disorders has been an area of research interest. Basal inflammation signals brain to defend the body, by inducting cascade of immune responses. However, continuous episode of systemic or basal inflammation over a period of time culminates into a loop or a vicious circle. The need of the hour is to find an approach which could potentially reverse the disease by eliminating the source and loop.

Modern medicine is successions of inventions and discoveries over the years. The advancing and fast running society has procured a lifestyle which pushes individuals towards metabolic diseases. Epithelial intestinal cells are closely bound sheets of cells that act as physical barrier against infections. They exert various functions such as- protection, adsorption of nutrients and digestion and secretion of undesirable matter [118-119]. Long and small intestine are the house of diverse microflora, which facilitate in maintaining colon function and immunity [119]. Intestinal microbiota plays a pivotal role in bestowing immunity by releasing chemotactic signals that attracts neutrophils at the site of inflammation [118-119]. Research has demonstrated that microorganisms such as *Lactobacillus* and *Bifidobacterium* prevent growth of pathogenic bacteria, thus mitigating intestinal inflammation [120-121]. On the flip side microorganisms such as *Clostridium perfringens* and *Escherichia coli* encourages inflammatory responses to relapse intestinal immune mechanism and thereby increasing the

risk of colon diseases such as trauma, sepsis, inflammatory bowel disease (IBD), and infectious diarrhea [122-125]. Studies have shown that intake of saturated fatty acids potentially increases the count of gram-negative bacteria, leading to leakage of LPS from the epithelial lining inside the body. Intestinal microflora such as, *H. pylori* secrets hydrogen peroxide causing oxidative stress in the gastrointestinal tract. Oxidative stress is the imbalance in the oxidation in antioxidant system of the body which proceeds in secondary loss of homeostasis of the body.

One of the major components present in outer membrane of Gram-negative bacteria, is lipopolysaccharide (LPS). LPS elicits an inflammatory response, externally through a bacterial infection and internally during growth or lysis of microorganism in intestine. LPS, has been identified as a potent stimulus and is used in various studies to induce inflammation. It actuates oxidative stress by increasing Reactive Oxygen Species (ROS) leading to activation of MAPK, NFKB pathways, followed by increasing the expression of pro-inflammatory markers such as IL-1 β,TNF α, iNOS and IL8 [126-127].

Pecan is a tree native to United States, whose various parts such as kernel, shell, bark and leaves have been studied for mitigating chronic diseases. It is a rich source of bioactive compounds, specifically ellagitannins. Ellagitannins on exposure to stomach acids hydrolyses to ellagic acid, which has been reported to show plethora of biological actions [128-129]. Very recently it was identified these ellagic acid are further metabolized by human colonic microflora to yield hydroxy- 6H-dibenzo[b,d]pyran-6-one derivatives (mainly urolithins A and B). Urolithins have shown to extenuate sequelae of chronic diseases such as obesity, inflammation, and reducing metastasis of cancer cells to name a few diseases [130-

[133]. The aim of this investigation is to quantify and identify the metabolites from pecan and identify anti-inflammatory properties in Caco-2 cells.

Materials and Methods:

Materials:

The following chemicals were used in the experiments: Lipopolysaccharide (LPS), 2′,7′-Dichlorofluorescin diacetate (DCFA), Dulbecco's Modified Eagle's Medium (DMEM)/low glucose, penicillin/streptomycin mixture, 0.25% Trypsin-EDTA solution, DMSO and Fetal Bovine Serum (FBS) were purchased from Sigma (St. Louis, MO). Glucose and sodium bicarbonate were purchased from Acros Organics (Fair Lawn, NJ) and sodium bicarbonate from Mallinckrodt Chemicals (Phillipsburg, NJ), respectively. The CellTiter 96® AQueous Non-Radioactive Cell Proliferation Assay kit was purchased from Promega (Madison, WI). Caco-2 (HTB-37) were purchased from American Type Culture Collection (ATCC, Rockville, MD). Urolithins A and B were purchased from Sigma (St. Louis, MO).

Pecan Extraction:

Three replicates of fifty grams of Pawnee (genotype of pecans) were finely grounded and defatted using (1:20 w/v) hexane. The mixture was kept on a shaker overnight. Then cake was defatted two more times with hexane. Subsequently, the cake (~10 g) was dried at room temperature. Ten grams of defatted pecan powder was homogenized with 200 ml aqueous acetone (70:30, v/v) solution and placed in an oscillatory shaker at 4°C overnight. Next day, the slurries were centrifuged at 18000 g and the supernatant was collected. The slurry was redissolved in acetone. This procedure was repeated two additional times with 50 ml acetone. The extract was then filtered through Whatman #1 filter paper and evaporated

at 45°C using a rotavapor (Büchi, Switzerland). Acetone from extracts was evaporated using a vacuum SpeedVac concentrator. The hexane fraction was used to quantify the oil content in pecan. The hexane was evaporated using a rotavapor. These extracts (around 1.5 g of dried yield was obtained out of which 300 mg each was used for each replicate) were further used for quantification of the phenolics from raw pecans. A portion from the acetone fraction was used for raw pecan phenolic acid profile. The rest of the extract was further used for acid hydrolyzation and dried using SpeedVac concentrator. The dried extracts were divided into two parts (300 mg each part) and 3 ml of 1N hydrochloric acid (pH=2) was added. One part was exposed to 37°C (Normal Condition) and other was exposed to 85°C (Extreme Condition) for 1 h. The two samples were neutralized using 3-4 ml of 1N NaOH. Small fraction (5 ml) from the hydrolysis samples were extracted using ethyl-acetate (5 ml) which was used for quantification using LC-MS/MS (30 mg/ml).

Subsequently, these hydrolyzed extracts were fermented in an anaerobic chamber with microorganisms from mice feces (10 weeks old C57BL/6J mice fed with chow (normal diet). Around 1g feces were collected and homogenized in 20 ml phosphate buffer. Fresh feces were collected from mice and were used the same day. Approximately, a concentration of 10^9 cfu/ml microorganisms were aliquoted in a liquid thioglycolate nutrient broth (quantified using Mile and Misra method)[134]. The hydrolyzed pecan samples (around 80 mg/ml) were exposed to 10^9 cfu/ ml fecal microorganisms for 24 and 48 h in inoculated in 7 ml liquid thioglycolate broth. The 5 ml of the fermented samples was extracted using 5ml ethyl-acetate and the production of metabolites were analyzed using LC-MS. Ethyl-acetate was evaporated until dryness and the samples were redissolved in methanol for LCMS analysis injected 10 µl with a concentration of 10 mg/ml.

For quantification of number of microorganisms in each fermented sample, Miles and Misra [134] method was adapted. Briefly, 20 µl of fermented samples were inoculated on a blood agar plate (5% Sheep Blood in Tryptic Soy Agar (TSA) Base, 15 x 100 mm plate, Hardy Diagnostics, Ohio) and incubated for 24 h. The number of micro-organisms were manually counted using a hemocytometer.

To identify urolithin from ellagic acid:

Pure ellagic acid (Sigma, St. Louis, MO) was dissolved in 100% DMSO (Sigma, St. Louis, MO) using a heat gun and inoculated in a liquid thioglycolate nutrient broth (BD Biosciences, Franklin Lakes, NJ) keeping the final concentrations to be 100, 200 and 300 µM containing approximately, 10^9 cfu/ml. Feces of mice were dissolved in a similar manner as mentioned before. Ellagic acid standard was fermented for 48 h in presence of microorganisms from mice feces (10 weeks old C57BL/6J mice) in an anaerobic chamber (the final concentration of DMSO was 1%). 5 ml samples were extracted using 5 ml ethylacetate dried with a speedvac concentrator and redissolved in methanol and the production of metabolites were analyzed using LC-MS. A volume of 10 µl with a concentration of 3 mg/ml was injected.

Analysis of Total Phenolics (TP):

Total phenolics were determined using the method described by Swain and Hillis [135]. The pecan extract was dissolved in methanol (30 mg of dried extract/ml of methanol). Methanolic extracts (13 µl) were diluted with nanopure water (208 µl) in a 96-well microplate well, followed by the addition of 0.25 N Folin–Ciocalteu reagent (13 µl). The mixture was incubated for 3 min, and then, 1 N Na_2CO_3 (26 µL) was added. The final mixture was incubated for 2 h at room temperature in the dark. Spectrophotometric readings at 725

nm were collected using a plate reader (Synergy HT, Bio-Tek Instruments, Inc., Winooski, VT). Total phenolics were expressed as mg chlorogenic acid equivalents (CAE)/mg of crude extract.

ORAC assay:

The procedure described by Wu et al. (2004) was used for hydrophilic AC (AC_{ORAC}) was adapted to measure the ORAC. The reagents were dissolved in 75 mM phosphate buffer pH 7.4. Clear-bottom 96-well black plates (Costar #3631, Corning, Inc., Corning, NY) was used and with 25 µl of extracts (~30mg/mL) were aliquoted and incubated at 37 °C for 45 min prior to analysis. Fluorescein sodium salt (FL) (protein probe) and AAPH (free radical source) were prepared. Stock solution (FL_1) were prepared by dissolving 112.5 mg of FL powder in 50 mL of phosphate buffer. A FL (FL_2) solution was made by diluting 100 µL of FL_1 in 10 mL of buffer. FL_1 and FL_2 solutions were stored at 2 °C after preparation. FL_3 was prepared by dissolving 400 µL of FL_2 in 25 mL of buffer. After incubation of buffer at 37 °C for 45 min APPH was prepared by dissolving 260 mg of AAPH pellets. Injectors were primed with, 200 µL of FL_3 and it injected in each well followed by 75 µL aliquots of APPH solution. Fluorescence readings was measured by plate reader (Synergy HT, Bio-Tek Instruments, Inc., Winooski, VT) using excitation and emission wavelengths were 485nm and 520 nm, respectively. Readings were made at 1 min intervals during 120 min. The samples were compared against Trolox standard and a blank curve prepared from normalized data using the area under the curve. Results were expressed as µmol Trolox equivalents/g defatted kernel (µmol TE/g).

LCMS methodology:

The determination of individual compounds were performed on a Surveyor HPLC/MS system equipped with an autosampler, a Surveyor 2000 quaternary pump, and a Surveyor UV 2000 PDA detector using a C18 reverse phase (150 mm × 4.6 mm, Atlantis, Waters, Ireland; particle size = 5 µm) column connected to a LCQ Deca XP Max MS^n system (Thermo Finnigan, San Jose, CA, USA) with a Z-spray ESI source run by Xcalibur software, version 1.3 (Thermo Finnigan-Surveyor, San Jose, CA). The mobile phase flow rate was set at 0.25 ml/min, while the elution gradients were performed with solvent A, consisting of acetonitrile/methanol (1:1) (containing 0.5% formic acid); and solvent B, consisting of water (containing 0.5% formic acid). The applied elution conditions were: 0-2 min, 2% A, 98% B; 3-5 min, 5% A, 95% B; 5-7 min, 25% A, 75% B; 7-12 min, 55% A, 45% B; 12-24 min, 55%A-80%A, 24-27 min held isocratic at 80%A, 28-30min 90% A, 10 % B; 31-33 min held isocratic, 100% A; 34-40 min, 2% A, 98% B, to the starting condition. The chromatograms were monitored at 280 nm, and complete spectral data were recorded in the range 200–600 nm. ESI was performed in the negative ionization mode, nitrogen was used as sheath gas with a flow of 59 arbitrary units, and He gas was used as dampening gas. The capillary voltage, -4.17 V; spray voltage, 5kV; capillary temperature, 275°C; and tube lens voltage at -55V. Collision energies of 30% were used for the MSn analysis. A 10 µl of 10 mg/ml of extracts were injected into LC-MS.

Phenolic compounds including urolithins were quantified by using external calibration curves for Ellagic Acid and concentrations reported as ellagic acid equivalents. Standard calibration curves were made with concentrations ranging from 0.1 – 100 µg/ml (r^2 value > 0.99).

Cell culture and proliferation:

Caco-2 were cultured and grown in 100 mm dishes (Nunclon, Sigma St. Louis, MO) in DMEM (Sigma, St. Louis, MO), adding the following components to the base medium: 10% fetal bovine serum (FBS) and antibiotics (100 units/ml penicillin and 100 µg/ml streptomycin) in a humidified atmosphere with 5% CO_2 at 37°C. Cells were used at a passage of 11-15 for this study. To reach confluency it took 5-7 days.

Cell viability assay:

Caco-2 were plated at a density of 0.5x 10^5 cells/well in 96 well plate (Costar, Cambridge, MA) in growth media and allowed to adhere overnight. Then the cells were exposed for 24 h with different concentrations of urolithins A and B (10, 20 and 50 µM). Pure urolithins were dissolved in 100% DMSO and then redissolved in the growth media to reach the final concentration in the cells. Cytotoxic effects of urolithins was evaluated in Caco-2 cells using the 3-(4,5-dimethylthiazol-2-yl)-5-(3-carboxymethoxyphenyl)-2-(4-sulfophenyl)-2H-tetrazolium MTS assay (CellTiter 96 AQueous One Solution Cell Proliferation assay, Promega Corp., Madison, WI), according to the manufacturer's instructions. Briefly, 20 µl of MTS solution was added in to the wells and the quantity of formazan product was measured at 490 nm using microplate reader (Synergy HT, Bio-Tek Instruments, Inc., Winooski, VT). The quantity of formazan produced is directly proportional to the activity of mitochondrial dehydrogenase. The final percentage of DMSO per well was 0.5%.

Measurement of reactive oxygen species production (ROS):

The Caco-2 were plated at a density of 0.5x 10^5 cells/well in a 96- well black and clear bottom plates (Costar, Cambridge, MA) and cultured overnight. The cells were

stimulated by 50 µg/ml LPS for 19 h with or without 5 h pretreatment of different concentrations of urolithins A and B (10, 20 and 50 µM). The measurement of intracellular ROS production was evaluated using 2′,7′-Dichlorofluorescin diacetate (DCFA) from Sigma (St. Louis, MO). Briefly, the cell culture medium was removed by aspiration and subsequently exposing the cells to 10 µM DCFA in PBS for 30 mins. Finally, fluorescence was read at wavelengths of 485 nm for excitation and 528 nm for emission on a 96-well microplate reader (Synergy HT, Bio-Tek Instruments, Inc., Winooski, VT)

Preparation of Total RNA and Gene Expression Analysis (Real-Time qRT-PCR):

At a density of 10^5cells/well Caco-2 were seeded in 6-well plate (BD Biosciences, Franklin Lakes, NJ). Total RNA was extracted from after challenging with 50 µg/ml LPS treatment for 19 h with or without 5 h pretreatment of different concentrations of urolithins A and B (10, 20 and 50 µM) using Zymo's RNA extraction kit with DNase I treatment (purchased from Zymos research, Irvine, CA) according to the manufacturer's instructions. RNA concentration was quantified using a NanoDrop ND-1000 spectrophotometer (NanoDrop Technologies, Willmington, DE). Around 1 µg of RNA was reversed transcribed for cDNA synthesis, using the SuperScript III first-strand synthesis super mix (Invitrogen, Carlsbad, CA), following the manufacturers protocol. cDNA amplification was analyzed using a LighterCycler 480 (Roche diagnostic) and Bullseye EvaGreen qPCR master mix for iNOS, IL1B, TNFa, LXRa, IL8. Sequences of the primer used are listed in Table 4.

Statistical analysis:

The data were analyzed using ANOVA and paired Student's t-test, using the software JMP v14.0 (Cary, NC). Results are expressed as means ± standard errors (S.E). (n=3-6)

Results and Discussion:

Total microbial count:

This analysis was performed to analyze toxicity of 115 mg/ml hydrolyzed pecan extracts which were inoculated in the fecal fermentation broth with 3 replicates. As presented in the Figure 6 there were no statistical loss of micro-organisms as compared to the control samples. Fecal microorganisms at a density of 10^9cfu/ml were inoculated into the fermentation broth. After the three time points (0, 24 and 48 h) using the Miles and Misra method[134] the number of microorganisms were quantified and no statistically difference between the control and pecan exposed samples ($p<0.05$) confirmed that no cytotoxic effect took place.

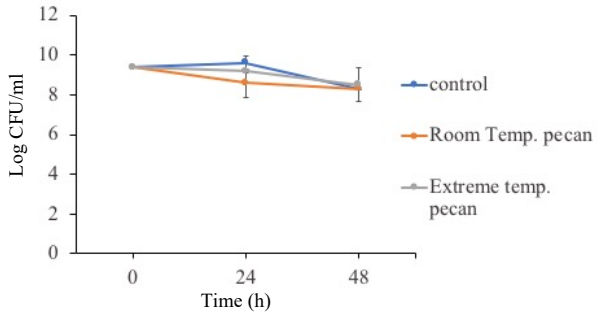

Figure 6: Quantitative evaluation of total microbial count of mice fecal microorganisms treated or not with hydrolyzed pecan pawnee extracts

Toxicity on total mice fecal microorganisms (10 weeks old C57BL/6J mice) of hydrolyzed pecan pawnee extracts at room/normal and extreme temperature, (37°C and 85°C) conditions and fermented for 0, 24 and 48 h by fecal microflora. Hydrolyzed pecan extracts did not show a decrease in microbial population through time ($p < 0.05$, $n = 3$) by a t-student analysis

Type of phenolics using LCMS:

As demonstrated with LC-MS analysis Table 1 and 2, Procyanidin B2, catechin hexoside, ellagic acid pentoside, methyl ellagic acid hexoside, methyl ellagic acid pentoside, Di-galloyl ellagic acid, ellagic acid galloyl pentoside, methyl ellagic acid galloyl pentose were identified in raw pecan pawnee samples which was similar to phenolics previously identified in the literature for pecan pawnee [17, 23, 136]. On acid hydrolysis at room temperature (37°C) similar phenolic profile was observed as the raw pecan. However, acid hydrolysis at extreme temperature (85°C), phenolic profile slightly shifted and catechin hexoside and Dimethyl ellagic acid were identified along with Procyanidin B2, ellagic acid pentoside, ellagic acid galloyl pentoside and methyl ellagic acid galloyl pentose. Furthermore, urolithin A and urolithin B were identified in fermentation samples at 24 and 48 h of fermentation with mice fecal microflora at 37 °C and 85°C in hydrolyzed sample. Table 1 and 2 show the identified peaks.

Peak **1** (14.87-14.96) showed a deprotonated ion [M-H]- m/z 577 in the negative mode ionization and yielded major fragment ion at m/z 289; which confirmed to be a procyanidin derivative. Procyanidins are the most prevalent Proanthocyanidin (PAC) found in foods, are composed of (−)-epicatechin monomers [137]. A PAC dimer with B-type linkages, procyanidin B2, was hence identified by the observed molecular ion $[M - H]^-$ at m/z 577 and due to the fragments [M-H-152]- m/z 425 and [M-H-170] m/z 407 due to the neutral loss of 152 and 170 amu [138]. Peak **1′** (15.02-15.06) gave a deprotonated ion [M-H]- m/z 331 and yielded a major fragment at [M-H-162]- m/z 169, due to the loss of a hexoside sugar and with a major base peak fragment ion of m/z 169 which corresponds to the mass of deprotonated gallic acid, the compound was identified as gallic acid hexoside. This peak **1′**

was not observed in original pecan extract, however it was observed at extreme hydrolysis (85°C), the concentration was found to be 0.0899 mg/100g of pecan. This peak was not observed in the pecan raw extract and was only observed on extreme condition hydrolysis. Peak **1a** (15.89-16.29) gave a deprotonated ion [M-H]- m/z 451 and yielded a major fragment at [M-H-162]- m/z 289; hence confirming to be a catechin derivative and hence the compound was identified as catechin hexoside. Catechins and ellagic acid derivatives are abundantly found in pecan extracts. Peak **1b** (16.30-16.33) & peak 2 (17.00) gave deprotonated ions [M-H]- m/z 463 & [M-H] m/z 433 respectively; and peaks **1b** and **2** yielded fragment $[M-H-162]^-$ m/z 301 and $[M-H-132]^-$ m/z 301 respectively due to the loss of hexose and pentose sugar and hence the peaks were identified as ellagic acid hexoside and ellagic acid pentoside respectively. Peaks **2a** (17.82-17.89) and **3** (18.69-18.82) gave [M-H]- m/z 477 and [M-H]- 447 and yielded fragments [M-H-162]- m/z 315 & $[M-H-132]^-$ m/z 315 due to the loss of hexoside and pentoside and both the peaks showed further loss of 14 amu which is due to the methyl group and gave a major fragment ion m/z 301 due to ellagic acid, hence the compounds were identified as methyl ellagic acid hexoside and methyl ellagic acid pentoside respectively. Peak 4 (19.49-19.56) and 4a (19.89) gave [M-H]- m/z 615 and [M-H]- m/z 585 and gave fragments [M-H-152] m/z 463 and [M-H-152]- m/z 433 due to the loss of galloyl moiety respectively; further loss of 162 amu resulted in the major ion 301 due to the loss of hexoside and hence the compounds were identified as di-galloyl ellagic acid and ellagic acid galloyl pentoside respectively. Peak 5 (20.36) gave [M-H]- m/z 599 and yielded fragments [M-H-152]- m/z 447 and [M-H-132]- m/z 315, due to the loss of galloyl moiety and pentoside group, the base fragment ion m/z 315 was due to

the methyl ellagic acid and hence the compound was identified as methyl ellagic acid galloyl pentose.

As also represented by Peak **6** (20.67-22.0) gave $[M-H]^-$ m/z 329 and yielded major fragment ion at m/z 315 due to the loss of methyl group and hence the compound was identified as dimethyl ellagic acid. Peak **6a** (22.17-22.19) gave [M-H]- m/z 387 and yielded a major fragment $[M-H-176]^-$ m/z 211 due to the loss of glucuronide moiety and the mass 211 amu corresponds to the Urolithin B, and it also showed UV max at 273nm and 326 nm hence the compound was identified as urolithin B-glucuronide [30] . Peak **6b** (22.3-22.5) gave UV 246nm, 280nm and 356 nm gave $[M-H]^-$ 227 and yielded MS fragments m/z 209, m/z 199, m/z 183 and m/z 113 and hence the compound was identified as Urolithin A. Intestinal microflora of mammals are able to metabolize ellagic acid and related products (the ellagitannin, punicalagin and ellagitannin-rich sources such as walnut or pomegranate extract) to produce dibenzopyran-6-one derivatives (urolithin like derivatives) [139]. Peak **7** (24.85-25.0) gave a deprotonated ion $[M-H]^-$ m/z 315 and yielded major fragment $[M-H-162]^-$ m/z 153 corresponds to the hexoside group and hence the compound was identified as protocatechuic acid hexoside.

In our experiments we observed that defatted pecan contains about (81.09% ±1.12) oil, which is similar to the amount observed by in the literature, reporting it to be around 65-75% fat content [10, 23]. The total phenolic analysis indicated that the pecan contained 60.033±19.08 mg CAE/g of defatted pecan respectively. The ORAC was measured and it was observed that pecan has 301.63±13.33 μmol Trolox equivalent/g defatted kernel. These results are in agreement with results observed by Flores-Cordova et al., (2017), Mallik et al., (2009), Villarreal-Lozoya et al. (2007) where they reported values of 62-106 mg CAE/g

defatted pecan and contains between 372 to 817 µmol Trolox equivalent/g defatted kernel which coincides with their results [21, 23, 140] These values could be influenced by the cultivar, cultivation procedures, location, climatic condition, horticultural practices, maturity and environment [23].

Table 1: Identification of chemical components from the fermented EA conc 100-300 µM after 48h

Retention time (mins)	$[M-H]^-$	MS fragments	Identification
15.91-15.93	563	443, 383, 353	Vicenin 1
17.40-17.44	449	**317**	Apigenin derivative
17.62-17.67	593	473, **383**, 353	Vicenin 2
18.39-18.43	417	**317**	Equol glucuronide
18.45-18.52	253	223, 117, **226**, 134	Diadzein
18.50-19.40	301	**165**	Ellagic acid
19.51-19.91	315	**162**	Protocatechuic acid hexoside
21.5-21.72	227	209, 199, 183, **113**	Urolithin A (UA)
23.0-23.14	211	183, **112**	Urolithin B (UB)

Table 2: Identification of compounds from raw Pecan extract, normal and extreme condition of acid hydrolysis and from the samples after fecal fermentation (peaks from figure 11-13)

Peak No	RT	M-H	MS fragments	Identification
1	14.87-14.96	577	451,425,407,**289**, 245	Procyanidin B2
1′	15.02-15.06	331	**169**, 125	Gallic acid hexoside
1a	15.89-16.29	451	289	Catechin hexoside
1b	16.30-16.33	463	301, 165	Ellagic acid hexoside
2	17.00	433	301, 165	Ellagic acid pentoside
2a	17.82-17.89	477	315, **301**	Methyl ellagic acid hexoside
3	18.69-18.82	447	315, **301**	Methyl ellagic acid pentoside
4	19.49-19.56	615	463, **301**	Di-galloyl ellagic acid
4a	19.89	585	433, 301	Ellagic acid galloyl pentoside
5	20.36	599	447, **315**	Methyl ellagic acid galloyl pentose
6	20.67-22.0	329	**315**	Dimethyl ellagic acid
6a	22.17-22.19	387	211	UB-glucuronide
6b	22.3-22.5	227	209, 199, 183, 113	Urolithin A (UA)
7	24.85-25.0	315	153	Protocatechuic acid hexoside

Phenolic concentrations:

To quantity polyphenols present in pecans, area under the chromatograms were quantified using Ellagic acid as the standard. Procyanidin B2, a condensed tannin was found to be the most abundant with a concentration of 3.32 mg/100 g defatted pecan followed by ellagic acid derivatives with a concentration of 2.3 mg/ 100g defatted pecan sample.

A combination of all derivatives of ellagic acid (Ellagic acid pentoside, Methyl ellagic acid hexoside, Methyl ellagic acid pentoside, Di-galloyl ellagic acid, Ellagic acid galloyl pentoside ,Methyl ellagic acid galloyl pentose) in raw pecan were around 3.24 mg/100g pecan which decreases on hydrolysis to 0.047 and 0.170 mg/100g in Normal condition (NC) and Extreme condition (EC) acid hydrolysis, respectively. These results are in coherence with Villarreal-Lozoya et al., 2007, where they observed extreme condition hydrolysis tend to increase the concentration of ellagic acid [23].

The occurrence of low concentrations or urolithin metabolites were found in the feces of mouse and humans after the intake of walnuts and pomegranate juice [141]. The concentrations of each phenolic compound were also calculated using ellagic acid standard. Each test was done in triplicates and chromatographs are represented in Figure 8-14. Figure 8-9 highlights concentration dependent synthesis of urolithin from pure ellagic acid fermentation. This was in coherence with the result we observed where, pure ellagic acid produced urolithins after 48 h exposure to fecal micro-organisms, as shown in figure 7. It can be observed that pure ellagic acid is being fermented and urolithin is being produced. The aim of this experiment was to demonstrate that ellagic acid is upstream responsible for production of urolithins from pecans. Thus, concluding that on exposure of pecan extracts to gut microbiota, these synthesize urolithins. This is the first report identifying the presence

of urolithin metabolites from pecans due to gut microbial fermentation. According to Larrosa et al., 2006, ellagic acid on exposure to microorganism produces urolithins[142] [143] [31] and Selma et al., 2014 identified *Gordonibacter urolithinfaciens sp* were responsible for converting ellagic acid to urolithins [143] . Plasma levels of urolithins reached a maximum concentration of 18.6 μM, after consumption of pomegranate juice containing 4.37 g ellagitannin (punicalagins)[144]. Thereby, for this investigation we used a range of concentrations, encompassing the physiological levels found in the body.

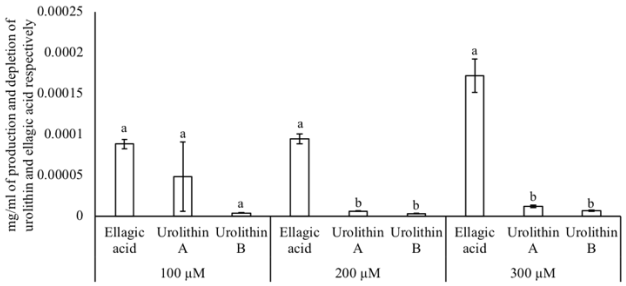

Figure 7: Production of urolithins in presence of pure ellagic acid after 48 h mice fecal fermentation.

This figure is schematic representation from the figures 8-9. Ellagic acid at a concentration of 100-300 μM inoculated in liquid thioglycolate broth for 48 h lead to synthesis of urolithin A and B. The concentrations were measured using ellagic acid standard calculated μg. extracts. Different letters denote differences ($p < 0.05$, $n = 3$) by Tukey HSD analysis

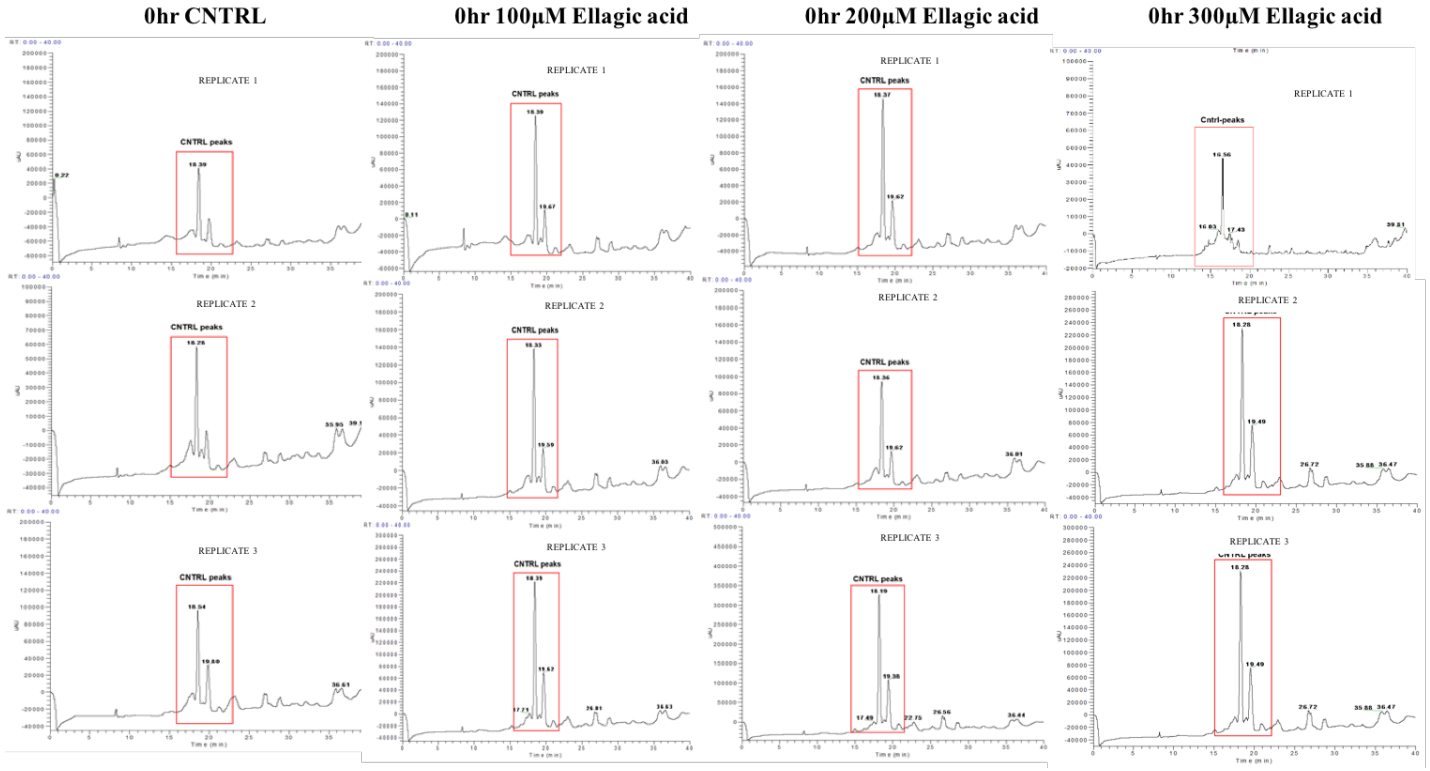

Figure 8: Chromatograms of ellagic acid (EA) at 100-300 µM in fermentation broth with mice feces at time 0h

LCMS chromatograms for ellagic acid (100-300 µM) was exposed to mice fecal microbiota inoculated in liquid thioglycolate broth at time 0 h.

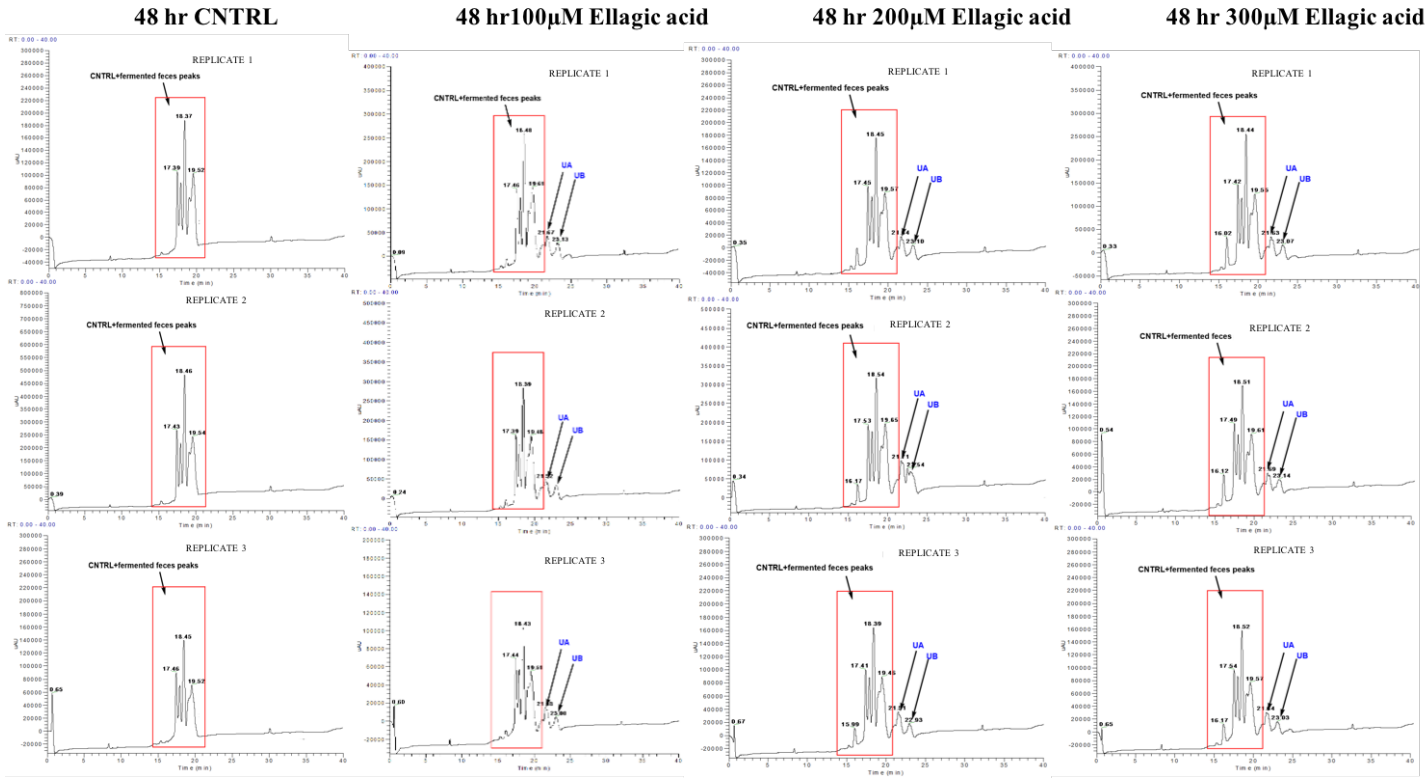

Figure 9: Chromatograms of ellagic acid (EA) at 100-300 µM in fermentation broth with mice feces after 48 h

LCMS chromatograms for ellagic acid (100-300 µM) was exposed to mice fecal microbiota inoculated in liquid thioglycolate broth for 48 h. (CNTRL: control)

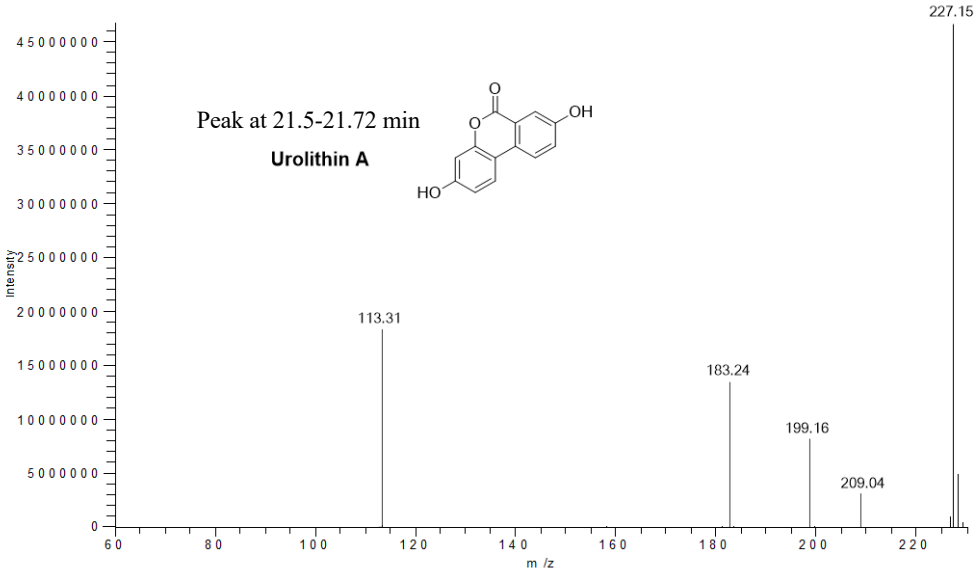

Figure 10: MS/MS fragmentation of urolithin A

From LC-MS profiles described in table 1 and figure 8, structure and mass spectral properties of urolithin A (m/z^- 227) peak identified at 21.3 min.

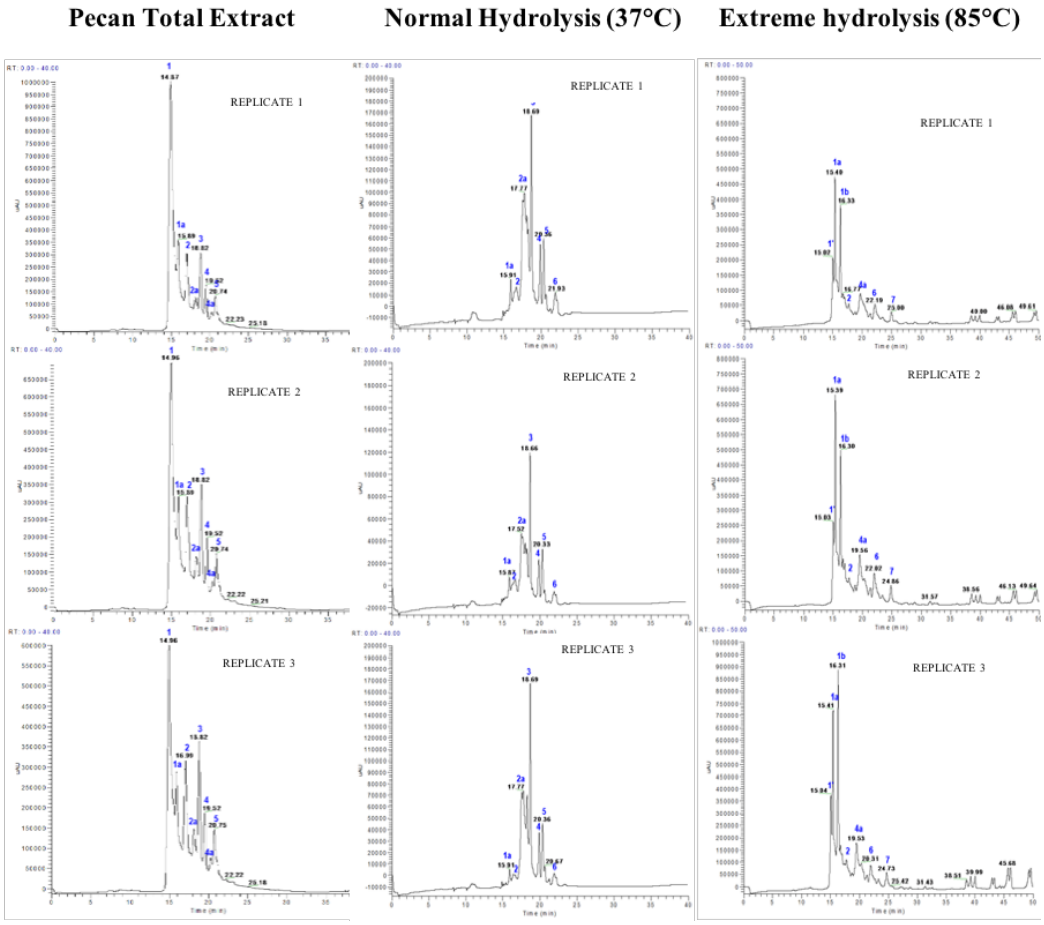

Figure 11: LCMS profiles of Total raw Pecan extract and after acid hydrolysis

LCMS chromatograms of total raw pecan pawnee, hydrolyzed at pH =2 at normal temperature, 37°C and extreme temperature, 85°C. Peak assignment of the identified phenolic compounds by LC-MS are presented in Table 2.

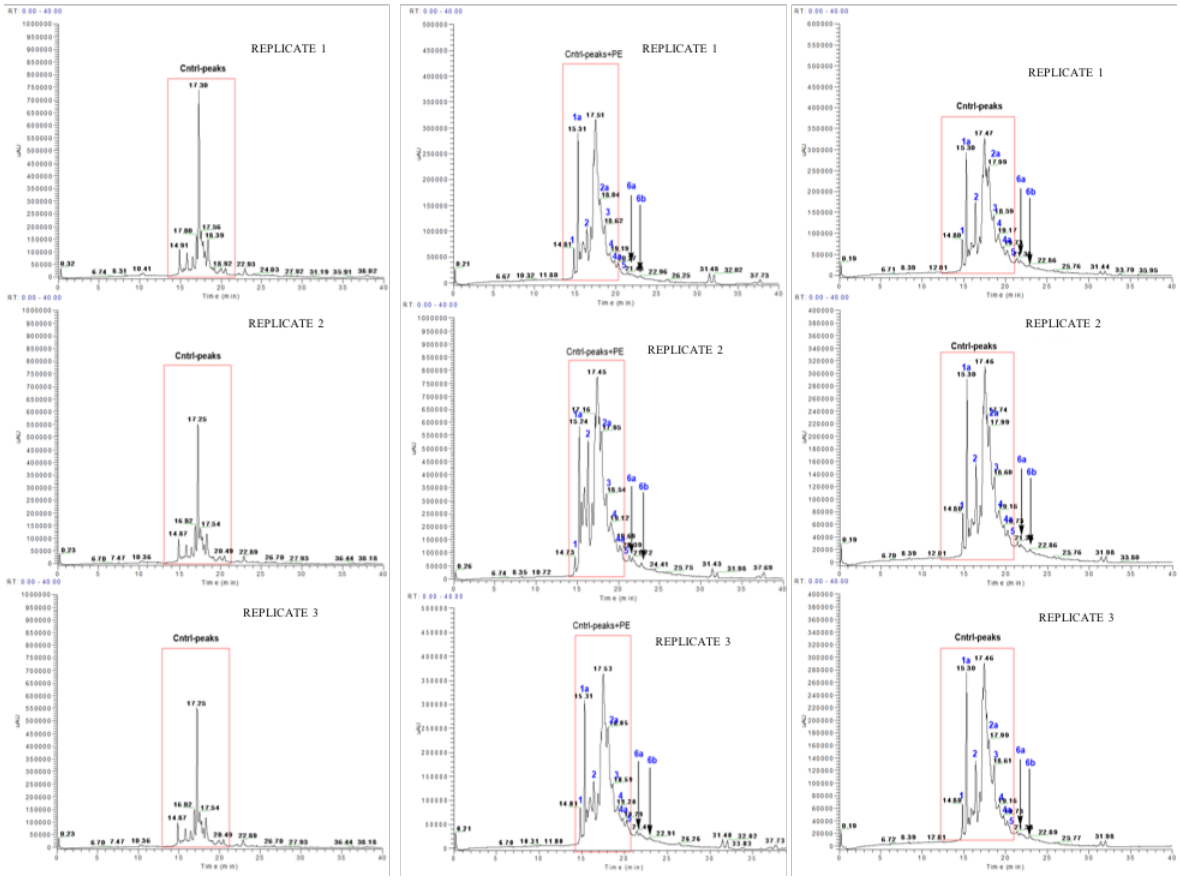

Figure 12: LCMS profiles of hydrolyzed Pecan under normal condition and after mice fecal fermentation for 24 and 48 h.

LCMS chromatograms of hydrolyzed pecan extracts at normal temperature, 37°C were exposed to mice fecal microflora at 24 and 48 h are shown and 0h represents control. Peak assignment of the identified phenolic compounds by LC-MS are presented in Table 2 and 3. 0hr control represents control which does not have any pecan extract added to it.

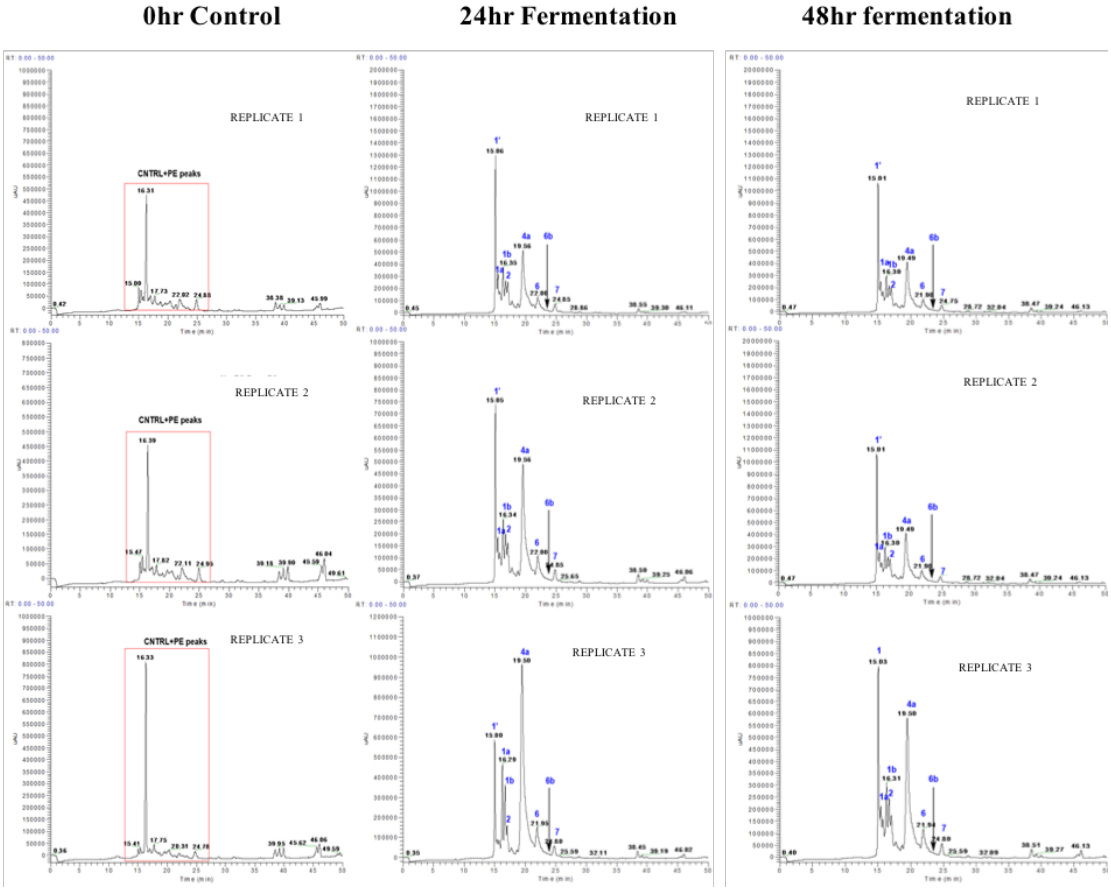

Figure 13: LCMS profiles of hydrolyzed Pecan under extreme condition and after mice fecal fermentation for 24 and 48 h.

LCMS chromatograms of hydrolyzed pecan extracts at extreme temperature, 85°C were exposed to mice fecal microflora at 24 and 48 h are shown and 0h represents control. Peak assignment of the identified phenolic compounds by LC-MS are presented in Table 2 and 3.0hr control represents control which does not have any pecan extract added to it.

Table 3: Quantification of compounds from raw Pecan extract, Normal and Extreme condition hydrolysis and from sample after fecal fermentation from the figures 11-13.

Peak No.	Identification	Raw Pecan (mg phenolics/100 g FW pecan)	Hydrolysis NC (mg phenolics/100 g FW pecan)	Hydrolysis EC (mg phenolics/100 g FW pecan)	Fermentation 24 h NC (mg phenolics/100 g FW pecan)	Fermentation 48 h NC (mg phenolics/100 g FW pecan)	Fermentation 24 h EC (mg phenolics/100 g FW pecan)	Fermentation 48 h EC (mg phenolics/100 g FW pecan)
1	Procyanidin B2	3.322 ±0.43	0.00114 ±0.0001	0.0220 ±0.0029	0.000256 ±0.0	0.00139 ±0.0001	-	-
1′	Gallic acid hexoside	-	-	0.0899 ±0.0103	-	-	0.0169 ±0.0005	0.0167 ±0.0005
1a	Catechin hexoside	1.583 ±0.69	0.00729 ±0.0009	-	0.00204 ±0.0003	0.00649 ±0.0005	0.000916 ±0.0001	0.00795 ±0.0001
1b	Ellagic acid hexoside	-	-	0.10006 ±0.0131	-	-	0.004459 ±0.0	0.000527 ±0.0
2	Ellagic acid pentoside	0.522 ±0.06	0.00564 ±0.0006	0.00404 ±0.0005	0.00123 ±0.0005	0.000985 ±0.0001	0.000551 ±0.0009	0.000381 ±0.0
2a	Methyl ellagic acid hexoside	0.090 ±0.004	0.00363 ±0.0001	-	0.0245 ±0.0005	0.004764 ±0.0007	-	-
3	Methyl ellagic acid pentoside	0.423 ±0.04	0.00395 ±0.0001	-	0.00651 ±0.0003	0.00138 ±0.0001	-	-
4	Di-galloyl ellagic acid	0.181 ±0.008	0.0152 ±0.0009	-	0.0490 ±0.0037	0.000461 ±0.0	-	-
4a	Ellagic acid galloyl pentoside	0.033 ±0.004	0.01561 ±0.0008	0.04474 ±0.0059	0.0151 ±0.0006	0.000133 ±0.0	0.0165 ±0.0001	0.1699 ±0.0004
5	Methyl ellagic acid galloyl pentose	0.095 ±0.001	0.00302 ±0.0003	-	0.00933 ±0.0007	-	-	-
6	Dimethyl ellagic acid	-	-	0.02147 ±0.0025	-	-	0.0019 ±0.0	0.0029 ±0.0
6a	Urolithin B-glucuronide				0.002566±0.0001	0.000267±0.00		
6b	Urolithin A (UA)				0.000411±0.0000	0.000113±0.0000	0.000025±0.00	0.0000372±0.0000
7	Protocatechuic acid hexoside	-	-	0.01819±0.0025	-	-	0.00182±0.0001	0.00142 ±0.0001
TOTAL PHENOLICS		6.249	0.05548	0.3004	0.1109	0.0159	0.04307	0.1998

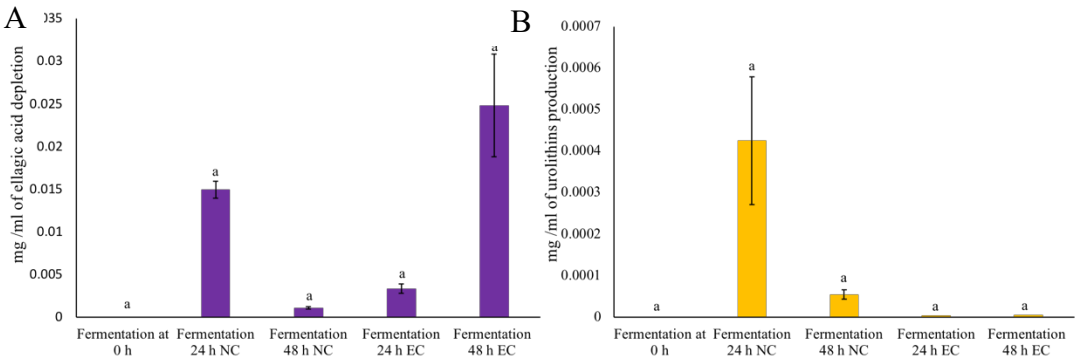

Figure 14: This figure is a schematic representation from figure 10-12 and Table 3

(A) Ellagic acid derivatives depleted when pecan pawnee (raw Pecan extract, Normal and Extreme condition hydrolysis) was exposed to mice fecal microorganism inoculated (10^9 cfu/ml) in liquid thioglycolate broth for 24 h and 48 h lead to (B) synthesis of urolithins from the ellagic acids present in pecan pawnee (raw Pecan extract, Normal and Extreme condition hydrolysis) after exposure to mice fecal microorganism inoculated in liquid thioglycolate broth for 24 h and 48 h. Different letters denote differences ($p < 0.05$, $n = 3$) by Tukey HSD analysis

Effect of urolithins A and B on cell viability:

In this study, concentrations of 10, 20 and 50 µM of urolithins A and B were exposed to Caco-2 cells. As shown in the Figure 15 compared to the control, urolithin were almost the same levels on cell viability. Thus, urolithins did not have any significant toxic effect on the cells. Hence (10 µM, 20 µM and 50 µM) of urolithin A and B were used for further analysis.

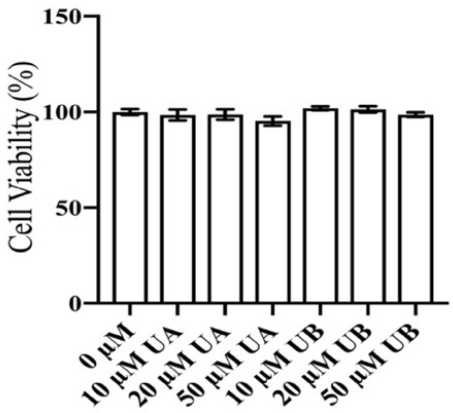

Figure 15: Effect of different concentrations of urolithin A and B on cell viability in Caco-2 cells

Colon Caco-2 cells (0.5×10^5 cells/well in 96-well culture plates) were pretreated with 0, 10, 20, 50 µM urolithin A and B for 24 h. The cell viability was measured using microplate reader (Synergy HT, Bio-Tek Instruments, Inc., Winooski, VT) with the MTS CellTiter 96®AQueous One Solution. The 0 µM is a control, indicating the pretreatment of 0.5 % DMSO in DMEM medium Data, obtained from triplicate repeats at least, are shown as mean ± SE. UA corresponds to urolithin A; UB corresponds to urolithin B. Statistical analysis was performed by the paired Student's t-test ($p < 0.05$).

Effect of urolithins A and B on intracellular ROS:

To further investigate the impact of urolithins A and B on LPS induced basal inflammation intracellular ROS levels were measured. LPS binds to TLR-4 (toll like receptor-4) and increases the levels of ROS (byproduct of the redox reaction from mitochondria and NADPH oxidases). Reactive oxygen species comprises of superoxide radical, hydrogen peroxide, hydroxyl radical and singlet oxygen species and at elevated levels they have shown to cause oxidative DNA damage, cell damage and finally apoptosis. Release of excessive free radicals and ROS during inflammation exacerbates tissue damage. ROS activates IκB/NF-κB pathway in epithelial cell. NF-κB is phosphorylated and

translocated into the nucleus where it increases the expression of pro-inflammatory genes. AP-1 is also activated by JNK phosphorylation to enhance the expression of inflammatory cytokines in Caco-2 [145].

Levels of intracellular ROS was measured using DCFA. Caco-2 were challenged with LPS for 19 h in presence or absence of pre-treatment of different concentration of urolithin A and B. As shown in the Figure 16 intracellular levels of ROS increased around 2x in the cells stimulated with 50 µg/ml LPS for 19 h as compared to the control cells, as indicated by increase in the fluorescence. The increase in the ROS levels were significantly ($p<0.05$) decreased by pretreatment of 20 µM and 50 µM of urolithin A and 10 µM urolithin B, thus, urolithin are capable of reducing intracellular ROS accumulation in LPS challenged colon cells.

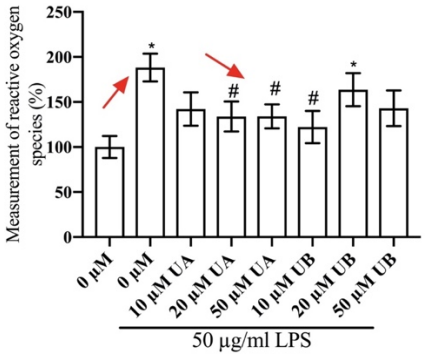

Figure 16:Effect of urolithin A and B on LPS-induced ROS production for 19 h in Caco-2 cells

Colon Caco-2 cells (0.5×10^5 cells/well in 96-well culture plates) were pretreated with 0, 10, 20, 50 µM urolithin A and B for 5 h and then stimulated with LPS (50 µg/ml) for 19 h. The levels of intracellular

ROS was measured using microplate reader (Synergy HT, Bio-Tek Instruments, Inc., Winooski, VT) with the DCFDA fluorescent dye. The 0 μM is a control, indicates the pretreatment of 0.5 % DMSO in DMEM medium in DMEM medium without any LPS stimulation. Data, obtained from triplicate repeats at least, are shown as mean ± SE. Different symbol indicate significant differences by the paired Student's t-test ($p < 0.05$). * significantly different from DMSO/control, $p<0.05$; # significantly different from LPS (50 μg/ml), $p<0.05$.

Effect of urolithins A and B on proinflammatory genes:

To determine the role of oxidative stress in inducing the expression of cytokines in Caco-2 model system, further analysis was performed by measuring the gene expression of pro-inflammatory genes (IL-8, iNOS, IL-1ß, TNFα, NFkB) as shown in Figure 17. The Caco-2 cells were stimulated with 50 μg/ml LPS for 19 h with or without pre-treatment of different concentration of urolithin A and B. Expression of genes increased by 3x, 18x, 3x, 1.4x and 2.5x for(IL8, IL-1ß, TNF-α, NFκB and iNOS, respectively in LPS treated Caco-2. All concentration of urolithin A significantly suppressed the expression of IL-1ß and IL8, whereas only 50 μM of urolithin A could suppress iNOS expression in LPS challenged cells as compared to the untreated control cells. Urolithin B at 20 μM and 50 μM decreased IL-1ß expression and 50 μM of urolithin suppressed IL8 expression in LPS stimulated cells. LPS increased the expression of NFκB, however only 50 μM urolithin A suppressed the increased levels. These results indicate that LPS induced levels of genes were suppressed mainly by urolithin A and partly by urolithin B.

To further explore the suppression molecular mechanism of urolithins, we hypothesized that anti-inflammatory activity of urolithin A and B might be mediated by promoting the expression of LXR-α. Liver X receptors (LXR) are members of nuclear hormone receptor that regulate cholesterol metabolism and have been implicated in inhibition of the inflammatory genes such as TNF α, IL-1B, iNOS etc [146] [147]. The underlying

mechanism of LXR is inadequately understood, however it has been illustrated that LXR agonists inhibits NF$\kappa\beta$ by inhibiting phosphorylation and degradation of I$\kappa\beta$ proteins, thus suppressing the NF-$\kappa\beta$ activity [148]. Here in our study we also saw upregulation of LXR-α by 20 μM and 50 μM urolithin A and 20 μM urolithin B. Urolithin A at a concentration of 50 μM have shown to downregulate the expression of iNOS and TNF-α; 10, 20 and 50 μM of urolithin A was able to downregulate IL-1β and IL-8, suggesting dual mechanism of action of urolithin A. It suppresses intracellular ROS and upregulates LXR-α facilitating downregulation of proinflammatory genes. On the other hand, 20 μM urolithin B increases the expression of LXR-α and 20 and 50 μM of urolithin B suppressed levels of IL-1β and 50 μM suppressed expression of IL-8 and TNF-α, suggesting that even though there was a partial suppression of intracellular ROS by urolithin B, it exerts its anti-inflammatory action by upregulating LXR-α.

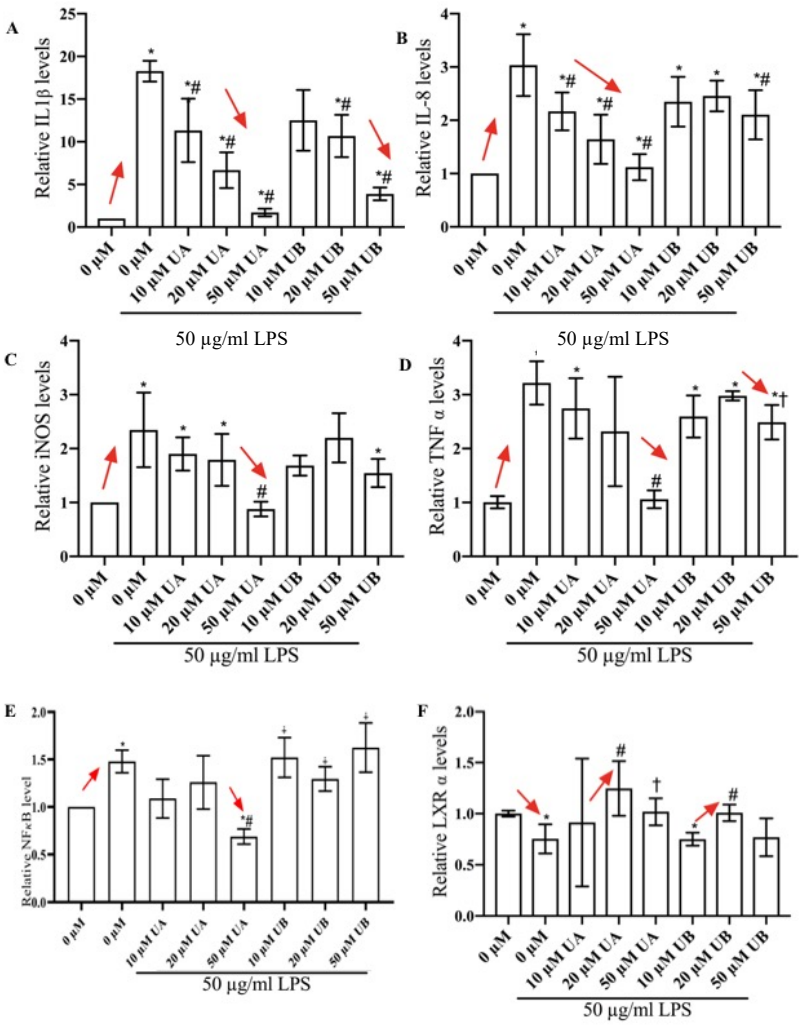

Figure 17: Effect of urolithin A and B on LPS-induced gene expression in Caco-2 cells

Colon Caco-2 cells (10^5cells/well were seeded in 6-well culture plates) were pretreated with 0, 10, 20, 50 µM urolithin A and B for 5 h and then stimulated with LPS (50 µg/ml) for 19 h. Subsequently, total RNAs were prepared and subjected to real-time qRT-PCR analysis using specific primer sets (Table 4), responsible for *IL-1 β* (a), *IL-8* (B), *iNOS* (C), *TNF-α* (D), *NFkB* (E) and *LXR-α* (F), genes. The 0 µM is a control, indicates the pretreatment of 0.5 % DMSO in DMEM medium in DMEM medium without any LPS stimulation. Data, obtained from triplicate repeats at least, are shown as mean ± SE. Different symbol indicate significant differences by the paired Student's t-test ($p < 0.05$). * significantly different from DMSO/control, $p<0.05$; # significantly different from LPS (50 µg/ml), $p<0.05$; † significantly different from LPS (50 µg/ml), $p<0.10$;┼ significantly different from DMSO/control, $p<0.10$.

Conclusion:

Figure 18 illustrates the proposed mode of action of urolithin A and B against LPS challenged Caco-2 cells. As shown in figure 16, Urolithin A ameliorates inflammation by two mechanisms, firstly, it suppresses intracellular ROS levels and thereby inhibits the downstream molecular mechanism by suppressing the NFκB induced pro-inflammatory genes. Secondly, it increases the expression of LXR-α. On the other hand, mechanism of urolithin B is by increasing expression of LXR-α, which facilitates it to impart anti-inflammatory effect as shown in Figure 17.

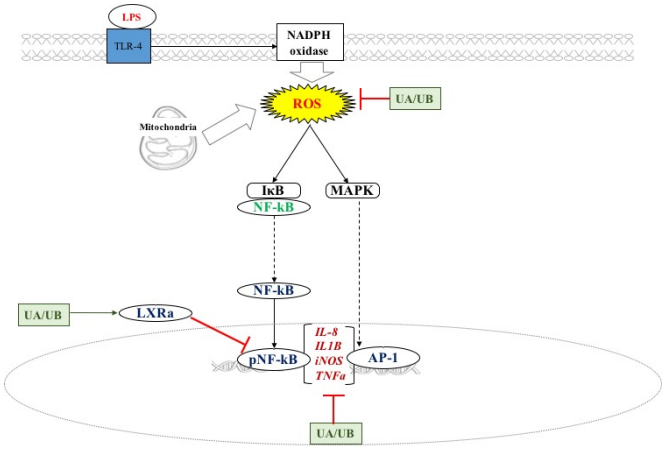

Figure 18: Anti-inflammatory role of urolithin A and B in colon Caco-2 cells

Binding of LPS to TLR4 receptor triggers a cascade of responses. ROS is generated from NOX and mitochondria. ROS mediates LPS-induced IL-1β, IL-8, iNOS, TNF α through NF κB and AP1 signaling. Urolithins A and B suppressed intracellular ROS, and thereby suppressed the action of downstream pro-inflammatory gene. Thus, suggesting that LPS mediated pathway in Caco-2 is ROS dependent. This study also demonstrates, urolithin A and B upregulates LXR α, which inhibits NFKB p65 subunit, thereby suppressing the proinflammatory genes.

CHAPTER III

MODE OF ACTION OF UROLITHINS A AND B AGAINST DIABETES IN PALMTIC ACID STIMULATED SKELETAL MUSCLE, HEPATIC AND PANCREATIC CELL MODEL SYSTEMS.

Summary:

Common causes of chronic diseases are- lack of physical activity, high body mass index (BMI) and poor nutrition (diets low in fruits, vegetables and whole grains and high in sodium, sugars and saturated fats) which culminates low grade inflammation into a pre-diseased state and finally transitions into chronic diseases such as diabetes. The aim of this chapter is to decipher the role of urolithin A and B against palmitic acid induced insulin resistance and glucose insensitivity. Insulin resistance and glucose insensitivity is an intermittent stage between pre-diseased state and diseased state. Urolithin A and B both suppressed ROS in palmitic acid stimulated hepatic cells (AML 12) and muscle cells (C2C12). Urolithins A and B also reverted the effect of glucose metabolism in muscle and liver cell. In muscle cells, it also upregulated the pAKT and pIRS protein expression and suppressed pJNK. On the other hand only urolithin B partially reversed insulin production in palmitic acid challenged pancreatic cell. However, neither urolithin A nor B could suppress levels of ROS in palmitic acid challenged pancreatic cells (βTC6) indicating urolithin B works through a non-ROS mediated mode of action. These results indicate urolithin A and B have the potential in amelioration of diabetes in invitro model by reversing insulin resistance and partially reverting glucose insensitivity.

Introduction:

Diabetes mellitus is a physiological dysfunction characterized by hyperglycemia resulting from insulin resistance, inadequate insulin secretion and excessive glucagon secretion. Obesity is speculated as one of the major instigators for insulin resistance. According to our disease model system adapted from Liu et al., 2011 [36] obesity is a pre-diseased state. It progresses due to increased levels of circulating free fatty acids leading to insulin resistance. This pathogenesis is associated with chronic inflammation such as type 2 diabetes (T2D). There are two types of diabetes- Type 1 Diabetes (T1D), classified as an autoimmune disease commonly occurs in childhood or adolescence, it is characterized by pancreatic beta cell destruction. It accounts for around 10% cases; however, its prevalence has increased over years worldwide [149].T1D, has an irreversible impact on the muscle health which can be detrimental on a long term [150].

Type 2 Diabetes (T2D), primarily occurs in presence of impaired glucose metabolism and regulation. It fosters in adulthood. It progresses with impairment in pancreatic B cells which advances in developing glucose insensitivity in pancreatic cells which triggers insulin resistance in liver and muscle.

Growing evidence has proposed that an inflammatory and oxidative stress in skeletal muscle, liver and pancreatic cells progresses to diabetes. Infiltration of immune cell and accumulation of FFAs (such as Palmitic acid) from diet, derivatives of lipids such as diacylglycerol and ceramide and elevated inflammatory cytokines are few of the potential mechanisms projected to link inflammation to diabetes in several tissues (hepatic, muscle and pancreatic B-cells)[151]. Studies have reported that stimulation of muscle cells and liver with lipopolysaccharide (LPS) and tumor necrosis α (TNF-α) elevates NFkB and

intracellular ROS levels (Frost et al. 2002; Lang et al. 2003). These elevated levels inhibit the insulin signaling pathway such as the insulin receptor, insulin receptor substrate-1 and Akt (Geng et al. 2017; Gupta et al. 2013). Thus, there is a necessity to identify and combat inflammation to ameliorate the insulin resistance and glucose insensitivity to reverse diabetes.

Insulin resistance and signaling:

Impairments in the insulin perception and activating insulin-dependent substrate proteins IRS-1 and IRS-2 mediated signaling pathway have been implicated in the progression of metabolic disorders such as diabetes. This cellular pathway involves insulin to stimulate protein kinases including the serine/threonine kinase Akt and protein kinase C (PKC) which phosphorylate a Ser/Thr residues in the insulin receptor substrate (IRS) proteins which are convoluted in the perceiving insulin to start the metabolic responses, such as translocation of glucose transporter and metabolism of glucose. Furthermore, other non-insulin dependent kinases such as AMP-activated protein kinase, c-Jun N-terminal protein kinase and G protein-coupled receptor kinase 2 are activated and phosphorylate insulin responsive substrates. Chronic diseases such as diabetes has been associated in development of hyperinsulinemia, dyslipidemia; in progression of these diseases, strong link has been found with defects in IRS, Akt and PKC kinases. Evidence have indicated environmental and cellular disturbances in lipid and glucose metabolism tissues such as pancreatic, hepatic and myocytes to contribute in development of insulin resistance. Inability to transport or metabolize glucose projects a shift in various cellular pathways. Especially in liver and muscles; impairment in liver to transport, dispose and control glucose production *via* gluconeogenesis, storage of glucose as glycogen, *de novo* lipogenesis causes the tissue to

progress the body into a state of hyperglycemia which proceeds into diabetes. Impairment in insulin pathway often progresses to diabetic myopathy. It is diabetic complication which develops and contributes in affecting muscle metabolic health. Evidences have demonstrated that it progresses with defects in glucose uptake, muscle contraction and accumulation of muscle progenitor cells leading to declining skeletal muscle health in diabetes mellitus.

Polyphenols from pecan bark have shown to ameliorate diabetes [15]. As seen in the previous chapter, pecan on exposure to gut microbiota synthesizes urolithins. There are different types of urolithins that are formulated inside the gut- urolithin A, B, C, D, and isourolithin. These urolithins have shown to placate diabetes by increasing the insulin release in pancreatic b-cells [152].. This study observed that a combination of urolithins could increase insulin release when pancreatic cells were induced with glucose insensitivity. The aim of this investigation is to study the role of urolithin A and B against palmitic acid induced insulin resistance and glucose insensitivity and proposing a mode of action.

Materials and Methods:

Materials:

The following chemicals were used in the experiments: Lipopolysaccharide (LPS), 2′,7′-Dichlorofluorescin diacetate (DCFA), Dulbecco's Modified Eagle's Medium (DMEM)/low glucose, penicillin/streptomycin mixture, 0.25% Trypsin-EDTA solution, DMSO, ITS mixture and Fetal Bovine Serum (FBS) were purchased from Sigma (St. Louis, MO). Glucose and sodium bicarbonate were purchased from Acros Organics (Fair Lawn, NJ) and sodium bicarbonate from Mallinckrodt Chemicals (Phillipsburg, NJ), respectively. The CellTiter 96® AQueous Non-Radioactive Cell Proliferation Assay kit was purchased from Promega (Madison, WI). The cell lines- AML 12, hepatocyte (cell line CRL-2254™),

Beta-TC-6, pancreatic beta cells (cell line CRL-11506™) and C2C12, muscle myoblast (cell line CRL-1772™) were obtained from the American Type Culture Collection (ATCC, Rockville, MD)

Cell culture and proliferation:

AML12:

Hepatic AML12 cells were left with DMEM-HAM'S F12/10% FBS medium supplemented with ITS mixture from Sigma (St. Louis, MO), cell were culture and grown in 100 mm dishes in DMEM (Sigma, St. Louis, MO), adding the following components to the base medium: 10% fetal bovine serum (FBS) and antibiotics (100 units/ml penicillin and 100 μg/ml streptomycin) in a humidified atmosphere with 5% CO_2 at 37°C. The cells were used at a passage of 3-9 in this study and it takes 4-5 days to reach confluency.

C2C12:

Muscle C2C12 cells were grown in 100 mm dishes supplemented with Low glucose DMEM/10% FBS medium and antibiotics (100 units/ml penicillin and 100 μg/ml streptomycin) in a humidified atmosphere with 5% CO_2 at 37°C. Medium was replaced every 2-3 days. Once cells were confluent, they were cultured with low glucose DMEM/10% Horse serum medium for four days, to induce myoblast formation. The cells were used at a passage of 3-9 in this study and it takes 3-4 days to reach confluency.

βTC6:

Pancreatic βTC6 cells were grown in 100 mm dishes supplemented with high glucose DMEM/15% inactivated FBS medium supplemented with antibiotics (100 units/ml penicillin and 100 μg/ml streptomycin) in a humidified atmosphere with 5% CO_2 at 37°C.

until they reached around 80% confluency. Medium was replaced every 2-3 days. The cells were used at a passage of 3-9 in this study.

Cell viability assay:

AML 12, BTC6, C2C12 were plated at a density of $5x10^4$, $5x10^4$, $1x10^4$ cells/ well respectively in 96 well plate in complete media and allowed to adhere for overnight. Then the cells were exposed to 24 h with different concentrations of urolithins A and B (10, 20 and 50 μM). Cytotoxic effects of urolithins was evaluated in AML 12, βTC6, C2C12 cells using the 3-(4,5-dimethylthiazol-2-yl)-5-(3-carboxymethoxyphenyl)-2-(4-sulfophenyl)-2H-tetrazolium MTS assay (CellTiter 96 AQueous One Solution Cell Proliferation assay, Promega Corp., Madison, WI), according to the manufacturer's instructions. Briefly, 20 μl of MTS solution was added in to the wells and the quantity of formazan product was measured at 490 nm using microplate reader (Synergy HT, Bio-Tek Instruments, Inc., Winooski, VT). The quantity of formazan produced is directly proportional to the activity of mitochondrial dehydrogenase. The final percentage of DMSO per well was 0.5%.

Measurement of reactive oxygen species production (ROS):

The AML 12, BTC6, C2C12 cells were plated at a density of $5x10^4$, $5x10^4$, $1x10^4$ cells/ well respectively in a 96- well black and clear bottom plates (Costar, Cambridge, MA) and cultured overnight. The cells were stimulated by 0.25 mM Palmitic acid for 12, 24 and 48 h with or without 18 h co-incubation with different concentrations of urolithins A and B (10, 20 and 50 μM). The measurement of intracellular ROS production was carried out using 2′,7′-Dichlorofluorescin diacetate (DCFA). Briefly, the cell culture medium was removed by aspiration and subsequently exposing the cells to 10 μM DCFA in PBS for 30 mins. Finally, fluorescence was read at wavelengths of 485 nm for excitation and 528 nm for

emission on a 96-well microplate reader (Synergy HT, Bio-Tek Instruments, Inc., Winooski, VT)

Measurement of Glucose uptake in AML12 and C2C12 cells:

Cells were seeded at a density of 10^5 cell/well (C2C12 and AML12) in 6-well plates, after reaching confluency, cells were stimulated with 0.25 mM palmitic acid for induction of insulin-resistance. After exposure to palmitic acid the cells were co-incubated with urolithin A and B for additional 18 h. Subsequently, the cells were exposed to 100 nM of insulin and 2 mM metformin (as a positive control) for 30 mins and 1h respectively. Then the cell culture was washed two times with warm PBS. Glucose concentrations was determined with a glucose assay kit from Abcam (cat. no. ab65333). Briefly, the cells were lysed using the assay buffer provided by the kit and the internal glucose was measured against the glucose standards curve.

Protein extraction and western blot preparation for C2C12 and AML12 cells:

C2C12 and AML 12 were seeded at a density of $5x10^5$ and $1x10^5$cells/well respectively in 6 well plate (BD Biosciences, Franklin Lakes, NJ). They were challenged with 0.25mM PA treatment for 24 h. Then co-incubated 18 h with or without different concentrations of urolithins A and B (50 μM). Subsequently, the cells were exposed to 100 nM of insulin and 2mM metformin (as a positive control) for 30 min and 1 h respectively. Before lysing the cells were washed twice with DPBS and then lysed using M-PER buffer (Pierce, California) supplemented with protease and phosphatase inhibitors. Concentrations of protein was determined by the Pierce BCA protein assay kit (Thermo Fisher Scientific, Rockford, IL). 25 μl of 2 mg/ml protein samples for muscle and 1 mg/ml protein for liver were loaded on a gel with a pre-stained, broad-range, molecular weight protein marker (Bio-

Rad, California). Proteins were fractionated by electrophoresis using 10 % polyacrylamide gels. The proteins on the gels were transferred by wet blotting over a PVDF membranes (Millipore, Bedford, MA). The membranes were blocked using 5% skim milk in Tris-buffered saline with 1% Tween-20 (TBS-T) for 1 h by gentle shaking. Membranes were then incubated overnight with a specific primary antibody against pJNK, pAKT, pIRS (1:1000) and Actin (1:1000) at 4 °C. The membranes were washed three times with TBS-T and incubated for 2 h at room temperature with the secondary antibody conjugated with horseradish peroxidase (HRP) at 1:5000 dilution. Protein specific bands were developed employing a SuperSignal West Femto enhanced chemiluminescence (ECL) western blotting detection kit (Pierce, Thermo Fisher Scientific, Inc., Rockford, IL). The signals were detected by ChemiDoc XRS (Bio-Rad Laboratories, Hercules, CA). The captured bands were quantified utilizing densitometry with ImageJ software (NIH, Bethesda, MD). After visualization, the primary antibody was removed using stripping buffer. Then it was blocked with 5% skim milk in Tris-buffered saline for overnight and then another primary antibody was used on the same membrane.

Quantification of insulin secretion in ßTC6:

ßTC6 cells were seeded in 96-well plates with growing medium (DMEM, 1mM glucose and 15% FBS). Cells were cultured for an additional day. For insulin resistance induction, medium was replaced with fresh medium and 0.25 mM palmitic acid was added and incubated for 48 h. Subsequently co-incubated with urolithin A and B for additional 18 h hours in the growing medium with 0.25 mM palmitic acid. In all cases, the medium was removed on the day of the experiment, and the cells washed two times with warm KRB medium (119 mM NaCl, 4.74 mM KCl, 2.54 mM $CaCl_2$, 1.19 mM $MgSO_4$, 1.19 mM

KH_2PO_4, 25 mM NaHC03, 10 mM HEPES [pH 7.4], 0.1 % BSA) and incubated with 200 µL of KRB at 37 C for 60 min. At the end of the incubation, cells were washed with warm KRB medium and then incubated with KRB containing 20 mM glucose for 1h at 37°C. The supernatant was collected, and insulin was measured by ELISA using mouse insulin as a standard (Millipore, MI). Following the manufacturer's instructions.

Statistical analysis:

The data were analyzed ANOVA and paired Student's t-test, using the software JMP v 14.0 (Cary, NC). Results are expressed as means± standard errors (S.E) where n=3-6.

Results and Discussion:

Effect of urolithins A and B on cell viability:

In this study, 10, 20 and 50 µM of urolithins A and B were exposed to AML 12, B-TC-6, and C2C12 cells. MTS assay demonstrates that 10, 20 and 50 µM of urolithins A and B did not have any significant cytotoxic effect on the cell viability. As shown in Figure 19, urolithins treated cells were almost the same levels as controls, indicating that urolithins did not have toxic effect to the any of the cell lines with (p-value>0.05). Thus, these concentrations were used for the following experiments.

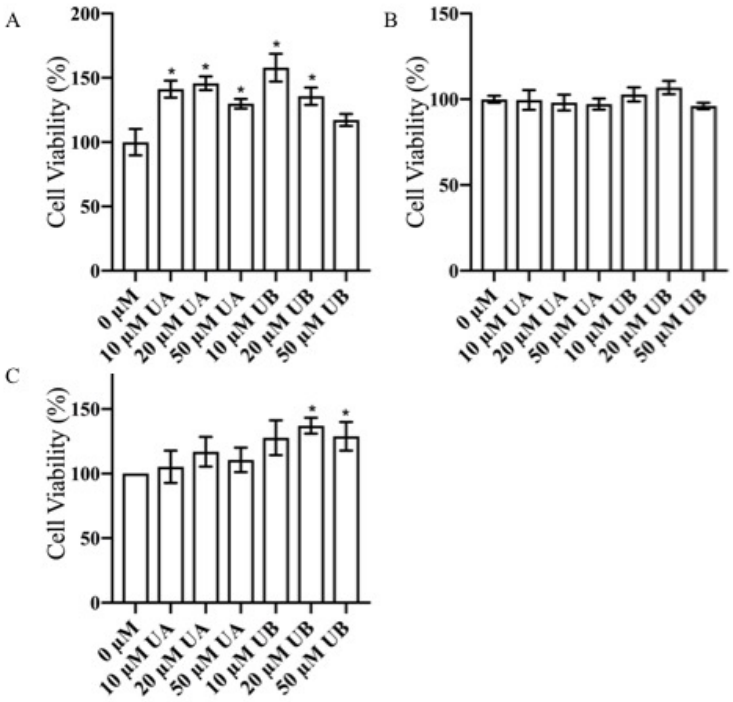

Figure 19: Effect of different concentrations of urolithin A and B on cell viability

Muscle C2C12 (A), hepatic AML12 (B) and pancreatic βTC6 (C); $5x10^4$, $5x10^4$, $1x10^4$ cells/ well respectively were treated with 0, 10, 20, 50 µM urolithin A and B for 24 h. The cell viability was measured using microplate reader (Synergy HT, Bio-Tek Instruments, Inc., Winooski, VT) with the MTS CellTiter 96®AQueous One Solution. The 0 µM is a control, indicating the pretreatment of 0.5 % DMSO in DMEM Data, obtained from triplicate repeats at least, are shown as mean ± SE. Different symbol indicate significant differences by the paired Student's t-test ($p < 0.05$). * significantly different from DMSO/control, $p<0.05$. UA corresponds to urolithin A; UB corresponds to urolithin B.

Effects of urolithin on Palmitic acid-induced ROS production in C2C12 cells:

To investigate whether anti-inflammatory effects of urolithin A and B are mediated through modulation of ROS production, intracellular levels of ROS was measured. Palmitic acid increases levels of ROS and stimulates different pathways by phosphorylating JNK, p38, MAPK and NFkB[153].

Differentiated C2C12 cell were stimulated with 0.25 mM palmitic acid for 12, 24 and 48 h and then co-incubated with different doses of (10, 20 and 50 μM) urolithin A and B. As shown in Figure 20, cells challenged with palmitic acid increased 1.16X, 1.4X and 1.5X times the levels of intracellular ROS levels after 12, 24 and 48 h. Urolithin A at a concentration of 20 and 50 μM suppressed ROS after 12 h and this suppression continued even after 24 and 48 h. Moreover, 10 μM urolithin A suppressed ROS at 24 and 48 h. Positive control metformin also suppressed levels of ROS after 24 and 48 h stimulation of palmitic acid. However, urolithin B did not suppress Palmitic acid stimulated intracellular ROS levels in C2C12 cells.

There are plethora of reports supporting association of obesity and inflammation. Fatty acid intake through diet or through increased levels in the serum due to an obesity state have demonstrated to have impact on insulin resistance. In coherence with our results, curcumin has shown to suppress levels of intracellular ROS in palmitate challenged C2C12 cells. In another study, levels of ROS were attenuated by oleate in palmitic acid treated myocytes[117]. These results indicate a strong role of inflammation induced increased levels of ROS in causation of insulin resistance.

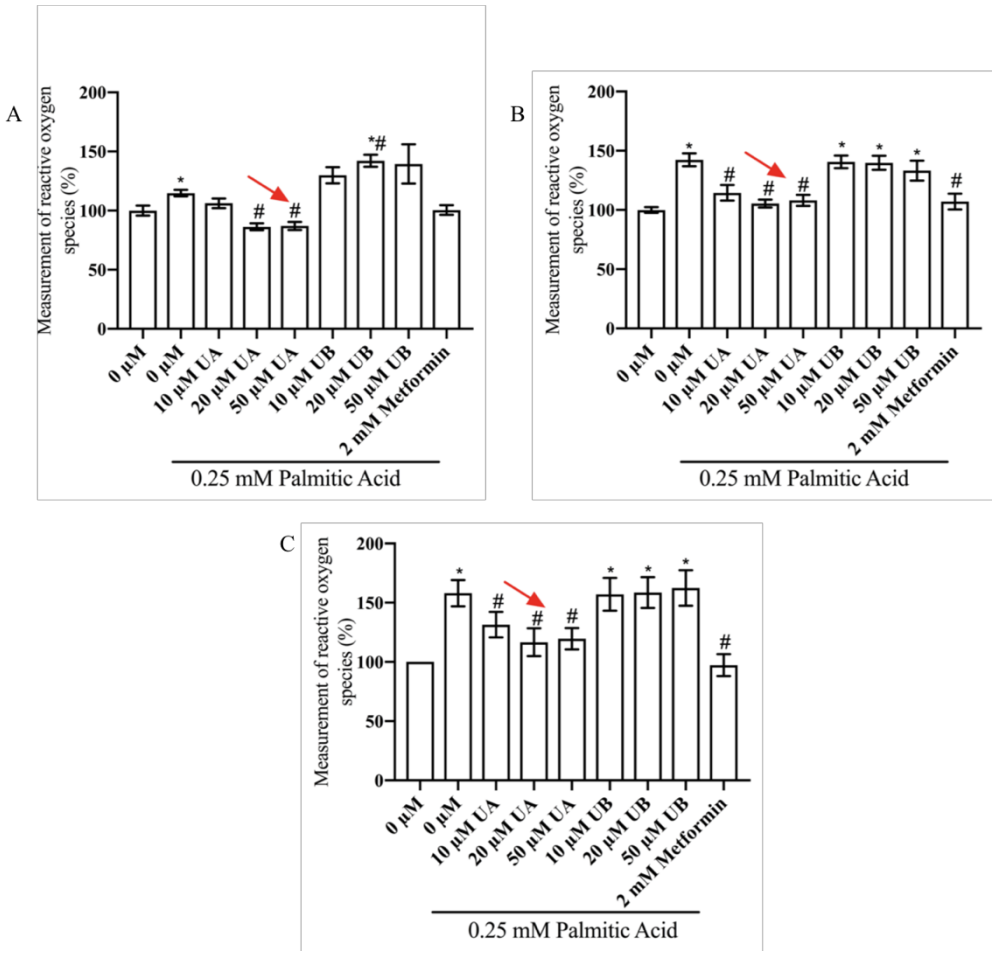

Figure 20: Effect of urolithin A and B on Palmitic acid-induced ROS production in muscle C2C12 cells through time

Muscle C2C12 (0.5×10^5 cells/well in 96-well culture plates) were exposed to 0.25 mM Palmitic acid for 12 h (A), 24 h (B) and 48 h (C) and subsequently co-incubated with 0, 10, 20, 50 µM urolithin A and B. The levels of intracellular ROS were measured using microplate reader (Synergy HT, Bio-Tek Instruments, Inc., Winooski, VT) with the DCFDA fluorescent dye. The 0 µM is a control, indicates the pretreatment of 0.5 % DMSO in DMEM medium in DMEM medium without any palmitic acid stimulation. Data, obtained from triplicate repeats at least, are shown as mean ± SE. Different symbol indicate significant differences by the paired Student's t-test ($p < 0.05$). * significantly different from DMSO/control, $p<0.05$; # significantly different from 0.25 mM Palmitic acid, $p<0.05$.

Effects of urolithin on Palmitic acid-induced Glucose uptake in C2C12 cells:

Insulin resistance progresses by decreasing the insulin stimulated glucose uptake and utilization. C2C12 cells perceive insulin and insulin binds to insulin receptor and phosphorylates three key tyrosine molecules on insulin receptor. After phosphorylation insulin receptor substrate (IRS-1) phosphorylates and activates p85 regulatory subunit of phosphatidylinositol-3kinase (PI3K) and activates catalytic subunit p110 which leads to activation of phosphotidyinositol-3,4,5, triphosphate. This activates protein kinase B (Akt) and phosphorylates AKT substrate 160 (AS160), leading to translocation of GLUT-4 to the cell membrane which facilitate glucose uptake. Reports have demonstrated that palmitate downregulated glucose uptake in C2C12 cells[154-155]. The results in our study were in coherence with literature wherein we observed palmitic acid impaired the perception of insulin causing decrease in glucose uptake. Interestingly, 50 µM Urolithin A reversed insulin resistance and significantly increased glucose uptake compared to untreated cells with added insulin and positive control metformin as shown in Figure 21. Similar results were observed by Hetta et al., 2017 where Eruca sativa leaf extracts increased the basal glucose uptake to insulin controls and metformin [156]. This suggests that urolithin A has the potential of reversing the insulin resistant state. However, urolithin B was not proficient in upregulating glucose uptake in palmitic acid stimulated insulin resistant cells.

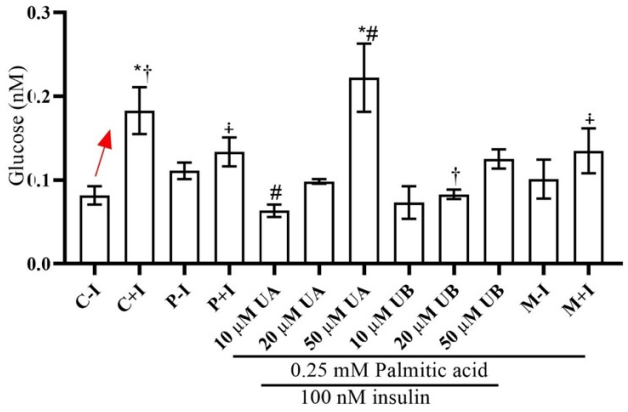

Figure 21: Effect of urolithins on measurement of Glucose uptake in muscle C2C12 cells

Muscle C2C12 cells were seeded at a density of 5x105 cell/ well and exposed to 0.25 mM of palmitic acid for 24 h to induce insulin resistance. It was co-incubated with palmitic acid and different concentrations of urolithin A and B for additional 18 h. Before measurement of glucose the samples were exposed to100 nM of insulin for 30 mins. The C-I is a control, indicates the pretreatment of 0.5 % DMSO in DMEM medium in DMEM medium without any 0.25 mM Palmitic acid stimulation, C+I indicate a control pretreatment of 0.5 % DMSO in DMEM medium in DMEM medium without any 0.25 mM Palmitic acid stimulation but treated with insulin; P-I is a control which is treated with palmitic acid and no additional insulin is added, P+I is a palmitic acid control where additional insulin is added. M-I corresponds to metformin control which is stimulated with 0.25 mM palmitic acid and is treated with 2 mM metformin for 60 min without any addition of insulin. M+I correspond to metformin control which is stimulated with 0.25 mM palmitic acid and is treated with 2 mM metformin for 60 min with addition of insulin. Data, obtained from triplicate repeats at least, are shown as mean ± SE. Different symbol indicate significant differences by the paired Student's t-test ($p < 0.05$). * significantly different from DMSO/control (C-I), $p<0.05$; # significantly different from 0.25 mM Palmitic acid, $p<0.05$(P+I); † significantly different from 0.25 mM Palmitic acid (P+I), $p<0.10$; ǂ significantly different from DMSO/control, $p<0.10$(C-I).

Effects of urolithin on Palmitic acid-induced protein expressions in insulin resistant C2C12 cells:

Skeletal muscle is a major location for glucose disposal. It accounts for around 80% insulin-stimulated glucose uptake. Defects in insulin sensitivity in skeletal muscle progresses to decrease in postprandial glucose uptake. Continuous manifestation precedes the onset of T2DM which could potentially progress in development of metabolic syndrome[157]. Insulin resistance is a complex cascade where defects in insulin mediated glucose oxidation or glycogen synthesis or glucose uptake takes place. To understand the underlying mechanism of urolithins in palmitic acid stimulated C2C12 cells we measured the expression of pAKT, pIRS and pJNK.

Incubation with palmitic acid for 24 h induced an insulin resistant state and C2C12 was unable to perceive insulin. Untreated cells when stimulated with insulin increase the levels of pAKT and pIRS, demonstrating that insulin pathway is activated by phosphorylation of IRS and Akt. pAKT is responsible for mediation of translocation of glucose transporter. Palmitic acid impairs the perception of insulin and decreases pIRS and pAKT. It induces PKC/NFkB inflammation pathway in diabetic or insulin resistant C2C12. Palmitic acid increases the accumulation of lipid intermediates such as ceramides and diacylglycerol. Consequently, activates JNK and interrupts the insulin signaling by inactivating IRS-1 and AKT insulin pathway. IRS or insulin receptor substrate serves as a key mediator in stimulating insulin in the peripheral tissues such as skeletal muscle and liver by activating downstream enzymes such as PI3K,PDK-1 and AKT. Saturated fatty acid such as palmitic acid upregulates JNK which further downregulates the expression of pIRS and pAKT in presence of insulin and thus initiating insulin resistance.

As observed in Figure 22, pJNK is upregulated in presence of palmitic acid. Presence of insulin in palmitic acid treated cells is incapable in reversing the effect of palmitic acid, thus demonstrating a state of insulin resistance. These results were in coherence where Salvado et al., 2013 and Li et al., 2015 observed insulin resistance leading to suppression of pAKT and pIRS in presence of palmitic acid. Bioactive compounds like silibinin and oleate were able to upregulate the expression of pAKT and pIRS thereby attenuating the insulin signaling inhibition [158-159]. In this investigation we observed that bioactive metabolite from pecan urolithin A at a concentration of 50 μM was able to revert the insulin resistance induced by palmitic acid by statistically suppressing the protein expression of pJNK and upregulating the expression of pIRS and pAKT. On the other hand, 50 μM urolithin B upregulated the expression of pIRS and pAKT and thus suppressed insulin resistance however could not suppress the increased expression of pJNK. More investigation is needed to understand the mechanism of urolithin B.

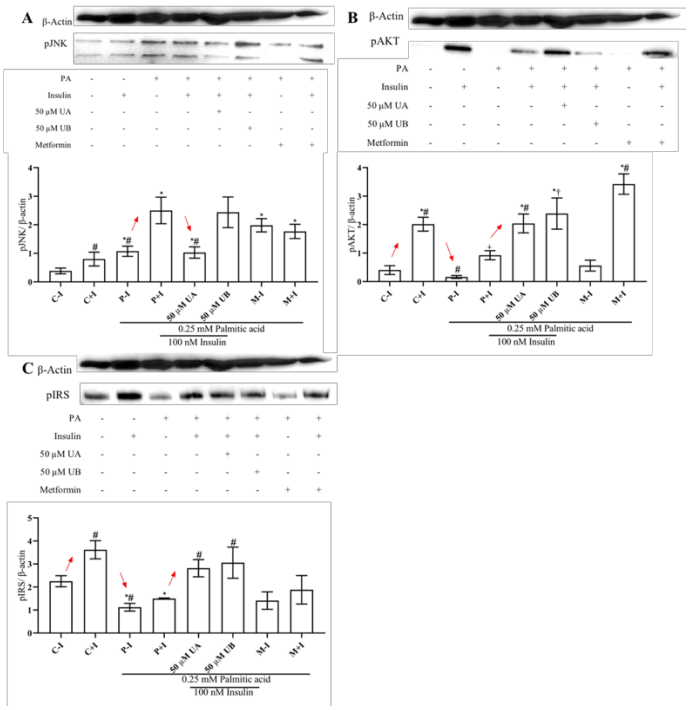

Figure 22: Effects of urolithin on Palmitic acid-induced protein expressions in muscle C2C12 cells

Muscle C2C12 cells (5x105cells/ well were seeded in 6-well culture plates) were challenged with 24 h with 0.25 mM Palmitic acid, followed by coincubation with 50 µM urolithin A and B for 18 h . Subsequently, total protein from cell lysates were subjected to SDS-PAGE and Western blot analysis using specific antibodies against pJNK (A), pAKT (B) and pIRS(C). The C-I is a control, indicates the pretreatment of 0.5 % DMSO in DMEM medium without any Palmitic acid stimulation. C+I indicate a control pretreatment of 0.5 % DMSO in DMEM medium without any 0.25 mM Palmitic acid stimulation but treated with insulin; P-I is a control which is treated with palmitic acid and no additional insulin is added, P+I is a palmitic acid control where additional insulin is added. M-I corresponds to metformin control which is stimulated with 0.25 mM palmitic acid and is treated with 2 mM metformin for 60 min without any addition of insulin. M+I correspond to metformin control which is stimulated with 0.25 mM palmitic acid and is treated with 2 mM metformin for 60 min with addition of insulin. Data, obtained from triplicate repeats at least, are shown as mean ± SE. Different symbol indicate significant differences by the paired Student's t-test ($p < 0.05$). * significantly different from DMSO/control (C-I), $p<0.05$; # significantly different from 0.25 mM Palmitic acid, $p<0.05$(P+I).

Effects of urolithin on Palmitic acid-induced ROS production and glucose uptake in AML 12 cells:

Increased levels of palmitic acid levels lead to intramyocellular lipid accumulation in humans which transition to obesity that is a causation and pathogenesis of hepatic insulin resistance. It is well known that occurrence of insulin resistance is first observed in liver, followed by muscle and lastly in adipocytes. Insulin resistance in hepatocytes leads to defect in glycogen synthesis (production of glycogen from glucose) and increase in gluconeogenesis (production of glucose) [74, 151, 160].

To understand the influx of FFA on hepatic cells and whether anti-inflammatory effects of urolithin A and B are mediated through modulation of ROS production, intracellular levels of ROS was measured in AML 12 cells. In coherence with the report in literature, wherein palmitate increased levels of intracellular ROS after 12, 24 and 36 h [74-75, 151]. We also observed, (figure 23) an increase in 1.2X, 1.4X and 1.5X times levels of intracellular ROS after 12, 24 and 48 h respectively in palmitic acid challenged AML 12 cells. Palmitic acid binds to Free fatty acid receptor. As shown in Figure 23 the positive control metformin suppressed ROS levels and as suspected urolithin A suppressed the levels of ROS after 12, 24 and 48 h. In case of urolithin B, 10 μM and 50 μM suppressed levels of ROS after 24 and 48 h. For understanding the role of urolithins on gluconeogenesis, we also measured glucose production in AML 12 cells. The results in our study were in coherence with the literature wherein we observed that, in insulin stimulated untreated cells basal levels of glucose was produced whereas palmitic acid impaired the perception of insulin and increased the levels of glucose production as shown in Figure 24 [74-75, 151]. Interestingly, all doses of urolithins were able to suppress elevated glucose levels.

These results also demonstrate that palmitic acid impairs the perception of insulin in a ROS mediated mechanism. Urolithin A and B downregulated ROS and therefore were able to suppress glucose production.

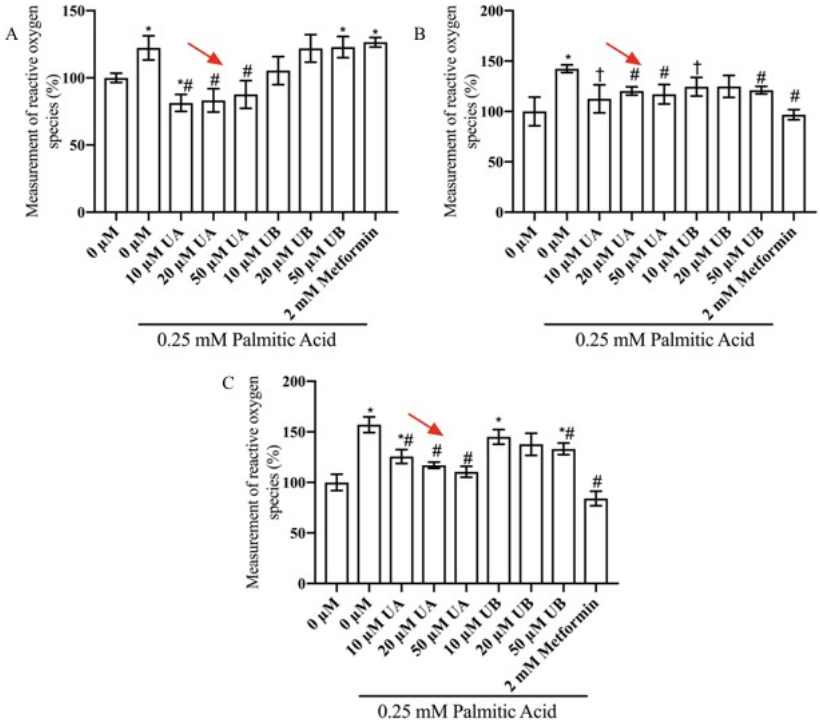

Figure 23:Effect of urolithin A and B on Palmitic acid-induced ROS production in hepatic AML 12 cells through time

Hepatic AML 12 cell (0.5×10^4 cells/well in 96-well 0.2% gelatin culture plates) were challenged with palmitic acid (0.25 mM) for 12 h (A), 24 h (B) and 48 h (C) and then co-incubated with 0, 10, 20, 50 µM urolithin A and B and PA for 18 h. The levels of intracellular ROS were measured using microplate reader (Synergy HT, Bio-Tek Instruments, Inc., Winooski, VT) with the DCFDA fluorescent dye. The 0 µM is a control, indicates the pretreatment of 0.5 % DMSO in DMEM medium without any LPS stimulation. Data, obtained from triplicate repeats at least, are shown as mean ± SE. Different symbol indicate significant differences by the paired Student's t-test ($p < 0.05$). * significantly different from DMSO/control, $p<0.05$; # significantly different from 0.25 mM Palmitic acid, $p<0.05$; † significantly different from 0.25 mM Palmitic acid, $p<0.10$ ǂ significantly different from DMSO/control, $p<0.10$.

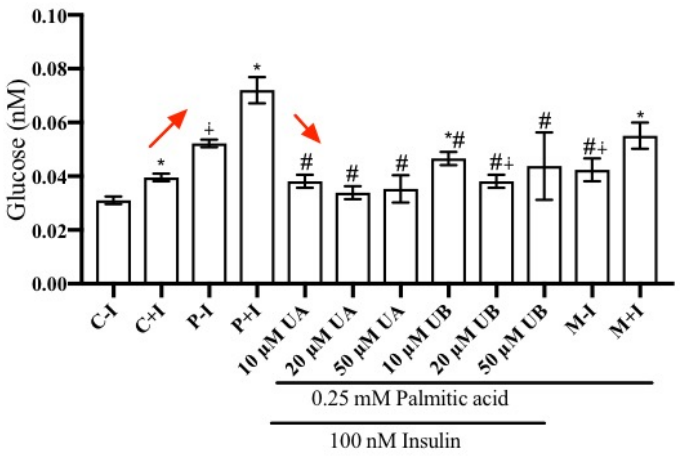

Figure 24: Effect of urolithins on measurement of Glucose uptake in hepatic AML12 cells

Hepatic AML 12 cells were seeded into 6 well 0.2% gelatin coated plate at a density of 10^5 cells/well They were exposed to 0.25 mM of palmitic acid for 24 h to induce insulin resistance and co-incubated with palmitic acid and different concentrations of urolithin A and B for additional 18 h. Before measurement of glucose the samples were exposed to100 nM of insulin for 30 mins. The C-I is a control, indicates the pretreatment of 0.5 % DMSO in DMEM medium without any 0.25 mM Palmitic acid stimulation, C+I indicate a control pretreatment of 0.5 % DMSO in DMEM medium without any 0.25 mM Palmitic acid stimulation but treated with insulin; P-I is a control which is treated with palmitic acid and no additional insulin is added, P+I is a palmitic acid control where additional insulin is added. M-I corresponds to metformin control which is stimulated with 0.25 mM palmitic acid and is treated with 2 mM metformin for 60 min without any addition of insulin. M+I correspond to metformin control which is stimulated with 0.25 mM palmitic acid and is treated with 2 mM metformin for 60 min with addition of insulin. Data, obtained from triplicate repeats at least, are shown as mean ± SE. Different symbol indicate significant differences by the paired Student's t-test ($p < 0.05$). * significantly different from DMSO/control (C-I), $p<0.05$; # significantly different from 0.25 mM Palmitic acid, $p<0.05$(P+I);+ significantly different from DMSO/control, $p<0.10$(C-I).

Effects of urolithin on Palmitic acid-induced protein expressions in insulin resistant AML 12 cells:

Studies have found association between free fatty acid intake especially saturated fatty acid such as palmitic acid and low consumption of polyunsaturated fat in causation of insulin resistance. One approach in linking palmitic acid to insulin resistance is through oxidative stresses. Elevated levels of ROS production leads to changes in the intracellular signaling which progresses to insulin resistance, hyperglycemia, development, and progression of diabetes complications. ROS damages the cells by oxidizing DNA, protein, and lipid and activating stress-sensitive intracellular signaling pathways, such as NF-kB, p38MAPK, and JNK.

As observed in Figure 25 palmitic acid induces insulin resistance in liver cells and cells are not perceiving insulin. This is in coherence with reports in the literature where presence of free fatty acids like palmitic acid induces insulin resistance, which is evident when the protein expression of phosphorylated AKT and IRS is downregulated in presence of palmitic acid [161]. Nevertheless, 50 μM urolithin A and B upregulated the expression of pIRS and pAKT and thus showing a potential mechanism of suppressed insulin resistance. These results demonstrate that urolithins are a potential candidate for suppressing insulin resistance in hepatocytes.

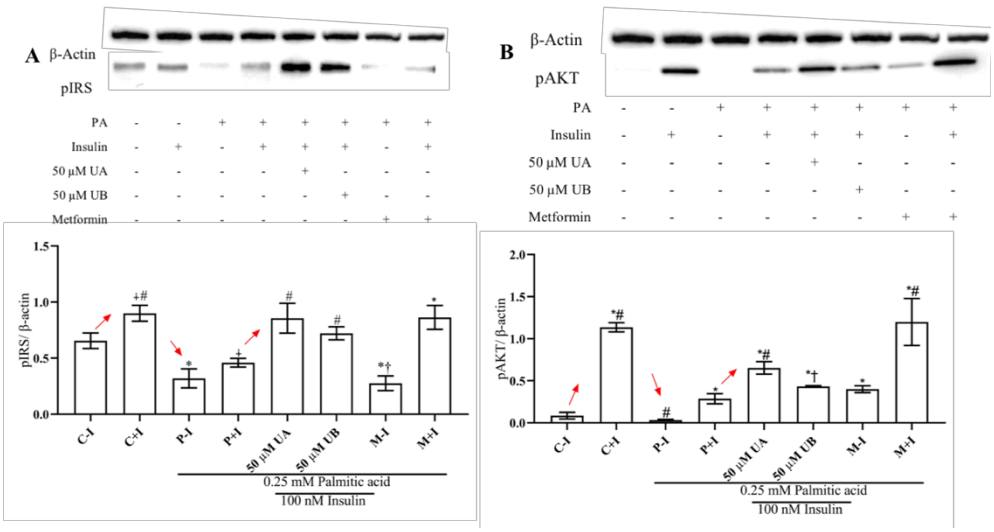

Figure 25:Effects of urolithin on Palmitic acid-induced protein expressions in liver AML 12 cells

Liver AML12 cells (1x10^{5}cells/ well were seeded in 6-well culture plates) were challenged with 24 h with 0.25 mM Palmitic acid, followed by coincubation with 50 µM urolithin A and B for 18 h . Subsequently, total protein from cell lysates were subjected to SDS-PAGE and Western blot analysis using specific antibodies against pIRS (A) and pAKT (B). The C-I is a control, indicates the pretreatment of 0.5 % DMSO in DMEM medium without any Palmitic acid stimulation. C+I indicate a control pretreatment of 0.5 % DMSO in DMEM medium without any 0.25 mM Palmitic acid stimulation but treated with insulin; P-I is a control which is treated with palmitic acid and no additional insulin is added, P+I is a palmitic acid control where additional insulin is added. M-I corresponds to metformin control which is stimulated with 0.25 mM palmitic acid and is treated with 2 mM metformin for 60 min without any addition of insulin. M+I correspond to metformin control which is stimulated with 0.25 mM palmitic acid and is treated with 2 mM metformin for 60 min with addition of insulin. Data, obtained from triplicate repeats at least, are shown as mean ± SE. Different symbol indicate significant differences by the paired Student's t-test ($p < 0.05$). * significantly different from DMSO/control (C-I), $p<0.05$; # significantly different from 0.25 mM Palmitic acid, $p<0.05$(P+I); † significantly different from 0.25 mM Palmitic acid (P+I), $p<0.10$; ┼ significantly different from DMSO/control, $p<0.10$(C-I).

Effects of urolithin on Palmitic acid-induced ROS production in BTC6 cells:

To investigate anti-inflammatory effects of urolithin A and B are mediated through modulation of ROS production, intracellular levels of ROS was measured in β-cells. Free Fatty Acids (FFA) such as palmitic acid has been considered as an antecedent in development of diabetes and impairment of β cells. Palmitic acid causes perturbation in Ca^{++} homeostasis and increases ROS [162]. Elevated levels of ROS causes DNA, lipid, RNA and protein damage and is also implicated in pathogenesis of chronic diseases such as cancer, diabetes and cardiovascular diseases [163]. Reports from literature suggest that incubation of pancreatic β cells with palmitate increases the levels of ROS after 48 h[160, 164]. Thereby for this investigation we stimulated β TC6 cells with palmitic acid for 24 and 48 h. As expected, palmitic acid significantly increased the intracellular ROS levels in β TC6 cells and the positive control metformin was proficient in suppressing it (Figure 26). However, none of the doses of urolithin A and B were adept to suppress the intracellular ROS levels in β TC6 cells as shown in Figure 24. Thus, suggesting urolithins were unable to suppress oxidative stress in palmitic acid stimulated β cell.

Effect of urolithins on insulin secretion in glucose insensitive pancreatic beta cells:

T2D is characterized by glucose insensitivity caused by β cells dysfunction and insulin resistance in liver and muscle.

As observed, exposure of palmitic acid for 48 h lead to glucose insensitivity and addition of glucose did not reverse the process confirming there was glucose insensitivity and positive control metformin reversed the process (Figure 27). These results were in coherence with the results obtained by Patanè et al., 2000 [107] where metformin upregulated the insulin release in fatty acid stimulated glucose insensitivity. Urolithin A was unable to

reverse the glucose insensitivity developed by palmitic acid however 50 µM of urolithin B partially increased the level of insulin secretion as compared to palmitic acid treated cells.

Both urolithin A and B could not suppress ROS, however 50 µM urolithin B partially increased insulin secretion showing that urolithin B functions in a ROS independent mechanism however more investigation is required to understand the mechanism for urolithin A .

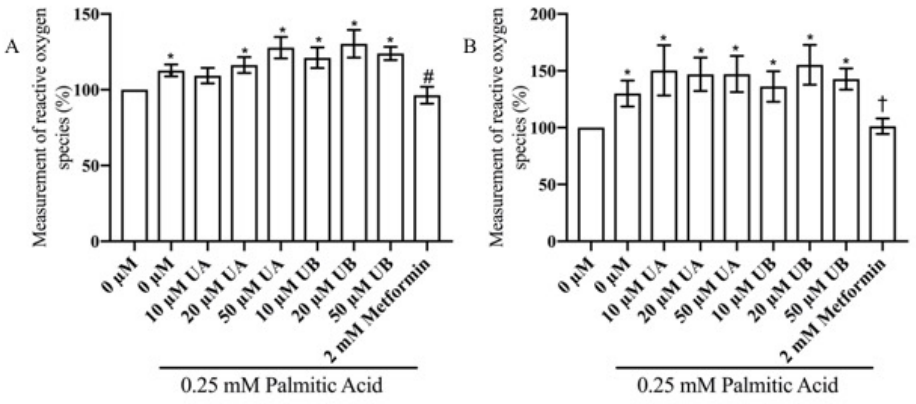

Figure 26:Effect of urolithin A and B on Palmitic acid-induced ROS production in pancreatic βTC6 cells through time

Pancreatic βTC6 ($1x10^4$ were seeded in 96-well culture plates) were stimulated with Palmitic acid (0.25 mM) 24 h (A) and 48 h (B) and then coincubated with palmitic acid and 0, 10, 20, 50 µM urolithin A and B for 18 h. The levels of intracellular ROS were measured using microplate reader (Synergy HT, Bio-Tek Instruments, Inc., Winooski, VT) with the DCFDA fluorescent dye. The 0 µM is a control, indicates the pretreatment of 0.5 % DMSO in DMEM medium without any 0.25 mM Palmitic acid stimulation. Data, obtained from triplicate repeats at least, are shown as mean ± SE. Different symbol indicate significant differences by the paired Student's t-test ($p < 0.05$). * significantly different from DMSO/control, $p<0.05$; # significantly different from 0.25 mM Palmitic acid, $p<0.05$; † significantly different from 0.25 mM Palmitic acid , $p<0.10$.

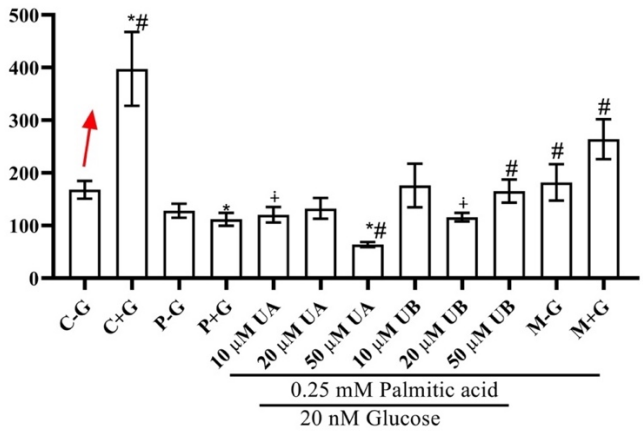

Figure 27: Effect of urolithin A and B on Palmitic acid induced glucose insensitivity in secretion of insulin in pancreatic βTC6 cells.

Pancreatic βTC6 cells were seeded into 6 well plate at a density of 10^5 cells/well They were exposed to 0.25 mM of palmitic acid for 48 h to induce glucose insensitivity and co-incubated with palmitic acid and different concentrations of urolithin A and B for additional 18 h. Before measurement of glucose the samples were exposed to 20 nM of glucose for 60 mins. The C-G is a control, indicates the pretreatment of 0.5 % DMSO in DMEM medium without any 0.25 mM Palmitic acid stimulation, C+G indicate a control pretreatment of 0.5 % DMSO in DMEM medium without any 0.25 mM Palmitic acid stimulation but treated with glucose; P-G is a control which is treated with palmitic acid and no additional glucose is added, P+G is a palmitic acid control where additional glucose is added. M-G corresponds to metformin control which is stimulated with 0.25 mM palmitic acid and is treated with 2 mM metformin for 60 min without any addition of glucose. M+G correspond to metformin control which is stimulated with 0.25 mM palmitic acid and is treated with 2 mM metformin for 60 min with addition of glucose. Data, obtained from triplicate repeats at least, are shown as mean ± SE. Different symbol indicate significant differences by the paired Student's t-test ($p < 0.05$). * significantly different from DMSO/control (C-G), $p<0.05$; # significantly different from 0.25 mM Palmitic acid (P+G), $p<0.05$; † significantly different from 0.25 mM Palmitic acid (P+G), $p<0.10$; ┼ significantly different from DMSO/control, $p<0.10$ (C-G).

Conclusion:

There are three conclusions drawn from this study:

- In C2C12 cells: As demonstrated in the investigation, urolithin A has more antioxidant, anti-inflammatory and anti-diabetic properties than urolithin B. Urolithin A significantly suppressed intracellular levels of ROS and expression of pJNK and increased glucose uptake. Whereas both urolithins upregulated expression of pAKT and pIRS. As shown in Figure 28.

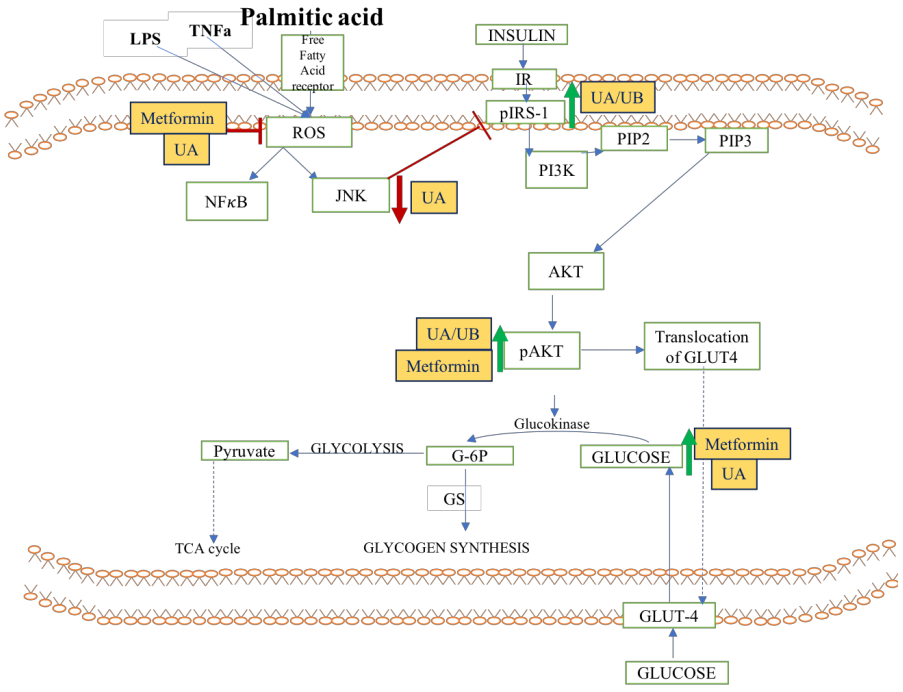

Figure 28: Anti-diabetic effect of urolithins A and B in muscle C2C12 cells

Palmitic Acid binds to FFA receptor and increases oxidative stresses by upregulating reactive oxygen species. ROS activates JNK mediated pathway inhibiting expression of insulin receptor substrate (IRS-1). Thus, downregulating phosphorylation of Akt and further decreasing the glucose uptake. As

demonstrated in the investigation, urolithin A and metformin significantly suppressed intracellular levels of ROS, Urolithin A significantly suppressed intracellular levels of ROS and expression of pJNK and increased glucose uptake. Whereas both urolithins A and B upregulated expression of pAKT and pIRS.

- In AML 12: It can be concluded from this investigation that both urolithin A and B significantly suppressed intracellular levels of ROS and glucose and upregulated expression of pAKT and pIRS levels in Palmitic acid stimulated insulin resistant hepatocytes as shown in Figure 29. However, more investigation is required to understand the underlying mechanism of action.

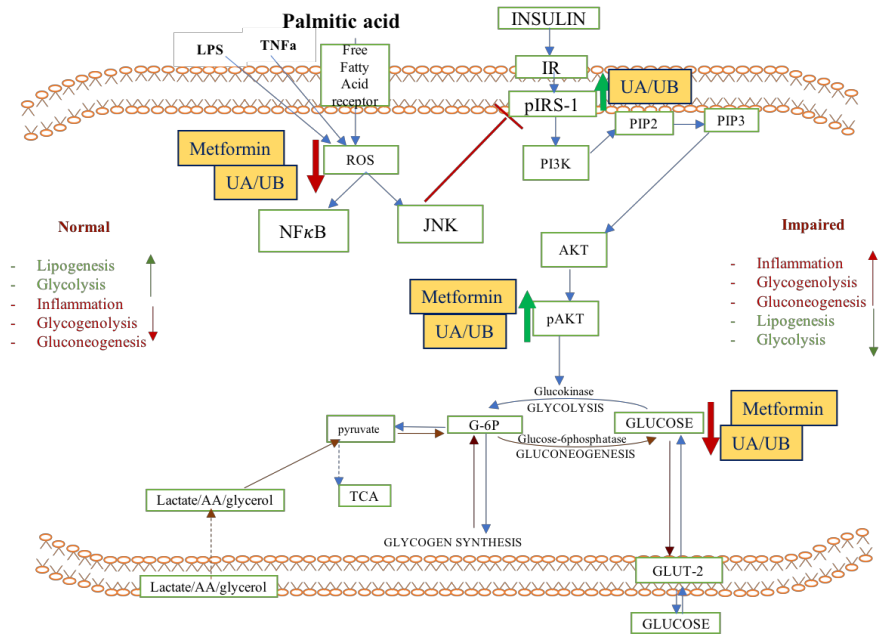

Figure 29: Anti-diabetic effect of urolithin A and B in hepatic AML 12 cell

Palmitic Acid binds to FFA receptor and increases oxidative stresses by upregulating reactive oxygen species. JNK inhibits insulin receptor substrate (IRS-1). Thereby, it downregulates phosphorylation of Akt and increases gluconeogenesis. Thus, there is an increase in the glucose production inside the cell.

As demonstrated in the investigation, urolithin A and B and metformin significantly suppressed intracellular levels of ROS, decreased glucose production in Palmitic acid stimulated insulin resistant hepatocyte. Also, urolithin A and B significantly upregulated expression of pAKT and pIRS levels in Palmitic acid stimulated insulin resistant hepatocytes.

- In βTC-6: Urolithin A did not have any effect on intracellular levels of ROS and insulin secretion, however 50 µM urolithin B partially increased the insulin secretion in Palmitic acid stimulated glucose resistant β-cells. However, more investigation is required to understand the underlying mechanism of action as shown in Figure 30.

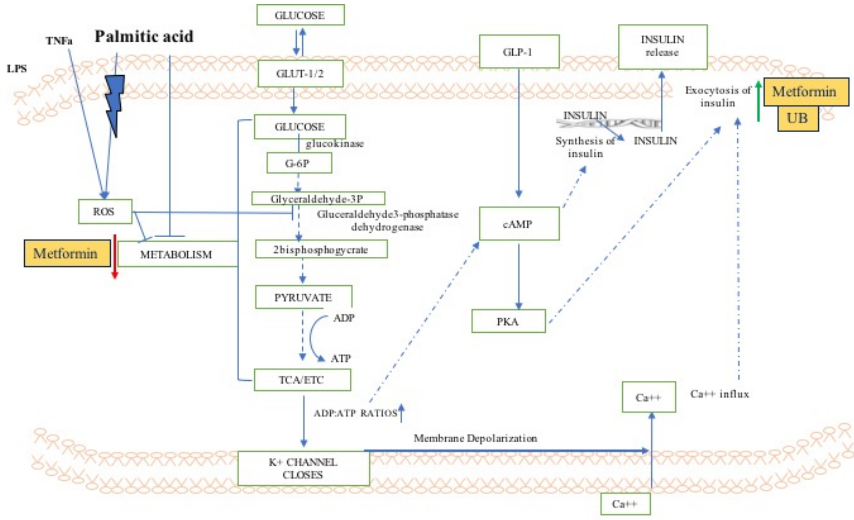

Figure 30: Anti-diabetic effect of urolithin A and B in pancreatic βTC6 cell

Palmitic Acid binds to FFA receptor and increases oxidative stresses by increasing reactive oxygen species. ROS inhibits the glucose metabolism pathway affecting the glucose sensitivity of B-cells. In a normal cell, glucose is transported inside the pancreas by GLUT-2, it undergoes glycolysis, oxidative metabolism which generates adenosine triphosphate (ATP) This increased ATP's leads to closure of ATP-sensitive K+-channels ($K_{ATP\text{-}channels}$). Allowing the calcium ions to seep inside the cell which facilitate insulin release. Elevated Ca^{2+} triggers exocytotic release of insulin granules. GLP-1 and ATP promotes formation of cAMP, amplifying secretion via protein kinase A (PKA). As demonstrated in the investigation, urolithin B and metformin significantly increases the secretion of insulin.

CHAPTER IV

MODE OF ACTION OF UROLITHINS A AND B AGAINST INFLAMMATION IN AN LPS AND TNF-α STIMULATED ENDOTHELIAL HUV-EC CELL MODEL SYSTEM

Summary:

Atherosclerosis in combination with chronic diseases like chronic inflammation, obesity and diabetes leads to metabolic syndrome. It is a leading cause of death which is characterized by dysfunction in endothelial cells (HUVEC). This work aims at accessing the in-vitro effects of ellagitannin derived metabolites of colonic origin on inflammation on primary human umbilical vein endothelial cell (HUVEC). Urolithin A and B were tested at a concentration of 50 μM on LPS and TNF α stimulated cells. Results indicate that urolithin A and B suppressed ROS in LPS challenged cells while not affecting pro-inflammatory genes. On the other hand, Urolithin A and B suppressed VCAM-1, MCP-1 and ESEL-1 in TNF α stimulated cells by both upregulating LXR α and ROS suppression by only UA. Thus, indicating that atherosclerosis process could be attenuated by urolithin A and B. These results also suggest that LPS and TNF stimulate inflammation in HUVEC cells in distinct mechanisms, while the former is basically ROS mediated the latter is through a dual mode of action including a ROS dependent and independent mechanism.

Introduction:

The key to sustain a balance in the cardiovascular system is by maintaining the homeostasis equilibrium of the body. It is maintained by a hierarchy of genetic and epigenetic systems interacting inside humans. A disequilibrium state contributes to the

pathogenesis of chronic disease such as atherosclerosis and its comorbid complications, myocardial infarction, and stroke.

Endothelial cells (EC) are thin lining of cells that maintain and regulate vessel wall permeability, described as physical barrier between circulating blood and tissues. It plays a physiological role in regulating vascular tone, proliferation, permeability of inflammatory inducers, and infiltration of leukocytes and is a key component in suppressing vascular inflammatory process [165-167]. In 1965, Swiss anatomist Wilhelm His coined the term "Endothelium" to differentiate them from epithelium cells [165-166]. Endothelial cell or endothelium is a ubiquitous cellophane like membrane that aligns throughout the circulatory system [167]. They are highly metabolically active, and the cell phenotypes are differentially regulated in space and time giving them their unique EC heterogeneity. An adult human is composed of approximately $6x10^{13}$ endothelial cells which weighs around 1 kilogram, and spreads around a surface area of $7m^2$.[168] Along with being the gate-keeper, endothelium is also recognized to have the presence of membrane receptors, proteins (such as, growth factors, coagulant, and anticoagulant proteins), lipid transporting particle (such as, low-density lipoprotein), nitrous oxide and serotonin, and endothelin-1[167].

Endothelial cell dysfunction is a lexicon attributed to the causation of cardiovascular diseases. The pathogenesis includes unavailability of endothelial derived nitric oxide, alteration of the anticoagulant and anti-inflammatory properties, impairment in vascular growth and lesions in the lining of endothelial cells. Endothelial cell dysfunction progresses to atherosclerosis, a chronic inflammatory disease which aggravates to stroke, myocardial infarctions and various other co-morbidities [167, 169].

Steps involved in transmigration:

During immune surveillance leukocytes migrates to the site of inflammation by breaching the endothelial lining. This migration is achieved by- rolling, attachment, and finally transmigration. The first step is rolling, when leukocyte accelerates on the luminal side of the endothelium. This step is regulated by selectins. Selectins are class of cell adhesion molecules expressed by endothelial cells. They bind to the protein present on leukocytes and facilitate rolling. Rolling is also mediated by interaction between leucocyte integrins and vascular cell adhesion molecules-1[166]. The second step is binding or attachment [170]. Selectins and leukocytes interaction stimulates endothelial cells to increase intracellular adhesion molecules-1 (ICAM-1) and vascular cell adhesion molecules-1 (VCAM-1) which initiates binding to leukocytes[171]. ICAM and VCAM are immunoglobulins present on endothelial cells in basal levels and upon stimulation they induce binding or attachment step. Leukocyte signals chemokine which arrests leukocytes on the surface of endothelial cells. The arrested leukocyte signals for chemotaxis on the surface of the endothelial cells. Then leukocytes progresses to the last step which is transmigration which is directed by the chemoattractant gradient allowing the leukocytes to migrate through endothelium extracellular matrix to the tissue of inflammation [166, 172].

Understanding the disease model:

Evidences in literature suggest significant role of bacterial lipopolysaccharide (LPS) in development of atherosclerotic lesions. In mice models, weekly injections of LPS lead to increase in NFκB along with increase in pro-inflammatory genes triggered increase atherosclerotic lesions [173-174]. LPS also causes oxidative stresses by increasing the reactive oxygen species, which have also been implicated to play a role in pathogenesis of

cardiovascular diseases [79, 175]. ROS is crucial in redox regulation of signal transduction, proliferation, differentiation and apoptosis[79, 176]. Increased levels of ROS have been implicated with endothelial dysfunction (ED). ED has pathophysiological involvement in causation of the diseased state such as CVD and metabolic syndrome [175-176] hypertension [177], hypercholesterolemia [177], diabetes [177] and obesity [178]. In endothelial cells, ROS has shown to decrease endothelial Nitric Oxide which leads to increase in the expression of pro-inflammatory cytokines and adhesion molecules [169]. Pro-inflammatory cytokine such as TNF- α, has shown to exacerbate the inflammatory cascade. It formulates the loop that creates a vicious circle which perpetuates the diseases. It increases expression of intracellular and vascular adhesion molecules (ICAM-1 AND VCAM-1) that have shown to exacerbate the intensity of atherosclerosis[167, 169]. TNF-α also increases oxidative stress by upregulating and translocation of nuclear factor kappa B (NFκB). In vascular endothelial cells, NADPH has been considered to be the main contributors of ROS[48, 175-176, 179]. Other sources include mitochondria. Thus, regulation of the loop caused by TNF-α leading to increase in inflammation and oxidative stress in ameliorating atherosclerosis is a crucial step.

Plant based polyphenols have shown to placate chronic diseases such as CVD at different fronts, because of the uniqueness in their structure and presence of phenolic groups which makes them ideal candidates to exert health benefiting properties. Back in time, treatment of all sort of diseases were done on the basis of herbal mixtures. However, recent scientific knowledge has elucidated mode of mechanisms for these herbal mixtures. Naringenin, a polyphenol found in fruits such as grapefruit, oranges, cherries, tomatoes have shown to suppress adhesion molecules (VCAM-1, ICAM-1) and proinflammatory markers such as IL-6, TNF-α in LPS stimulated endothelial cells [180]. Blueberry extracts rich in

polyphenols such as anthocyanins have shown to suppressed elevated levels of chemokines such as IL8 and MCP-1, adhesion molecules such as VCAM-1, ESEL-1 in palmitate stimulated endothelial cells [181].

Pecans originates from the Algonquin Indian word "pacaan" used to describe "all nuts requiring a stone to crack". Pecans, native from US was widely used by precolonial residents. Native American tribes consumed wild pecans as a major food source [182]. It is a popular nut and is widely relished as a snack food (roasted/salted), pie, baked goods, confections, dessert toppings and salads. Pecan nut seeds is considered as a high-energy food with about 690 kcal/100 g and about 75% lipids (w/ w) and 18% carbohydrates [24, 183].

It is well established that bioavailability of polyphenols from natural plant-based compounds is low. However, likelihood of absorption increases after biotransformation of polyphenols by the intestinal bacteria. Pecan is a rich source of ellagitannins. Dietary ellagitannins have shown to be converted into urolithin by action of intestinal microbiota primarily including *Gordonibacter pamelaeae* (DSM 19378^T) and *Gordonibacter urolithinfaciens* [184]. Reports suggest that these urolithins have been studied for anti-inflammatory, antioxidant, cardioprotective, neuroprotective, and cancer preventive compound[184]. However, literature lacks the molecular mechanism of how oxidative stresses play a role[30, 35, 130-132, 142, 184]. The aim of the current investigation is to understand the molecular role of oxidative stresses in mechanism of urolithins A and B against LPS and TNF-α stimulated inflammatory model in HUVEC system.

Materials and Methods:

Materials:

The following chemicals were used in the experiments: Lipopolysaccharide (LPS), 2′,7′-Dichlorofluorescin diacetate (DCFA), penicillin/streptomycin mixture, 0.25% Trypsin-EDTA solution, Diphenylene iodonium (DPI), DMEM/F-12 medium, DMSO and Fetal Bovine Serum (FBS) were purchased from Sigma (St. Louis, MO). Tumor Necrosis Factor (TNFα), glucose and sodium bicarbonate were purchased from Acros Organics (Fair Lawn, NJ) and sodium bicarbonate from Mallinckrodt Chemicals (Phillipsburg, NJ), respectively. The CellTiter 96® AQueous Non-Radioactive Cell Proliferation Assay kit was purchased from Promega (Madison, WI). The Human Umbilical Vein Endothelial Cells (cell line CRL-1730™) was obtained from the American Type Culture Collection (ATCC, Rockville, MD).

Cell culture:

Human Umbilical Vein Endothelial Cells (HUVEC) were cultured and grown in 100 mm dishes Biocoat gelatin (BD Biosciences, Franklin Lakes, NJ) supplemented with DMEM/F-12 medium (Sigma, St. Louis, MO), with a combination of the following components to the base medium: 0.1 mg/ml heparin; 0.03 mg/ml endothelial cell growth supplement (ECGS); 10% fetal bovine serum (FBS) and antibiotics (100 units/ml penicillin and 100 µg/ml streptomycin). The cells were proliferated in a humidified atmosphere with 5% CO_2 at 37°C. HUVEC cells reached 100% confluence were pre-treated with various concentrations of urolithins (10, 20 and 50 µM) for 5 h before stimulating with LPS (1 µg/mL) or 20ng/ml of TNF-α. These cells reach confluency in 5-6 days and were used between 2-8 passage number.

Cell Count protocol:

Human Umbilical Vein Endothelial Cells were plated in Biocoat Multidish 6 well plate (BD Biosciences, Franklin Lakes, NJ) at 1×10^5 cells/well and were maintained in culture for 24 h. Then cells were pretreated with different concentration of urolithin for 24 h (50 μM). At least three independent trials were performed for each assay. After 24 h cells were harvested by treating with 500 μl 0.05% trypsin and 0.02% EDTA for 5 min at 37 °C. The trypsin was deactivated with 500 μl of complete medium. Cell number was assessed by trypan blue exclusion assay. The cell suspension aliquots were incubated in trypan blue solution (0.4%) for 5 min followed by quantifying the cells number in a Countess automated cell counter (Invitrogen, Carlsbad, CA). The final percentage of DMSO per well was 0.5%.

Measurement of reactive oxygen species production (ROS):

The HUVEC were plated at a density of 5x 10^4 cells/well in a 96- well black and clear bottom plates (Costar, Cambridge, MA) and cultured overnight. In separate experiments the cells were stimulated by 1 μg/ml LPS or 20 ng/ml TNF-α for 19 h with or without 5 h pretreatment of 50 μM of urolithins A and B and 5 μM of DPI, used as a positive control. The measurement of intracellular ROS production was evaluated using 2′,7′-Dichlorofluorescin diacetate (DCFA). Briefly, the cell culture medium was removed by aspiration and subsequently exposing the cells to 10 μM DCFA in PBS for 30 mins. Finally, fluorescence was read at wavelengths of 485 nm for excitation and 528 nm for emission on a 96-well microplate reader (Synergy HT, Bio-Tek Instruments, Inc., Winooski, VT).The final concentration of DMSO per well was 0.5%.

Preparation of Total RNA and Gene Expression Analysis (Real-Time qRT-PCR):

Total RNA was extracted from HUV-EC in 6 well plate (BD Biosciences, Franklin Lakes, NJ) after challenging with 1 µg/ml LPS or 20 ng/ml TNF-α treatment for 19 h with or without 5 h pretreatment of 50 µM urolithins A and B using Zymo's RNA extraction kit with DNase I treatment according to the manufacturer's instructions (purchased from Zymos research, Irvine, CA). RNA concentration was quantified using a NanoDrop ND-1000 spectrophotometer (NanoDrop Technologies, Willmington, DE). Around 1 µg of RNA was reversed transcribed for cDNA synthesis, using the SuperScript III first-strand synthesis super mix (Invitrogen, Carlsbad, CA), following the manufacturers protocol. cDNA amplification was analyzed using a LighterCycler 480 (Roche diagnostic) and Bullseye EvaGreen qPCR master mix (Midscientific, St. Louis). The list of primers used are in Table 4. For this work, the expression of ICAM-1, VCAM-1, MCP-1, ESEL-1 and LXRa were measured.

Statistical analysis:

The data were analyzed using ANOVA and paired Student's t-test, using the software JMP v 14.0 (Cary, NC). Results are expressed as means± standard errors (S.E), n=3-6.

Results and Discussion:

Effect of urolithins A and B on cell viability:

Urolithin A and B were exposed at a concentration of 50 µM for cell viability in HUVEC using cell counter to measure cell toxicity employing the trypan blue technique, as shown in Figure 31. The number of viable cells in urolithin pre-treated and untreated wells, were not significantly different, suggesting no cytotoxic effect of urolithins on HUVEC. Thus, further

experiments were performed using 50 µM urolithins A and B. Also, 5 µM DPI a ROS inhibitor did not show any cytotoxic effect.

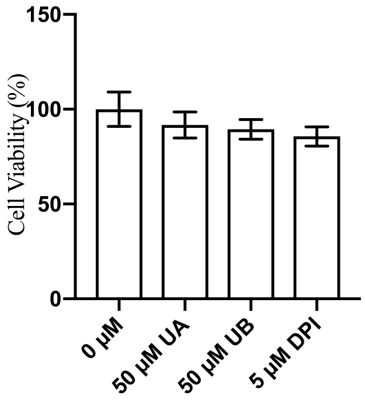

Figure 31: Effect of urolithin A and B on cell viability in HUVEC cells

HUVEC cells (0.5×10^4 cells/well in 96-well culture plates) were treated with 0 and 50 µM urolithin A and B for 24 h. The cell viability was measured by with trypan blue staining. The 0 µM is a control, indicating the pretreatment of 0.5 % DMSO in DMEM medium Data, obtained from triplicate repeats at least, are shown as mean ± SE. UA corresponds to urolithin A; UB corresponds to urolithin B and DPI corresponds to Diphenyleneiodonium.

Effect of urolithins A and B on intracellular ROS in LPS treated HUV-EC:

Increased levels of ROS induce an inflammatory state resulting in leukocyte adhesion on to the endothelial cells and transmigration into the subendothelial spaces, which further progresses into atherosclerosis. ROS activates several pathways including MAPK, Akt and NFKB. To understand the role of oxidative stress in HUVEC model system, levels of intracellular ROS was measured using DCFDA. The cells were challenged with 1 µg/ml LPS.

Lipopolysaccharide (LPS), a bacterial endotoxin is used to stimulate endothelial dysfunction. It binds to TLR-4 receptor which activates NFκB pathway. NFκB is an important inflammatory transcription factor which is activated directly by LPS. To understand the role of oxidative stresses in endothelial dysfunction and how urolithins play a role we measured intracellular ROS in LPS stimulated HUVEC. In vascular cells ROS is produced through NADPH oxidases and mitochondrial including O_2^- and H_2O_2 derived from the xanthine oxidase, cyclooxygenase, lipoxygenase, nitric oxide synthase, hemeoxygenases, peroxidases, hemoproteins such as heme and hematin as part of cellular processes[79, 175-176, 180].

HUV-EC were challenged with 1 µg/ml LPS for 3 h and 19 h in presence or absence of pre-treatment of 50 µM urolithin A and B and 5 µM DPI (NADPH oxidase inhibitor). On stimulation with LPS endothelial cells undergo oxidative stress and produce intracellular ROS level, as reported previously [175, 185-186]. As shown in the Figure 32, intracellular levels of ROS increased around 1.5x and 3x times in the cells stimulated with 1 µg/ml LPS for 3 h and 19 h respectively, as compared to the control cells and 5 µM DPI. Compounds such as allicin, quercetin, chitosan, paeonol have shown suppression of LPS stimulated ROS in endothelial cells[175, 185-187]. In our investigation also, we observed similar results when pre-treatment of urolithin A and B (50 µM) and DPI (a positive control) significantly suppressed the levels of elevated intracellular ROS at the two time points. Considering, suppression of ROS was higher at 19 h so further investigation was done at 19 h stimulation of LPS. DPI suppression also indicates that NADPH is a major source of ROS as it suppressed the intracellular levels of ROS comparable to the untreated cells. Similar observations were made by Li et al., 2014 when intracellular ROS was suppressed by DPI. These results suggest

that urolithins A and B exhibit antioxidant nature which ameliorates intracellular ROS accumulation in LPS challenged cells.

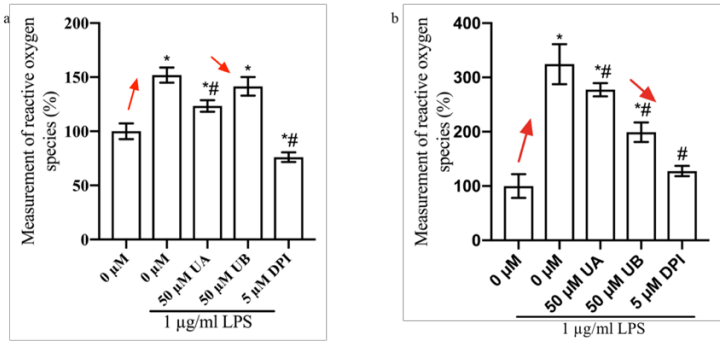

Figure 32: Effect of urolithin A and B on LPS-induced intracellular ROS production at 3 and 19 h in HUVEC cells

HUVEC (0.5×10^4 cells/well in 96-well culture plates) were pretreated with 0 and 50 µM urolithin A and B for 5 h and then stimulated with LPS (1 µg/ml). The levels of intracellular ROS were measured at 3 h (a) and 19 h (b) using microplate reader (Synergy HT, Bio-Tek Instruments, Inc., Winooski, VT) with the DCFDA fluorescent dye. The 0 µM is a control, indicates the pretreatment of 0.5 % DMSO in DMEM medium without any LPS stimulation. Data, obtained from triplicate repeats at least, are shown as mean ± SE. Different symbol indicate significant differences by the paired Student's t-test ($p < 0.05$). * significantly different from DMSO/control, $p<0.05$; # significantly different from LPS (1 µg/ml), $p<0.05$.

Effect of urolithins A and B on proinflammatory genes in LPS stimulated cells:

Endothelial dysfunction has been attributed for progression of vascular diseases, such as atherosclerosis (chronic inflammation). Endothelial cells produce TNF-α, a proinflammatory cytokine that upregulates the expression of Cell Adhesion Molecules (CAM) [188]. CAM expression, including ICAM-1, VCAM-1, and E-selectin arbitrate inflammation and proceeds to the formation of atheromas leading to atherosclerosis.

Endothelial dysfunction represents progression of plaque and lesion formation leading to atherosclerosis [188-189].

The next step in inflammation model was to understand the role of ROS on pro-inflammatory genes. The expression of pro-inflammatory genes ICAM-1, VCAM-1, ESEL-1 and MCP-1 increased in LPS challenged cells (Figure 35). These adhesion molecules play a pivotal role in leukocyte transmigration and increased expression of them progresses to cardiovascular diseases. Hence, we decided to study the effect of urolithins against these genes. As shown in the Figure 35, urolithin A and B (50 μM) were unable to inhibit the expression of the pro-inflammatory genes. However, urolithin B partially suppressed the expression of MCP-1 in LPS challenged HUVEC cells. These results suggested that even though urolithins suppressed intracellular ROS levels, urolithin A and B (50 μM) were unable to inhibit the expression of the pro-inflammatory genes. This could potentially suggest that LPS activates NFκB in a ROS independent mechanism. This hypothesis was in coherence with Li *et al*., 2016 who also observed that LPS stimulation increases the expression of NFκB in a ROS independent mechanism [175]. On binding to TLR-4, LPS stimulates NF-kB signaling pathway which triggers proinflammatory cytokine TNF-α expression and induces the activation of protein kinase C followed by phosphorylation of $p47^{phos}$ and activates NOX, thus producing ROS which potentiates NFκB signaling [190]. Also, the transcription of ICAM-1, VCAM-1 are regulated by AP-1 and NFκB [180]. They both are modulated distinctively in LPS induced system. In a study by Zheng et al., 2010, flavan-3-ol, epigallocatechin gallate (EGCG), suppressed atherosclerosis and inflammation by inhibiting expression of MCP-1 through AP-1, however it did not affect the DNA binding of NFκB [191].

This brought us to hypothesize that urolithins may function via TNF-α, that is urolithins suppresses the ROS which in turn suppresses the expression of adhesion molecules.

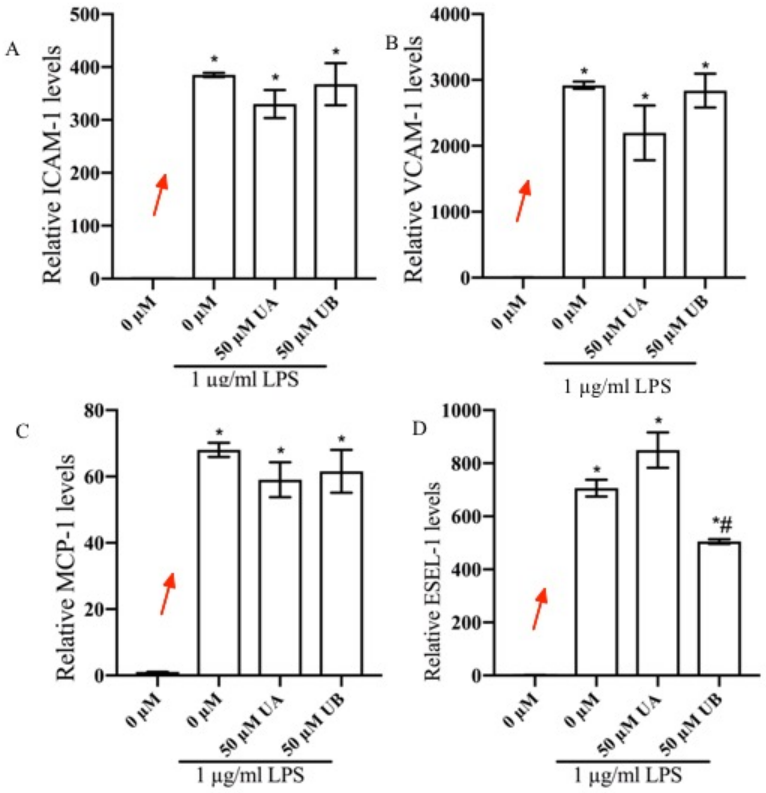

Figure 33: Effect of urolithin A and B on LPS-induced gene expression in HUVEC cells

HUVEC cells (1×10^5 cells/well in 6-well culture plates) were pretreated with 0 and 50 μM urolithin A and B for 5 h and then stimulated with LPS (1 μg/ml) for 19 h. Subsequently, total RNAs were prepared and subjected to real-time qRT-PCR analysis using specific primer sets, responsible for *ICAM-1* (a), *VCAM-1* (B), *MCP-1* (C), and *ESEL-1* (D) genes were measured. The 0 μM is a control, indicates the pretreatment of 0.5 % DMSO in DMEM medium in DMEM medium without any LPS stimulation. Data, obtained from triplicate repeats at least, are shown as mean ± SE. Different symbol indicate

significant differences by the paired Student's t-test ($p < 0.05$). * significantly different from DMSO/control, $p<0.05$; # significantly different from LPS (1 μg/ml), $p<0.05$.

Effect of urolithins A and B on intracellular ROS in TNF-α treated HUV-EC:

HUV-EC were challenged with 20 ng/ml TNF-α for 3 and 19 h in presence or absence of pre-treatment of 50 μM of urolithin A and B. Our second hypothesis was to test urolithins against the TNF-α stimulated HUVEC and demonstrate urolithin could potentially suppress the loop since TNF-α is also, a proinflammatory cytokine perceived as an inflammatory stimulant and has the capacity to perpetuate inflammation. Endothelial cells when exposed to TNF-α have shown to increase the levels of intracellular levels of ROS [192-194]. As shown in the Figure 34, intracellular levels of ROS increased around 1.5x in the cells stimulated with 20 ng/ml TNF-α for 19 h as compared to the control cells similar to the results reported previously. However, after 3 h stimulation of TNF-α, no significant increase of intracellular ROS levels was observed. At concentration of 50 μM of urolithin A suppressed the levels of ROS after 19 h exposure to TNF-α. In spite of many ROS producing systems in a cell, NOX is speculated as a major contributor of ROS in HUVEC system[176], thus similar to what we observed in LPS, DPI adequately suppressed TNF-α stimulated cells in the present study Naringin suppressed the increased level of ROS[176], similar to observation of this report where Urolithin A suppressed ROS. These results suggest that urolithin A exhibit capability in reducing intracellular ROS accumulation in TNF-α challenged cells whereas urolithin B did not have any effect on intracellular ROS in TNF-α stimulated cells.

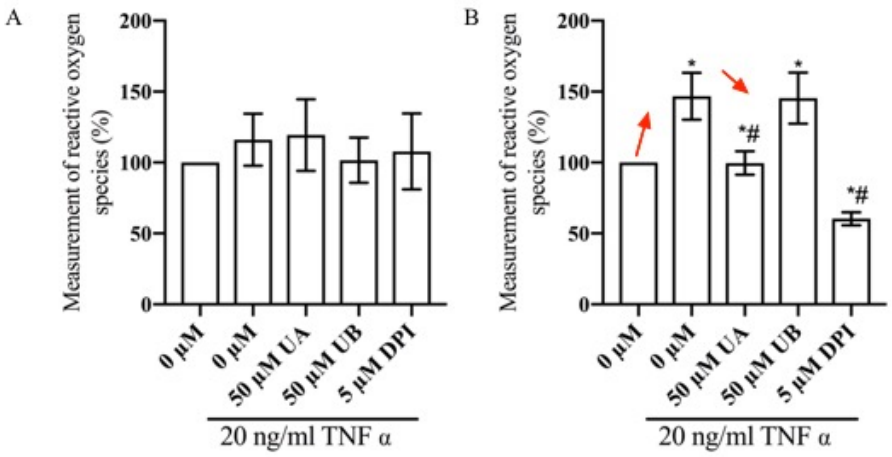

Figure 34: Effect of urolithin A and B on TNF*α*-induced intracellular ROS production at 3 and 19 h in HUVEC cells

HUVEC (0.5×10^4 cells/well in 96-well culture plates) were pretreated with 0 and 50 µM urolithin A and B for 5 h and then stimulated with TNF*α* (20 ng/ml). The levels of intracellular ROS were measured at 3 h (a) and 19 h (b) using microplate reader (Synergy HT, Bio-Tek Instruments, Inc., Winooski, VT) with the DCFDA fluorescent dye. The 0 µM is a control, indicates the pretreatment of 0.5 % DMSO in DMEM medium without any TNF*α* stimulation. Data, obtained from triplicate repeats at least, are shown as mean ± SE. Different symbol indicate significant differences by the paired Student's t-test ($p < 0.05$). * significantly different from DMSO/control, $p<0.05$; # significantly different from TNF *α* (20 ng/ml), $p<0.05$.

Effect of urolithins A and B on proinflammatory genes in TNF- α stimulated cells:

Our second hypothesis was to test urolithins against the TNF- α stimulated HUVEC. TNF- α is a proinflammatory cytokine which induces inflammation by perpetuating basal inflammation into chronic inflammation. As shown in Figure 34, cells were stimulated with TNF-α, significantly increased the expression of ICAM-1, VCAM-1, MCP-1, E-Sel-1. As hypothesized pretreatment of 50 µM urolithin A and B downregulated the expression of VCAM-1, MCP-1 and ESEL-1. Thus suggesting the potential mechanism of urolithins in

TNFα induced cells similar to EGCG, allicin where they suppressed the expression of the adhesion molecules to suppress inflammation via suppressing the adhesion molecules (Zheng, Toborek et al. 2010) [185]. However, expression of ICAM was not suppressed by neither urolithins A nor B. This could be explained by the fact that ICAM is activated through AP-1 and NFkB within the ICAM -1 promoter site [172, 179]. Thus, urolithins suppress the expression of VCAM, ESEL-1 and MCP-1 genes modulated through TNFα induced NFκB.

Urolithin A significantly suppressed levels of ROS and proinflammatory genes, suggesting that mechanism of action is ROS dependent. On the other hand, urolithin B, downregulated the expression of pro-inflammatory genes, however, did not have any effect on ROS. To further scrutinize the molecular mechanism of urolithins A and B, we hypothesized that anti-inflammatory activity of urolithin A and B might be mediated by upregulating the expression of LXR-α. LXR-α stimulates reverse cholesterol transport (RCT), thereby inducing an increase in HDL cholesterol which ameliorates hypercholesterolemia, reduces cholesterol absorption, improves NO bioavailability, expedites fecal cholesterol disposal and increases apoptosis [195]. As suspected, expression of LXR-α decreased in presence of TNF-α and urolithin A and B upregulated the expression of LXR-α. Similar results were observed by Zhang et al. (2017) where allicin compound found in garlic has shown to suppress inflammation in HUVEC by upregulating LXR-α[185]. Capsaicin also demonstrated inhibition of proinflammatory genes in LPS stimulated monocyte THP-1 by partially upregulating LXR-α[87, 148]. These studies are in coherence with the results we observed, thus demonstrate that the anti-inflammatory mechanism for urolithins A and B is upregulating expression of LXR-α as shown in Figure 34.

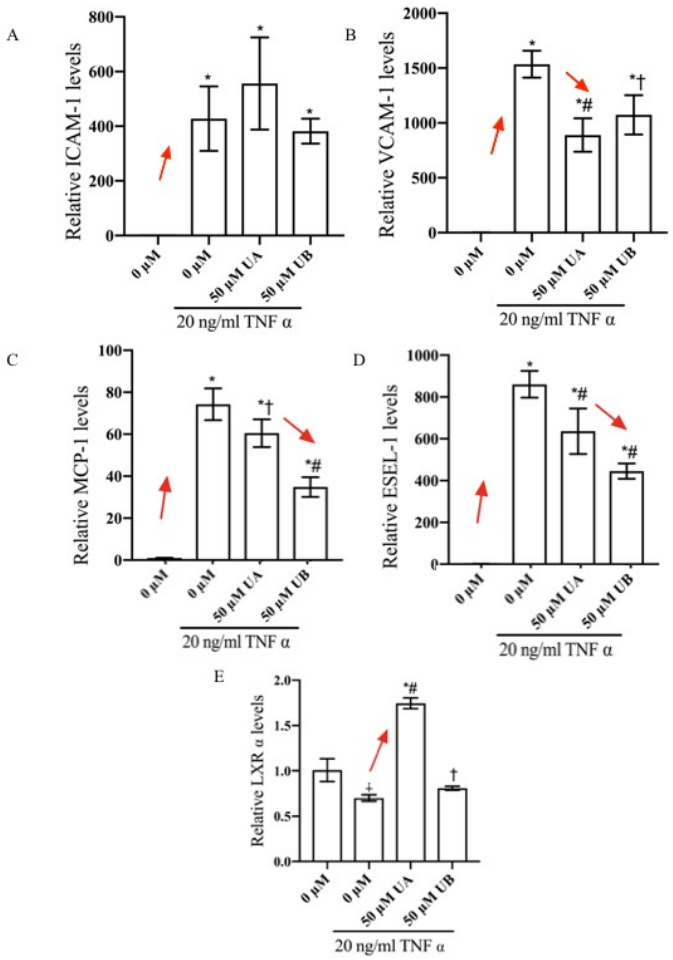

Figure 35: Effect of urolithin A and B on LPS-induced gene expression in HUV-EC cells

HUVEC cells (1×10^5 cells/well in 6-well culture plates) were pretreated with 0 and 50 µM urolithin A and B for 5 h and then stimulated with TNF α (20 ng/ml) for 19 h. Subsequently, total RNAs were prepared and subjected to real-time qRT-PCR analysis using specific primer sets, responsible for ICAM-1 (a), VCAM-1 (B), MCP-1 (C), ESEL-1 (D) and LXR α (E) genes were measured. The 0 µM is a control, indicates the pretreatment of 0.5 % DMSO in DMEM medium without any LPS stimulation. Data, obtained from triplicate repeats at least, are shown as mean ± SE. Different symbol indicate significant differences by the paired Student's t-test ($p < 0.05$). * significantly different from DMSO/control, $p<0.05$; ∔ significantly different from DMSO/control, $p<0.10$; # significantly different from TNF α (20 ng/ml), $p<0.05$.

Conclusion:

From this study, it was concluded that urolithin A and B have two different mode of action in suppressing LPS/TNFa induced inflammation as represented in Figure 36 and 37. Urolithin A suppressed intracellular levels of ROS in LPS and TNF α stimulated cells demonstrating its antioxidant nature. It also suppressed the levels of VCAM-1, MCP-1 and ESEL-1 by promoting the expression of LXR- α in TNF α stimulated cells. On the other hand, urolithin B, suppressed the levels of VCAM-1, MCP-1 and ESEL-1 and partially increased the expression of LXR-α, however it was inadequate in suppressing intracellular ROS in TNF α stimulated cells, thus suggesting a ROS independent mechanism of action. More studies are required to understand the underlying mechanism of AP-1 to elucidate urolithins mechanism.

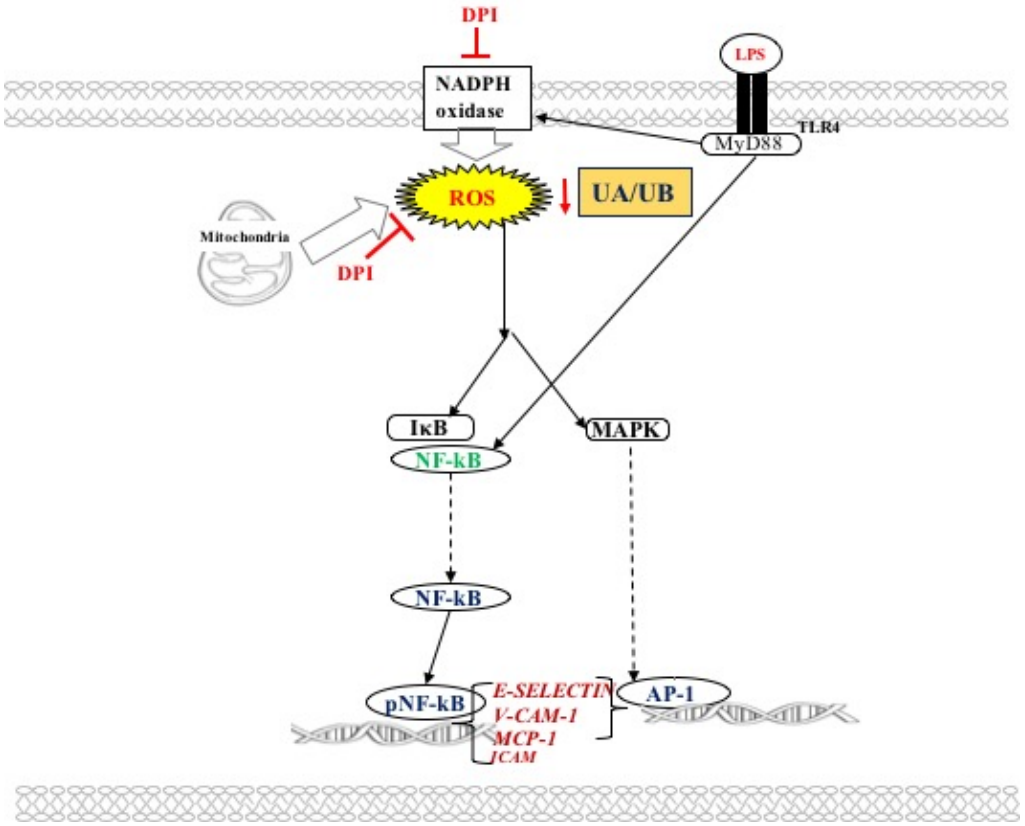

Figure 36: Anti-inflammatory mode of action of urolithin A and B in LPS-stimulated HUVEC cells

Binding of LPS to TLR4 receptor triggers a cascade of responses. ROS is generated from NOX and mitochondria. LPS increases the expression of NFκB in a ROS independent mechanism and increases the expression of VCAM, ICAM-1, ESEL-1, MCP-1 through NF κB and AP1 signaling. Urolithins A and B suppresses intracellular ROS in HUVEC while not affecting expression of those pro-inflammatory genes due to the unique direct ROS independent LPS stimulation of NF κB and the corresponding pro-inflammatory genes

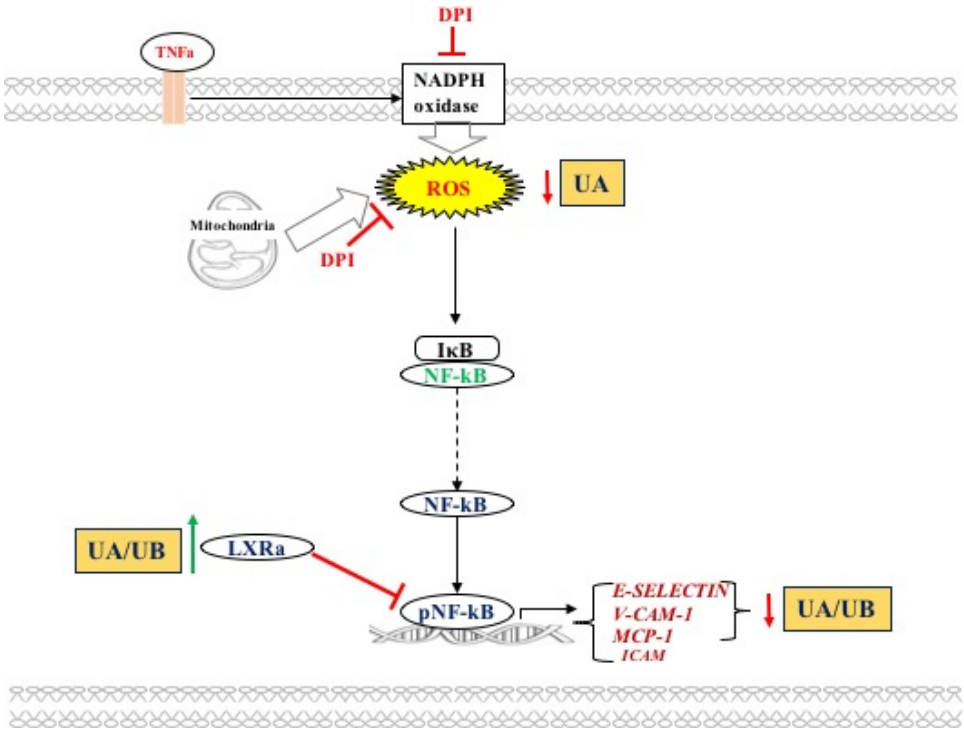

Figure 37: Anti-inflammatory mode of action of urolithin A and B in TNF a-stimulated HUVEC cells

Binding of LPS to TLR4 receptor triggers production of different pro-inflammatory genes including TNFα. TNFα binds to TNFR-1 and increases intracellular levels of ROS. The major sources of ROS are NOX and mitochondria. ROS mediates to produce ICAM-1, VCAM-1, MCP-1, ESEL-1 through NF*κ*B and AP-1 signaling. Urolithins A suppressed intracellular ROS, and thereby suppressed the action of downstream pro-inflammatory gene. Thus, suggesting that urolithin A suppresses proinflammatory genes in a ROS dependent mechanism in HUVEC. This study also demonstrates, urolithin A and B upregulates LXR α, which inhibits NFKB p65 subunit, thereby suppressing the proinflammatory genes. This suggests that urolithin B functions in a ROS independent mechanism.

Table 4: Sequences of primers used in gene expression studies of different cells lines

Primer	Sequence
TNFα-F	5'-ACTGGCAGAAGAGGCACTCC -3'
TNFα-R	5'-CGATCACCCCGAAGTTCA-3'
IL-1β-F	5'-GAGCACCTTCTTTTCCTTCATCT-3'
IL-1β-R	5'-GATATTCTGTCCATTGAGGTGGA-3'
iNOS-F	5'-GCTCGCTTTGCCACGGACGA-3'
iNOS-R	5'-AAGGCAGCGGGCACATGCAA-3'
β-Actin-F	5'-CCCAGGCATTGCTGACAGG-3'
β-Actin-R	5'-TGGAAGGTGGACAGTGAGGC-3'
E-Selectin-F	5'- TGCATGGAGGGTTGTTAATGG -3'
E-Selectin-R	5'- GGATGAAAGTGATTAAATTGTGCATAG -3'
ICAM-F	5'- GCTATGCCTTGTCCTCTTG -3'
ICAM-R	5'- ATACACACACACACACACGC -3'
VCAM-F	5'- CAAATCCTTGATACTGCTCATC -3'
VCAM-R	5'- TTGACTTCTTGCTCACAGC -3'
MCP-1-F	5'- CAGCCAGATGCAATCAATGC -3'
MCP-1-R	5'- GTGGTCCATGGAATCCTGAA -3'
GAPDH-F	5'- GCACCGTCAAGGCTGAGAAC -3'
GAPDH-R	5'- ATGGTGGTGAAGACGCCAGT -3'
LXR α-F	5'-AAGCCCTGCATGCCTACGT-3'
LXR α-R	5'-TGCAGACGCAGTGCAAACA-3'

The primer sets are listed were provided by Integrated DNA Technologies (IDT, Coralville, IA). The relative expression of each gene was normalized by β-Actin or GAPDH [196], and was calculated following the comparative Ct method (ΔΔCt), also known as the $2^{-\Delta\Delta Ct}$ method [197].

CHAPTER V

GENERAL CONCLUSION

Cell culture/cell line technique is cost effective, bypasses ethical concerns and are easily available. Cell lines are pure population of cells which provide valuable information regarding testing the metabolism and toxicity of drugs, vaccine and antibody; facilitate understanding the cytokine productions and studying expression of genes and proteins; aid in synthesis of artificial tissues and biological compounds. Working with cell culture we could precisely controlled physiological conditions such as quantity of nutrients, pH, temperature, osmolarity and concentrations of toxins. Cell lines being pure population of cells mimics the functionality of the organs in-vivo and has become the first step for understanding the functionality of those organs under different condition such as chronic or acute inflammation, diabetes, obesity, etc. and understand the underlying molecular pathways[198-199].

Through this research we identified anti-inflammatory and anti-diabetic properties of urolithins, the gut microbial metabolites of ellagic acid from pecans. This research is a stepping stone for future animal and human trials for understanding the nutraceutical effect of urolithin A and B. However, working in aseptic in-vitro controlled culture of animal cells has its disadvantages also. These tests were done with pure population of cells thereby, possibility of metabolism, phase II modifications of these compounds and their cross-talks with other organs were not considered. Therefore, the beneficial properties urolithin A and B should be evaluated in vivo in animals and clinical studies in human to understand their functionality and propose urolithins as nutraceutical supplements against the metabolic syndrome.

These cell lines- Caco-2, AML12, C2C12, βTC6 and HUVEC are involved in pathogenesis of metabolic syndrome. They have been used as model cell lines for understanding chronic diseases and preventing them utilizing various metabolites such as urolithins from plants. Urolithins have elicited anti-inflammatory properties by suppressing the metabolic stress during maladaptation through a feed forward signaling pathway leading to activation of various transcription factors. In presence of external (LPS) and internal stresses (PA and TNF α) urolithin A proficiently suppressed elevated levels of intracellular ROS and thus downregulating the pathways involved in inflammation insulin resistance. Whereas urolithin B demonstrated a ROS independent mechanism in HUVEC, Caco-2 and C2C12 cells. In skeletal muscle and liver cells (C2C12 and AML 12 cell lines), urolithin A and B upregulated expression of insulin receptor substrate (IRS-1) and protein kinase B (AKT) demonstrating potential candidate in ameliorating insulin resistance effect at a cell model system.

This study aimed at annotating a holistic approach to elucidate effect of urolithin A and B in abating the sequence of events in the model of diseases utilizing cell model systems. Urolithins were successful in mitigating epithelial inflammation, insulin resistance, glucose insensitivity and endothelial dysfunction in cell models. Further investigation is required in understanding the mechanism of urolithin B in glucose resistant pancreatic B cells.

REFERENCES

1. Milani, R. V.; Lavie, C. J., Health Care 2020: Reengineering Health Care Delivery to Combat Chronic Disease. *The American Journal of Medicine* 2015, *128* (4), 337-343.

2. Deaton, C.; Froelicher, E. S.; Wu, L. H.; Ho, C.; Shishani, K.; Jaarsma, T., The global burden of cardiovascular disease. *European Journal of Cardiovascular Nursing* 2011, *10* (2_suppl), S5-S13.

3. Lee, L.; Sanders, R. A., Metabolic syndrome. *Pediatrics in review* 2012, *33* (10), 459.

4. Shaw, J. E.; Sicree, R. A.; Zimmet, P. Z., Global estimates of the prevalence of diabetes for 2010 and 2030. *Diabetes Research and Clinical Practice 87* (1), 4-14.

5. Kaur, J., A comprehensive review on metabolic syndrome. *Cardiology research and practice* 2014, *2014*.

6. Romieu, I.; Dossus, L.; Barquera, S.; Blottière, H. M.; Franks, P. W.; Gunter, M.; Hwalla, N.; Hursting, S. D.; Leitzmann, M.; Margetts, B., Energy balance and obesity: what are the main drivers? *Cancer Causes & Control* 2017, *28* (3), 247-258.

7. Saris, W.; Blair, S.; Van Baak, M.; Eaton, S.; Davies, P.; Di Pietro, L.; Fogelholm, M.; Rissanen, A.; Schoeller, D.; Swinburn, B., How much physical activity is enough to prevent unhealthy weight gain? Outcome of the IASO 1st Stock Conference and consensus statement. *Obesity reviews* 2003, *4* (2), 101-114.

8. Mendis, S., Cardiovascular risk assessment and management in developing countries. *Vascular health and risk management* 2005, *1* (1), 15.

9. Wetzstein, H. Y.; Rodriguez, A. P.; Burns, J. A.; Magner, H. N., Carya illinoensis (pecan). In *Trees IV*, Springer: 1996; pp 50-75.

10. Wakeling, L. T.; Mason, R. L.; D'Arc, B. R.; Caffin, N. A., Composition of pecan cultivars Wichita and western Schley [Carya illinoinensis (Wangenh.) K. Koch] grown in Australia. *Journal of agricultural and food chemistry* 2001, *49* (3), 1277-1281.

11. Zhang, R.; Peng, F.; Li, Y., Pecan production in China. *Scientia Horticulturae* 2015, *197*, 719-727.

12. Sathe, S. K.; Monaghan, E. K.; Kshirsagar, H. H.; Venkatachalam, M., Chemical composition of edible nut seeds and its implications in human health. *Tree nuts: composition, phytochemicals, and health effects* 2009, 11-35.

13. Bottari, N. B.; Lopes, L. Q. S.; Pizzuti, K.; dos Santos Alves, C. F.; Corrêa, M. S.; Bolzan, L. P.; Zago, A.; de Almeida Vaucher, R.; Boligon, A. A.; Giongo, J. L., Antimicrobial activity and phytochemical characterization of Carya illinoensis. *Microbial pathogenesis* 2017, *104*, 190-195.

14. Babu, D.; Crandall, P. G.; Johnson, C. L.; O'Bryan, C. A.; Ricke, S. C., Efficacy of antimicrobials extracted from organic pecan shell for inhibiting the growth of Listeria spp. *Journal of food science* 2013, *78* (12), M1899-M1903.

15. El Hawary, S. S.; Saad, S.; El Halawany, A. M.; Ali, Z. Y.; El Bishbishy, M., Phenolic content and anti-hyperglycemic activity of pecan cultivars from Egypt. *Pharmaceutical biology* 2016, *54* (5), 788-798.

16. Porto, L. C. S.; da Silva, J.; Ferraz, A. B.; Ethur, E. M.; Porto, C. D.; Marroni, N. P.; Picada, J. N., The antidiabetic and antihypercholesterolemic effects of an aqueous extract from pecan shells in wistar rats. *Plant foods for human nutrition* 2015, *70* (4), 414-419.

17. Robbins, K. S.; Greenspan, P.; Pegg, R. B., Effect of pecan phenolics on the release of nitric oxide from murine RAW 264.7 macrophage cells. *Food chemistry* 2016, *212*, 681-687.

18. Senter, S.; Horvat, R.; Forbus Jr, W., Relation between phenolic acid content and stability of pecans in accelerated storage. *Journal of Food Science* 1980, *45* (5), 1380-1382.

19. Grimmer, H. R.; Parbhoo, V.; McGrath, R. M., Antimutagenicity of polyphenol-rich fractions from sorghum bicolor grain. *Journal of the Science of Food and Agriculture* 1992, *59* (2), 251-256.

20. Gu, L.; Kelm, M. A.; Hammerstone, J. F.; Beecher, G.; Holden, J.; Haytowitz, D.; Gebhardt, S.; Prior, R. L., Concentrations of proanthocyanidins in common foods and estimations of normal consumption. *The Journal of nutrition* 2004, *134* (3), 613-617.

21. Malik, N. S.; Perez, J. L.; Lombardini, L.; Cornacchia, R.; Cisneros-Zevallos, L.; Braford, J., Phenolic compounds and fatty acid composition of organic and conventional grown pecan kernels. *Journal of the Science of Food and Agriculture* 2009, *89* (13), 2207-2213.

22. Lipińska, L.; Klewicka, E.; Sójka, M., Structure, occurrence and biological activity of ellagitannins: a general review. *Acta scientiarum polonorum. Technologia alimentaria* 2014, *13* (3).

23. Villarreal-Lozoya, J. E.; Lombardini, L.; Cisneros-Zevallos, L., Phytochemical constituents and antioxidant capacity of different pecan [Carya illinoinensis (Wangenh.) K. Koch] cultivars. *Food Chemistry* 2007, *102* (4), 1241-1249.

24. Venkatachalam, M.; Kshirsagar, H. H.; Seeram, N. P.; Heber, D.; Thompson, T. E.; Roux, K. H.; Sathe, S. K., Biochemical composition and immunological comparison of

select pecan [Carya illinoinensis (Wangenh.) K. Koch] cultivars. *Journal of agricultural and food chemistry* 2007, *55* (24), 9899-9907.

25. Hilbig, J.; de Britto Policarpi, P.; de Souza Grinevicius, V. M. A.; Mota, N. S. R. S.; Toaldo, I. M.; Luiz, M. T. B.; Pedrosa, R. C.; Block, J. M., Aqueous extract from pecan nut [Carya illinoinensis (Wangenh) C. Koch] shell show activity against breast cancer cell line MCF-7 and Ehrlich ascites tumor in Balb-C mice. *Journal of ethnopharmacology* 2018, *211*, 256-266.

26. Porto, L. C. S.; Silva, J. d.; Sousa, K.; Ambrozio, M. L.; de Almeida, A.; dos Santos, C. E. I.; Dias, J. F.; Allgayer, M. C.; dos Santos, M. S.; Pereira, P., Evaluation of Toxicological Effects of an Aqueous Extract of Shells from the Pecan Nut Carya illinoinensis (Wangenh.) K. Koch and the Possible Association with Its Inorganic Constituents and Major Phenolic Compounds. *Evidence-Based Complementary and Alternative Medicine* 2016, *2016*.

27. Rajaram, S.; Myint, T.; Connell, B.; Burke, K.; Sabaté, J. In *Effect of pecan rich diet on serum lipids and lipoproteins in healthy men and women*, FASEB JOURNAL, FEDERATION AMER SOC EXP BIOL 9650 ROCKVILLE PIKE, BETHESDA, MD 20814-3998 USA: 2000; pp A293-A293.

28. Rajaram, S.; Burke, K.; Connell, B.; Myint, T.; Sabate, J., A monounsaturated fatty acid–rich pecan-enriched diet favorably alters the serum lipid profile of healthy men and women. *The Journal of nutrition* 2001, *131* (9), 2275-2279.

29. Figueira, I.; Garcia, G.; Pimpão, R.; Terrasso, A.; Costa, I.; Almeida, A.; Tavares, L.; Pais, T.; Pinto, P.; Ventura, M., Polyphenols journey through blood-brain barrier towards neuronal protection. *Scientific reports* 2017, *7* (1), 11456.

30. González-Barrio, R. o.; Truchado, P.; Ito, H.; Espín, J. C.; Tomás-Barberán, F. A., UV and MS identification of urolithins and nasutins, the bioavailable metabolites of ellagitannins and ellagic acid in different mammals. *Journal of agricultural and food chemistry* 2011, *59* (4), 1152-1162.

31. García-Villalba, R.; Beltrán, D.; Espín, J. C.; Selma, M. V.; Tomás-Barberán, F. A., Time course production of urolithins from ellagic acid by human gut microbiota. *Journal of agricultural and food chemistry* 2013, *61* (37), 8797-8806.

32. Piwowarski, J. P.; Granica, S.; Zwierzyńska, M.; Stefańska, J.; Schopohl, P.; Melzig, M. F.; Kiss, A. K., Role of human gut microbiota metabolism in the anti-inflammatory effect of traditionally used ellagitannin-rich plant materials. *Journal of ethnopharmacology* 2014, *155* (1), 801-809.

33. DaSilva, N. A.; Nahar, P. P.; Ma, H.; Eid, A.; Wei, Z.; Meschwitz, S.; Zawia, N. H.; Slitt, A. L.; Seeram, N. P., Pomegranate ellagitannin-gut microbial-derived metabolites, urolithins, inhibit neuroinflammation in vitro. *Nutritional neuroscience* 2017, 1-11.

34. Mele, L.; Mena, P.; Piemontese, A.; Marino, V.; López-Gutiérrez, N.; Bernini, F.; Brighenti, F.; Zanotti, I.; Del Rio, D., Antiatherogenic effects of ellagic acid and urolithins in vitro. *Archives of biochemistry and biophysics* 2016, *599*, 42-50.

35. Savi, M.; Bocchi, L.; Bresciani, L.; Falco, A.; Quaini, F.; Mena, P.; Brighenti, F.; Crozier, A.; Stilli, D.; Del Rio, D., Trimethylamine-N-Oxide (TMAO)-Induced Impairment of Cardiomyocyte Function and the Protective Role of Urolithin B-Glucuronide. *Molecules* 2018, *23* (3), 549.

36. Liu, R.; Chen, L.; Aihara, K. In *The early warning signal of complex diseases based on the network transition entropy*, Systems Biology (ISB), 2011 IEEE International Conference on, IEEE: 2011; pp 362-367.

37. Osorio, C.; Schreckinger, E.; Bhargava, P.; Bang, W. Y.; Jacobo-Velázquez, D. A.; Cisneros-Zevallos, L., Golden berry and selected tropical (açai, acerola and maqui) juices. *Handbook of Functional Beverages and Human Health; Shahidi, F., Alasalvar, C., Eds* 2016, 251-269.

38. Cheng, C.-W.; Villani, V.; Buono, R.; Wei, M.; Kumar, S.; Yilmaz, O. H.; Cohen, P.; Sneddon, J. B.; Perin, L.; Longo, V. D., Fasting-mimicking diet promotes Ngn3-driven β-cell regeneration to reverse diabetes. *Cell* 2017, *168* (5), 775-788. e12.

39. Yamaoka, M.; Maeda, N.; Nakamura, S.; Kashine, S.; Nakagawa, Y.; Hiuge-Shimizu, A.; Okita, K.; Imagawa, A.; Matsuzawa, Y.; Matsubara, K.-i., A pilot investigation of visceral fat adiposity and gene expression profile in peripheral blood cells. *PLoS One* 2012, *7* (10), e47377.

40. Lumeng, C. N.; Saltiel, A. R., Inflammatory links between obesity and metabolic disease. *The Journal of clinical investigation* 2011, *121* (6), 2111-2117.

41. Teran-Garcia, M.; Bouchard, C., Genetics of the metabolic syndrome. *Applied Physiology, Nutrition, and Metabolism* 2007, *32* (1), 89-114.

42. Peppa, M.; Raptis, S. A., Advanced glycation end products and cardiovascular disease. *Current diabetes reviews* 2008, *4* (2), 92-100.

43. Maury, E.; Ramsey, K. M.; Bass, J., Circadian rhythms and metabolic syndrome: from experimental genetics to human disease. *Circulation research* 2010, *106* (3), 447-462.

44. Giugliano, D.; Ceriello, A.; Esposito, K., The effects of diet on inflammation: emphasis on the metabolic syndrome. *Journal of the American College of Cardiology* 2006, *48* (4), 677-85.

45. Pan, M.-H.; Lai, C.-S.; Ho, C.-T., Anti-inflammatory activity of natural dietary flavonoids. *Food & function* 2010, *1* (1), 15-31.

46. Courts, F. L.; Williamson, G., The occurrence, fate and biological activities of C-glycosyl flavonoids in the human diet. *Critical reviews in food science and nutrition* 2015, *55* (10), 1352-1367.

47. Xiao, J.; Capanoglu, E.; Jassbi, A. R.; Miron, A., Advance on the Flavonoid C-glycosides and Health Benefits. *Critical Reviews in Food Science and Nutrition* 2016, *56* (sup1), S29-S45.

48. Yuan, S. Y.; Rigor, R. R. In *Regulation of endothelial barrier function*, Colloquium Series on Integrated Systems Physiology: From Molecule to Function, Morgan & Claypool Life Sciences: 2011; pp 1-146.

49. Naydenov, N. G.; Ivanov, A. I., Adducins regulate remodeling of apical junctions in human epithelial cells. *Molecular biology of the cell* 2010, *21* (20), 3506-3517.

50. Blandino, G.; Inturri, R.; Lazzara, F.; Di Rosa, M.; Malaguarnera, L., Impact of gut microbiota on diabetes mellitus. *Diabetes & metabolism* 2016, *42* (5), 303-315.

51. Gassler, N.; Rohr, C.; Schneider, A.; Kartenbeck, J. r.; Bach, A.; Obermüller, N.; Otto, H. F.; Autschbach, F., Inflammatory bowel disease is associated with changes of enterocytic junctions. *American Journal of Physiology-Gastrointestinal and Liver Physiology* 2001, *281* (1), G216-G228.

52. Guttman, J. A.; Li, Y.; Wickham, M. E.; Deng, W.; Vogl, A. W.; Finlay, B. B., Attaching and effacing pathogen-induced tight junction disruption in vivo. *Cellular microbiology* 2006, *8* (4), 634-645.

53. Ferrero-Miliani, L.; Nielsen, O.; Andersen, P.; Girardin, S., Chronic inflammation: importance of NOD2 and NALP3 in interleukin-1β generation. *Clinical & Experimental Immunology* 2007, *147* (2), 227-235.

54. Bauer, U. E.; Briss, P. A.; Goodman, R. A.; Bowman, B. A., Prevention of chronic disease in the 21st century: elimination of the leading preventable causes of premature death and disability in the USA. *The Lancet* 2014, *384* (9937), 45-52.

55. McArdle, M. A.; Finucane, O. M.; Connaughton, R. M.; McMorrow, A. M.; Roche, H. M., Mechanisms of obesity-induced inflammation and insulin resistance: insights into the emerging role of nutritional strategies. *Frontiers in endocrinology* 2013, *4*.

56. Cani, P. D.; Amar, J.; Iglesias, M. A.; Poggi, M.; Knauf, C.; Bastelica, D.; Neyrinck, A. M.; Fava, F.; Tuohy, K. M.; Chabo, C., Metabolic endotoxemia initiates obesity and insulin resistance. *Diabetes* 2007, *56* (7), 1761-1772.

57. Song, J. D.; Lee, S. K.; Kim, K. M.; Kim, J. W.; Kim, J. M.; Yoo, Y. H.; Park, Y. C., Redox factor-1 mediates NF-κB nuclear translocation for LPS-induced iNOS expression in murine macrophage cell line RAW 264.7. *Immunology* 2008, (1).

58. Kabe, Y.; Ando, K.; Hirao, S.; Yoshida, M.; Handa, H., Redox regulation of NF-κB activation: Distinct redox regulation between the cytoplasm and the nucleus. *Antioxidants and Redox Signaling* 2005, *7* (3-4), 395-403.

59. Biswas, Subhra K.; Mantovani, A., Minireview: Orchestration of Metabolism by Macrophages. *Cell metabolism* 2012, *15*, 432-437.

60. Chan, E. D.; Riches, D. W. H., IFN-γ + LPS induction of iNOS is modulated by ERK, JNK/SAPK, and p38mapk in a mouse macrophage cell line. *American Journal of Physiology* 2001, *280* (3), C441-C450.

61. Jacobs, A. T.; Ignarro, L. J., Lipopolysaccharide-induced Expression of Interferon-β Mediates the Timing of Inducible Nitric-oxide Synthase Induction in RAW 264.7 Macrophages. *Journal of Biological Chemistry* 2001, *276* (51), 47950-47957.

62. Mittal, M.; Siddiqui, M. R.; Tran, K.; Reddy, S. P.; Malik, A. B., Reactive oxygen species in inflammation and tissue injury. *Antioxidants & Redox Signaling* 2014, *20* (7), 1126-1167.

63. Clària, J.; González-Périz, A.; López-Vicario, C.; Rius, B.; Titos, E., New insights into the role of macrophages in adipose tissue inflammation and Fatty liver disease: modulation by endogenous omega-3 Fatty Acid-derived lipid mediators. *Frontiers in immunology* 2011, *2*, 49.

64. Adams, K. F.; Schatzkin, A.; Harris, T. B.; Kipnis, V.; Mouw, T.; Ballard-Barbash, R.; Hollenbeck, A.; Leitzmann, M. F., Overweight, obesity, and mortality in a large prospective cohort of persons 50 to 71 years old. *New England Journal of Medicine* 2006, *355* (8), 763-778.

65. Finucane, M. M.; Stevens, G. A.; Cowan, M. J.; Danaei, G.; Lin, J. K.; Paciorek, C. J.; Singh, G. M.; Gutierrez, H. R.; Lu, Y.; Bahalim, A. N., National, regional, and global trends in body-mass index since 1980: systematic analysis of health examination surveys and epidemiological studies with 960 country-years and 9· 1 million participants. *The Lancet* 2011, *377* (9765), 557-567.

66. Lopez-Legarrea, P.; Fuller, N. R.; Zulet, M. A.; Martinez, J. A.; Caterson, I. D., The influence of Mediterranean, carbohydrate and high protein diets on gut microbiota composition in the treatment of obesity and associated inflammatory state. *Asia Pacific Journal of Clinical Nutrition* 2014, *23* (3), 360-368.

67. J Chu, A., Antagonism by bioactive polyphenols against inflammation: a systematic view. *Inflammation & Allergy-Drug Targets (Formerly Current Drug Targets-Inflammation & Allergy)* 2014, *13* (1), 34-64.

68. Schwiertz, A.; Taras, D.; Schäfer, K.; Beijer, S.; Bos, N. A.; Donus, C.; Hardt, P. D., Microbiota and SCFA in lean and overweight healthy subjects. *Obesity* 2010, *18* (1), 190-195.

69. Rui, L., Energy metabolism in the liver. *Comprehensive physiology* 2011, *4* (1), 177-197.

70. Braun, M., The somatostatin receptor in human pancreatic β-cells. In *Vitamins & Hormones*, Elsevier: 2014; Vol. 95, pp 165-193.

71. Sakai, K.; Matsumoto, K.; Nishikawa, T.; Suefuji, M.; Nakamaru, K.; Hirashima, Y.; Kawashima, J.; Shirotani, T.; Ichinose, K.; Brownlee, M., Mitochondrial reactive oxygen species reduce insulin secretion by pancreatic β-cells. *Biochemical and biophysical research communications* 2003, *300* (1), 216-222.

72. Newsholme, P.; Keane, K.; de Bittencourt Jr, P. I. H.; Krause, M., The impact of inflammation on pancreatic β-cell metabolism, function and failure in T1DM and T2DM: commonalities and differences. In *Type 1 diabetes*, InTech: 2013.

73. Röder, P. V.; Wu, B.; Liu, Y.; Han, W., Pancreatic regulation of glucose homeostasis. *Experimental & molecular medicine* 2016, *48* (3), e219.

74. Nakamura, S.; Takamura, T.; Matsuzawa-Nagata, N.; Takayama, H.; Misu, H.; Noda, H.; Nabemoto, S.; Kurita, S.; Ota, T.; Ando, H., Palmitate induces insulin resistance in H4IIEC3 hepatocytes through reactive oxygen species produced by mitochondria. *Journal of Biological Chemistry* 2009, *284* (22), 14809-14818.

75. Gao, D.; Nong, S.; Huang, X.; Lu, Y.; Zhao, H.; Lin, Y.; Man, Y.; Wang, S.; Yang, J.; Li, J., The effects of palmitate on hepatic insulin resistance are mediated by NADPH Oxidase 3-derived reactive oxygen species through JNK and p38MAPK pathways. *Journal of Biological Chemistry* 2010, *285* (39), 29965-29973.

76. DeFronzo, R. A.; Tripathy, D., Skeletal muscle insulin resistance is the primary defect in type 2 diabetes. *Diabetes care* 2009, *32* (suppl 2), S157-S163.

77. Kim, S.-H.; Hwang, J.-T.; Park, H. S.; Kwon, D. Y.; Kim, M.-S., Capsaicin stimulates glucose uptake in C2C12 muscle cells via the reactive oxygen species (ROS)/AMPK/p38 MAPK pathway. *Biochemical and biophysical research communications* 2013, *439* (1), 66-70.

78. Sargis, R. M., An Overview of the Pancreas Understanding Insulin and Diabetes. *Endocrine Web* 2015.

79. Schieber, M.; Chandel, N. S., ROS function in redox signaling and oxidative stress. *Current biology* 2014, *24* (10), R453-R462.

80. Zeyda, M.; Stulnig, T. M., Obesity, inflammation, and insulin resistance–a mini-review. *Gerontology* 2009, *55* (4), 379-386.

81. Liang, H.; Hussey, S. E.; Sanchez-Avila, A.; Tantiwong, P.; Musi, N., Effect of lipopolysaccharide on inflammation and insulin action in human muscle. *PloS one* 2013, *8* (5), e63983.

82. Yang, M.; Wei, D.; Mo, C.; Zhang, J.; Wang, X.; Han, X.; Wang, Z.; Xiao, H., Saturated fatty acid palmitate-induced insulin resistance is accompanied with myotube loss and the impaired expression of health benefit myokine genes in C2C12 myotubes. *Lipids in health and disease* 2013, *12* (1), 104.

83. Eckel, R. H.; Grundy, S. M.; Zimmet, P. Z., The metabolic syndrome. *The lancet* 2005, *365* (9468), 1415-1428.

84. Kühnau, J., The flavonoids. A class of semi-essential food components: their role in human nutrition. In *World review of nutrition and dietetics*, Karger Publishers: 1976; Vol. 24, pp 117-191.

85. Scalbert, A.; Manach, C.; Morand, C.; Rémésy, C.; Jiménez, L., Dietary polyphenols and the prevention of diseases. *Critical reviews in food science and nutrition* 2005, *45* (4), 287-306.

86. Pérez-Jiménez, J.; Neveu, V.; Vos, F.; Scalbert, A., Identification of the 100 richest dietary sources of polyphenols: an application of the Phenol-Explorer database. *European journal of clinical nutrition* 2010, *64* (S3), S112.

87. Kim, C.-S.; Kawada, T.; Kim, B.-S.; Han, I.-S.; Choe, S.-Y.; Kurata, T.; Yu, R., Capsaicin exhibits anti-inflammatory property by inhibiting IkB-a degradation in LPS-stimulated peritoneal macrophages. *Cellular signalling* 2003, *15* (3), 299-306.

88. Kang, J.-H.; Kim, C.-S.; Han, I.-S.; Kawada, T.; Yu, R., Capsaicin, a spicy component of hot peppers, modulates adipokine gene expression and protein release from obese-mouse adipose tissues and isolated adipocytes, and suppresses the inflammatory responses of adipose tissue macrophages. *FEBS letters* 2007, *581* (23), 4389-4396.

89. Park, C. E.; Kim, M.-J.; Lee, J. H.; Min, B.-I.; Bae, H.; Choe, W.; Kim, S.-S.; Ha, J., Resveratrol stimulates glucose transport in C2C12 myotubes by activating AMP-activated protein kinase. *Experimental & molecular medicine* 2007, *39* (2), 222.

90. Pournourmohammadi, S.; Grimaldi, M.; Stridh, M. H.; Lavallard, V.; Waagepetersen, H. S.; Wollheim, C. B.; Maechler, P., Epigallocatechin-3-gallate (EGCG) activates AMPK through the inhibition of glutamate dehydrogenase in muscle and pancreatic ß-cells: A potential beneficial effect in the pre-diabetic state? *The international journal of biochemistry & cell biology* 2017, *88*, 220-225.

91. Deng, Y.-T.; Chang, T.-W.; Lee, M.-S.; Lin, J.-K., Suppression of free fatty acid-induced insulin resistance by phytopolyphenols in C2C12 mouse skeletal muscle cells. *Journal of agricultural and food chemistry* 2012, *60* (4), 1059-1066.

92. Mohar, D. S.; Malik, S., The sirtuin system: the holy grail of resveratrol? *Journal of clinical & experimental cardiology* 2012, *3* (11).

93. Biasutto, L.; Mattarei, A.; Zoratti, M., Resveratrol and health: the starting point. *Chembiochem* 2012, *13* (9), 1256-1259.

94. Mcdougall, G. J.; Stewart, D., The inhibitory effects of berry polyphenols on digestive enzymes. *Biofactors* 2005, *23* (4), 189-195.

95. Ji, G.; Zhang, Y.; Yang, Q.; Cheng, S.; Hao, J.; Zhao, X.; Jiang, Z., Genistein suppresses LPS-induced inflammatory response through inhibiting NF-κB following AMP kinase activation in RAW 264.7 macrophages. *PLoS One* 2012, *7* (12), e53101.

96. Hämäläinen, M.; Nieminen, R.; Vuorela, P.; Heinonen, M.; Moilanen, E., Anti-inflammatory effects of flavonoids: genistein, kaempferol, quercetin, and daidzein inhibit STAT-1 and NF-κB activations, whereas flavone, isorhamnetin, naringenin, and

pelargonidin inhibit only NF-κB activation along with their inhibitory effect on iNOS expression and NO production in activated macrophages. *Mediators of inflammation* 2007, *2007*.

97. Wadsworth, T. L.; Koop, D. R., Effects of the wine polyphenolics quercetin and resveratrol on pro-inflammatory cytokine expression in RAW 264.7 macrophages. *Biochemical pharmacology* 1999, *57* (8), 941-949.

98. Siddiqui, A. M.; Cui, X.; Wu, R.; Dong, W.; Zhou, M.; Hu, M.; Simms, H. H.; Wang, P., The anti-inflammatory effect of curcumin in an experimental model of sepsis is mediated by up-regulation of peroxisome proliferator-activated receptor-γ. *Critical care medicine* 2006, *34* (7), 1874-1882.

99. Brouet, I.; Ohshima, H., Curcumin, an anti-tumor promoter and anti-inflammatory agent, inhibits induction of nitric oxide synthase in activated macrophages. *Biochemical and biophysical research communications* 1995, *206* (2), 533-540.

100. Kim, D.-C.; Lee, W.; Bae, J.-S., Vascular anti-inflammatory effects of curcumin on HMGB1-mediated responses in vitro. *Inflammation Research* 2011, *60* (12), 1161-1168.

101. Simonyi, A.; Wang, Q.; Miller, R. L.; Yusof, M.; Shelat, P. B.; Sun, A. Y.; Sun, G. Y., Polyphenols in cerebral ischemia. *Molecular neurobiology* 2005, *31* (1-3), 135-147.

102. Patil, C. S.; Singh, V. P.; Satyanarayan, P.; Jain, N. K.; Singh, A.; Kulkarni, S. K., Protective effect of flavonoids against aging-and lipopolysaccharide-induced cognitive impairment in mice. *Pharmacology* 2003, *69* (2), 59-67.

103. Ross, R., Atherosclerosis—an inflammatory disease. *New England journal of medicine* 1999, *340* (2), 115-126.

104. Silva, B.; Oliveira, P. J.; Dias, A.; Malva, J. O., Quercetin, kaempferol and biapigenin fromhypericum perforatum are neuroprotective against excitotoxic insults. *Neurotoxicity research* 2008, *13* (3-4), 265-279.

105. Echeverry, C.; Arredondo, F.; Abin-Carriquiry, J. A.; Midiwo, J. O.; Ochieng, C.; Kerubo, L.; Dajas, F., Pretreatment with natural flavones and neuronal cell survival after oxidative stress: a structure− activity relationship study. *Journal of agricultural and food chemistry* 2010, *58* (4), 2111-2115.

106. Wang, X.; Ouyang, Y. Y.; Liu, J.; Zhao, G., Flavonoid intake and risk of CVD: a systematic review and meta-analysis of prospective cohort studies. *British Journal of Nutrition* 2014, *111* (1), 1-11.

107. Patanè, G.; Piro, S.; Rabuazzo, A. M.; Anello, M.; Vigneri, R.; Purrello, F., Metformin restores insulin secretion altered by chronic exposure to free fatty acids or high glucose: a direct metformin effect on pancreatic beta-cells. *Diabetes* 2000, *49* (5), 735-740.

108. Gehrmann, W.; Elsner, M.; Lenzen, S., Role of metabolically generated reactive oxygen species for lipotoxicity in pancreatic β-cells. *Diabetes, Obesity and Metabolism* 2010, *12*, 149-158.

109. Munhoz, A. C.; Riva, P.; Simões, D.; Curi, R.; Carpinelli, A. R., Control of insulin secretion by production of reactive oxygen species: study performed in pancreatic islets from fed and 48-hour fasted Wistar rats. *PloS one* 2016, *11* (6), e0158166.

110. Viollet, B.; Guigas, B.; Garcia, N. S.; Leclerc, J.; Foretz, M.; Andreelli, F., Cellular and molecular mechanisms of metformin: an overview. *Clinical science* 2012, *122* (6), 253-270.

111. Valenti, L.; Rametta, R.; Dongiovanni, P.; Maggioni, M.; Fracanzani, A. L.; Zappa, M.; Lattuada, E.; Roviaro, G.; Fargion, S., Increased expression and activity of the transcription factor FOXO1 in nonalcoholic steatohepatitis. *Diabetes* 2008.

112. Gunton, J. E.; Delhanty, P. J.; Takahashi, S.-I.; Baxter, R. C., Metformin rapidly increases insulin receptor activation in human liver and signals preferentially through insulin-receptor substrate-2. *The Journal of Clinical Endocrinology & Metabolism* 2003, *88* (3), 1323-1332.

113. Zheng, J.; Woo, S.-L.; Hu, X.; Botchlett, R.; Chen, L.; Huo, Y.; Wu, C., Metformin and metabolic diseases: a focus on hepatic aspects. *Frontiers of medicine* 2015, *9* (2), 173-186.

114. Xu, H.; Zhou, Y.; Liu, Y.; Ping, J.; Shou, Q.; Chen, F.; Ruo, R., Metformin improves hepatic IRS2/PI3K/Akt signaling in insulin-resistant rats of NASH and cirrhosis. *Journal of Endocrinology* 2016, *229* (2), 133-144.

115. Kumar, N.; Dey, C. S., Metformin enhances insulin signalling in insulin-dependent and-independent pathways in insulin resistant muscle cells. *British journal of pharmacology* 2002, *137* (3), 329-336.

116. Park, S. Y.; Kim, M. H.; Ahn, J. H.; Lee, S. J.; Lee, J. H.; Eum, W. S.; Choi, S. Y.; Kwon, H. Y., The stimulatory effect of essential fatty acids on glucose uptake involves both Akt and AMPK activation in C2C12 skeletal muscle cells. *The Korean Journal of Physiology & Pharmacology* 2014, *18* (3), 255-261.

117. Lee, H.; Lim, J.-Y.; Choi, S.-J., Oleate Prevents Palmitate-Induced Atrophy via Modulation of Mitochondrial ROS Production in Skeletal Myotubes. *Oxidative medicine and cellular longevity* 2017, *2017*.

118. Ganz, T., Epithelia: not just physical barriers. *Proceedings of the National Academy of Sciences* 2002, *99* (6), 3357-3358.

119. Terzić, J.; Grivennikov, S.; Karin, E.; Karin, M., Inflammation and colon cancer. *Gastroenterology* 2010, *138* (6), 2101-2114. e5.

120. Tien, M.-T.; Girardin, S. E.; Regnault, B.; Le Bourhis, L.; Dillies, M.-A.; Coppée, J.-Y.; Bourdet-Sicard, R.; Sansonetti, P. J.; Pédron, T., Anti-inflammatory effect of Lactobacillus casei on Shigella-infected human intestinal epithelial cells. *The Journal of Immunology* 2006, *176* (2), 1228-1237.

121. Roselli, M.; Finamore, A.; Britti, M. S.; Mengheri, E., Probiotic bacteria Bifidobacterium animalis MB5 and Lactobacillus rhamnosus GG protect intestinal Caco-2 cells from the inflammation-associated response induced by enterotoxigenic Escherichia coli K88. *British Journal of Nutrition* 2006, *95* (6), 1177-1184.

122. Walmsley, R.; Anthony, A.; Sim, R.; Pounder, R.; Wakefield, A., Absence of Escherichia coli, Listeria monocytogenes, and Klebsiella pneumoniae antigens within inflammatory bowel disease tissues. *Journal of clinical pathology* 1998, *51* (9), 657-661.

123. Subramanian, S.; Rhodes, J. M.; Hart, A. C.; Tam, B.; Roberts, C. L.; Smith, S. L.; Corkill, J. E.; Winstanley, C.; Virji, M.; Campbell, B. J., Characterization of epithelial IL-8 response to inflammatory bowel disease mucosal E. coli and its inhibition by mesalamine. *Inflammatory bowel diseases* 2007, *14* (2), 162-175.

124. Gosain, A.; Gamelli, R. L., Role of the gastrointestinal tract in burn sepsis. *The Journal of burn care & rehabilitation* 2005, *26* (1), 85-91.

125. Diebel, L. N.; Liberati, D. M., Intestinal epithelial cells mediate lung injury after ethanol exposure and hypoxic insult. *Journal of Trauma and Acute Care Surgery* 2009, *67* (2), 296-302.

126. Holst, O.; Ulmer, A. J.; Brade, H.; Flad, H. D.; Rietschel, E. T., Biochemistry and cell biology of bacterial endotoxins. *FEMS Immunology & Medical Microbiology* 1996, *16* (2), 83-104.

127. Tobias, P. S.; Tapping, R. I.; Gegner, J. A., Endotoxin interactions with lipopolysaccharide-responsive cells. *Clinical infectious diseases* 1999, *28* (3), 476-481.

128. Losso, J. N.; Bansode, R. R.; Trappey II, A.; Bawadi, H. A.; Truax, R., In vitro anti-proliferative activities of ellagic acid. *The Journal of nutritional biochemistry* 2004, *15* (11), 672-678.

129. Larrosa, M.; Tomás-Barberán, F. A.; Espín, J. C., The dietary hydrolysable tannin punicalagin releases ellagic acid that induces apoptosis in human colon adenocarcinoma Caco-2 cells by using the mitochondrial pathway. *The Journal of nutritional biochemistry* 2006, *17* (9), 611-625.

130. Sánchez-González, C.; Noé, V.; Izquierdo-Pulido, M., Walnut polyphenol metabolites, urolithins A and B, inhibit the expression of the prostate-specific antigen and the androgen receptor in prostate cancer cells. *Food & function* 2014, *5* (11), 2922-2930.

131. Kang, I.; Kim, Y.; Tomás-Barberán, F. A.; Espín, J. C.; Chung, S., Urolithin A, C, and D, but not iso-urolithin A and urolithin B, attenuate triglyceride accumulation in human cultures of adipocytes and hepatocytes. *Molecular nutrition & food research* 2016, *60* (5), 1129-1138.

132. Piwowarski, J. P.; Granica, S.; Kiss, A. K., Influence of Gut Microbiota-Derived Ellagitannins' Metabolites Urolithins on Pro-Inflammatory Activities of Human Neutrophils. *Planta medica* 2014, *80* (11), 887-895.

133. González-Sarrías, A.; Giménez-Bastida, J. A.; Núñez-Sánchez, M. Á.; Larrosa, M.; García-Conesa, M. T.; Tomás-Barberán, F. A.; Espín, J. C., Phase-II metabolism limits the antiproliferative activity of urolithins in human colon cancer cells. *European journal of nutrition* 2014, *53* (3), 853-864.

134. Hedges, A.; Shannon, R.; Hobbs, R., Comparison of the precision obtained in counting viable bacteria by the spiral plate maker, the droplette and the Miles & Misra methods. *Journal of Applied Bacteriology* 1978, *45* (1), 57-65.

135. Swain, T., The phenolic constituents of Prunus domestica. I.-The quantitative analysis of phenolic constituents. *Journal of the Science of Food and Agriculture* 1959, *10* (1), 63-68.

136. Ortiz-Quezada, A. G.; Lombardini, L.; Cisneros-Zevallos, L., Antioxidants in pecan nut cultivars [Carya illinoinensis (Wangenh.) K. Koch]. In *Nuts and Seeds in Health and Disease Prevention*, Elsevier: 2011; pp 881-889.

137. Rigaud, J.; Escribano-Bailon, M.; Prieur, C.; Souquet, J.-M.; Cheynier, V., Normal-phase high-performance liquid chromatographic separation of procyanidins from cacao beans and grape seeds. *Journal of Chromatography A* 1993, *654* (2), 255-260.

138. Robbins, K. S.; Ma, Y.; Wells, M. L.; Greenspan, P.; Pegg, R. B., Separation and characterization of phenolic compounds from US pecans by liquid chromatography–tandem mass spectrometry. *Journal of agricultural and food chemistry* 2014, *62* (19), 4332-4341.

139. Cerdá, B.; Periago, P.; Espín, J. C.; Tomás-Barberán, F. A., Identification of urolithin A as a metabolite produced by human colon microflora from ellagic acid and related compounds. *Journal of agricultural and food chemistry* 2005, *53* (14), 5571-5576.

140. Flores-Cordova, M.; Muñoz-Márquez, E.; Muñoz-Márquez, E.; Ojeda-Barrios, D. L.; Soto-Parra, J. M.; Preciado-Rangel, P., Phytochemical composition and antioxidant capacity in Mexican pecan nut. *Emirates Journal of Food and Agriculture* 2017, 346-350.

141. González-Sarrías, A.; Giménez-Bastida, J. A.; García-Conesa, M. T.; Gómez-Sánchez, M. B.; García-Talavera, N. V.; Gil-Izquierdo, A.; Sánchez-Álvarez, C.; Fontana-Compiano, L. O.; Morga-Egea, J. P.; Pastor-Quirante, F. A., Occurrence of urolithins, gut microbiota ellagic acid metabolites and proliferation markers expression response in the human prostate gland upon consumption of walnuts and pomegranate juice. *Molecular nutrition & food research* 2010, *54* (3), 311-322.

142. Larrosa, M.; González-Sarrías, A.; García-Conesa, M. T.; Tomás-Barberán, F. A.; Espín, J. C., Urolithins, ellagic acid-derived metabolites produced by human colonic microflora, exhibit estrogenic and antiestrogenic activities. *Journal of agricultural and food chemistry* 2006, *54* (5), 1611-1620.

143. Selma, M. V.; Tomas-Barberan, F. A.; Beltran, D.; García-Villalba, R.; Espín, J. C., Gordonibacter urolithinfaciens sp. nov., a urolithin-producing bacterium isolated from the human gut. *International journal of systematic and evolutionary microbiology* 2014, *64* (7), 2346-2352.

144. Cerdá, B.; Espín, J. C.; Parra, S.; Martínez, P.; Tomás-Barberán, F. A., The potent in vitro antioxidant ellagitannins from pomegranate juice are metabolised into bioavailable but

poor antioxidant hydroxy–6H–dibenzopyran–6–one derivatives by the colonic microflora of healthy humans. *European journal of nutrition* 2004, *43* (4), 205-220.

145. Shaulian, E.; Karin, M., AP-1 in cell proliferation and survival. *Oncogene* 2001, *20* (19), 2390.

146. Joseph, S. B.; Bradley, M. N.; Castrillo, A.; Bruhn, K. W.; Mak, P. A.; Pei, L.; Hogenesch, J.; O'Connell, R. M.; Cheng, G.; Saez, E., LXR-dependent gene expression is important for macrophage survival and the innate immune response. *Cell* 2004, *119* (2), 299-309.

147. Hong, C.; Tontonoz, P., Coordination of inflammation and metabolism by PPAR and LXR nuclear receptors. *Current opinion in genetics & development* 2008, *18* (5), 461-467.

148. Tang, J.; Luo, K.; Li, Y.; Chen, Q.; Tang, D.; Wang, D.; Xiao, J., Capsaicin attenuates LPS-induced inflammatory cytokine production by upregulation of LXRα. *International immunopharmacology* 2015, *28* (1), 264-269.

149. Onkamo, P.; Väänänen, S.; Karvonen, M.; Tuomilehto, J., Worldwide increase in incidence of Type I diabetes–the analysis of the data on published incidence trends. *Diabetologia* 1999, *42* (12), 1395-1403.

150. Mozdziak, P.; Pulvermacher, P.; Schultz, E., Unloading of juvenile muscle results in a reduced muscle size 9 wk after reloading. *Journal of Applied Physiology* 2000, *88* (1), 158-164.

151. Li, L.; He, Q.; Huang, X.; Man, Y.; Zhou, Y.; Wang, S.; Wang, J.; Li, J., NOX3-derived reactive oxygen species promote TNF-α-induced reductions in hepatocyte glycogen levels via a JNK pathway. *FEBS letters* 2010, *584* (5), 995-1000.

152. Cros, G.; Crozier, A.; Dall'asta, M.; Del Rio, D.; Magous, R.; Oiry, C., Compositions comprising urolithins and uses thereof for the stimulation of insulin secretion. Google Patents: 2016.

153. Sadeghi, A.; Rostamirad, A.; Seyyedebrahimi, S.; Meshkani, R., Curcumin ameliorates palmitate-induced inflammation in skeletal muscle cells by regulating JNK/NF-kB pathway and ROS production. *Inflammopharmacology* 2018, 1-8.

154. Mäkinen, S.; Nguyen, Y. H.; Skrobuk, P.; Koistinen, H. A., Palmitate and oleate exert differential effects on insulin signalling and glucose uptake in human skeletal muscle cells. *Endocrine connections* 2017, *6* (5), 331-339.

155. Tatebe, J.; Morita, T., Enhancement of TNF-α expression and inhibition of glucose uptake by nicotine in the presence of a free fatty acid in C2C12 skeletal myocytes. *Hormone and metabolic research* 2011, *43* (01), 11-16.

156. Hetta, M. H.; Owis, A. I.; Haddad, P. S.; Eid, H. M., The fatty acid-rich fraction of Eruca sativa (rocket salad) leaf extract exerts antidiabetic effects in cultured skeletal muscle, adipocytes and liver cells. *Pharmaceutical biology* 2017, *55* (1), 810-818.

157. Abdul-Ghani, M. A.; DeFronzo, R. A., Pathogenesis of insulin resistance in skeletal muscle. *BioMed Research International* 2010, *2010*.

158. Salvado, L.; Coll, T.; Gomez-Foix, A.; Salmeron, E.; Barroso, E.; Palomer, X.; Vazquez-Carrera, M., Oleate prevents saturated-fatty-acid-induced ER stress, inflammation and insulin resistance in skeletal muscle cells through an AMPK-dependent mechanism. *Diabetologia* 2013, *56* (6), 1372-1382.

159. Li, H.; Yang, Y.; Mo, Z.; Ding, Y.; Jiang, W., Silibinin improves palmitate-induced insulin resistance in C2C12 myotubes by attenuating IRS-1/PI3K/Akt pathway inhibition. *Brazilian Journal of Medical and Biological Research* 2015, *48* (5), 440-446.

160. Yuan, H.; Zhang, X.; Huang, X.; Lu, Y.; Tang, W.; Man, Y.; Wang, S.; Xi, J.; Li, J., NADPH oxidase 2-derived reactive oxygen species mediate FFAs-induced dysfunction and apoptosis of β-cells via JNK, p38 MAPK and p53 pathways. *PloS one* 2010, *5* (12), e15726.

161. Lee, M. Y.; Choi, R.; Kim, H. M.; Cho, E. J.; Kim, B. H.; Choi, Y. S.; Naowaboot, J.; Lee, E. Y.; Yang, Y. C.; Shin, J. Y., Peroxisome proliferator-activated receptor δ agonist attenuates hepatic steatosis by anti-inflammatory mechanism. *Experimental & molecular medicine* 2012, *44* (10), 578.

162. Dai Ly, L.; Xu, S.; Choi, S.-K.; Ha, C.-M.; Thoudam, T.; Cha, S.-K.; Wiederkehr, A.; Wollheim, C. B.; Lee, I.-K.; Park, K.-S., Oxidative stress and calcium dysregulation by palmitate in type 2 diabetes. *Experimental & molecular medicine* 2017, *49* (2), e291.

163. Tiganis, T., Reactive oxygen species and insulin resistance: the good, the bad and the ugly. *Trends in pharmacological sciences* 2011, *32* (2), 82-89.

164. Liang, H.; Zhong, Y.; Zhou, S.; Li, Q. Q., Palmitic acid-induced apoptosis in pancreatic β-cells is increased by liver X receptor agonist and attenuated by eicosapentaenoate. *in vivo* 2011, *25* (5), 711-718.

165. Aird, W. C., Phenotypic heterogeneity of the endothelium: I. Structure, function, and mechanisms. *Circulation research* 2007, *100* (2), 158-173.

166. Cook-Mills, J. M.; Deem, T. L., Active participation of endothelial cells in inflammation. *Journal of leukocyte biology* 2005, *77* (4), 487-495.

167. Cines, D. B.; Pollak, E. S.; Buck, C. A.; Loscalzo, J.; Zimmerman, G. A.; McEver, R. P.; Pober, J. S.; Wick, T. M.; Konkle, B. A.; Schwartz, B. S., Endothelial cells in physiology and in the pathophysiology of vascular disorders. *Blood* 1998, *91* (10), 3527-3561.

168. Augustin, H. G.; Kozian, D. H.; Johnson, R. C., Differentiation of endothelial cells: analysis of the constitutive and activated endothelial cell phenotypes. *Bioessays* 1994, *16* (12), 901-906.

169. Forstermann, U.; Munzel, T., Endothelial nitric oxide synthase in vascular disease: from marvel to menace. *Circulation* 2006, *113* (13), 1708-1714.

170. Alon, R.; Feigelson, S. In *From rolling to arrest on blood vessels: leukocyte tap dancing on endothelial integrin ligands and chemokines at sub-second contacts*, Seminars in immunology, Elsevier: 2002; pp 93-104.

171. Campbell, J. J.; Qin, S.; Bacon, K. B.; Mackay, C. R.; Butcher, E. C., Biology of chemokine and classical chemoattractant receptors: differential requirements for adhesion-triggering versus chemotactic responses in lymphoid cells. *The Journal of Cell Biology* 1996, *134* (1), 255-266.

172. Middleton, J.; Patterson, A. M.; Gardner, L.; Schmutz, C.; Ashton, B. A., Leukocyte extravasation: chemokine transport and presentation by the endothelium. *Blood* 2002, *100* (12), 3853-3860.

173. Cuaz-Pérolin, C.; Billiet, L.; Baugé, E.; Copin, C.; Scott-Algara, D.; Genze, F.; Büchele, B.; Syrovets, T.; Simmet, T.; Rouis, M., Antiinflammatory and antiatherogenic effects of the NF-κB inhibitor acetyl-11-keto-β-boswellic acid in LPS-challenged ApoE−/− mice. *Arteriosclerosis, thrombosis, and vascular biology* 2008, *28* (2), 272-277.

174. Gitlin, J. M.; Loftin, C. D., Cyclooxygenase-2 inhibition increases lipopolysaccharide-induced atherosclerosis in mice. *Cardiovascular research* 2008, *81* (2), 400-407.

175. Li, C.; Zhang, W.-J.; Frei, B., Quercetin inhibits LPS-induced adhesion molecule expression and oxidant production in human aortic endothelial cells by p38-mediated Nrf2 activation and antioxidant enzyme induction. *Redox biology* 2016, *9*, 104-113.

176. Thannickal, V. J.; Fanburg, B. L., Reactive oxygen species in cell signaling. *American Journal of Physiology-Lung Cellular and Molecular Physiology* 2000, *279* (6), L1005-L1028.

177. Ting, H. H.; Timimi, F. K.; Boles, K. S.; Creager, S. J.; Ganz, P.; Creager, M. A., Vitamin C improves endothelium-dependent vasodilation in patients with non-insulin-dependent diabetes mellitus. *The Journal of clinical investigation* 1996, *97* (1), 22-28.

178. Perticone, F.; Ceravolo, R.; Candigliota, M.; Ventura, G.; Iacopino, S.; Sinopoli, F.; Mattioli, P. L., Obesity and body fat distribution induce endothelial dysfunction by oxidative stress: protective effect of vitamin C. *Diabetes* 2001, *50* (1), 159-165.

179. Roebuck, K. A.; Rahman, A.; Lakshminarayanan, V.; Janakidevi, K.; Malik, A. B., H_2O_2 and tumor necrosis factor-α activate intercellular adhesion molecule 1 (ICAM-1) gene transcription through distinct cis-regulatory elements within the ICAM-1 promoter. *Journal of Biological Chemistry* 1995, *270* (32), 18966-18974.

180. Sawa, Y.; Ueki, T.; Hata, M.; Iwasawa, K.; Tsuruga, E.; Kojima, H.; Ishikawa, H.; Yoshida, S., LPS-induced IL-6, IL-8, VCAM-1, and ICAM-1 expression in human lymphatic endothelium. *Journal of Histochemistry & Cytochemistry* 2008, *56* (2), 97-109.

181. Bharat, D.; Cavalcanti, R. R. M.; Petersen, C.; Begaye, N.; Cutler, B. R.; Costa, M. M. A.; Ramos, R. K. L. G.; Ferreira, M. R.; Li, Y.; Bharath, L. P., Blueberry Metabolites Attenuate Lipotoxicity-Induced Endothelial Dysfunction. *Molecular nutrition & food research* 2018, *62* (2), 1700601.

182. Rosengarten Jr, F., *The book of edible nuts*. Courier Corporation: 2004.

183. Eitenmiller, R. R.; Pegg, R. B., Compositional characteristics and health effects of pecan [Carya illinoinensis (Wangenh.) K. Koch]. CRC Press: Boca Raton, FL: 2009; pp 259-283.

184. Selma, M. V.; Beltrán, D.; García-Villalba, R.; Espín, J. C.; Tomás-Barberán, F. A., Description of urolithin production capacity from ellagic acid of two human intestinal Gordonibacter species. *Food & function* 2014, *5* (8), 1779-1784.

185. Zhang, M.; Pan, H.; Xu, Y.; Wang, X.; Qiu, Z.; Jiang, L., Allicin decreases lipopolysaccharide-induced oxidative stress and inflammation in human umbilical vein endothelial cells through suppression of mitochondrial dysfunction and activation of Nrf2. *Cellular Physiology and Biochemistry* 2017, *41* (6), 2255-2267.

186. Choy, K. W.; Lau, Y. S.; Murugan, D.; Vanhoutte, P. M.; Mustafa, M. R., Paeonol Attenuates LPS-Induced Endothelial Dysfunction and Apoptosis by Inhibiting BMP4 and TLR4 Signaling Simultaneously but Independently. *Journal of Pharmacology and Experimental Therapeutics* 2018, *364* (3), 420-432.

187. Li, J.; He, J.; Yu, C., Chitosan oligosaccharide inhibits LPS-induced apoptosis of vascular endothelial cells through the BKCa channel and the p38 signaling pathway. *International journal of molecular medicine* 2012, *30* (1), 157-164.

188. Pober, J. S.; Sessa, W. C., Evolving functions of endothelial cells in inflammation. *Nature Reviews Immunology* 2007, *7* (10), 803.

189. Yang, J.-X.; Pan, Y.-Y.; Ge, J.-H.; Chen, B.; Mao, W.; Qiu, Y.-G.; Wang, X.-X., Tanshinone II A attenuates TNF-α-induced expression of VCAM-1 and ICAM-1 in endothelial progenitor cells by blocking activation of NF-κB. *Cellular Physiology and Biochemistry* 2016, *40* (1-2), 195-206.

190. Simon, F.; Fernández, R., Early lipopolysaccharide-induced reactive oxygen species production evokes necrotic cell death in human umbilical vein endothelial cells. *Journal of hypertension* 2009, *27* (6), 1202-1216.

191. Zheng, Y.; Toborek, M.; Hennig, B., Epigallocatechin gallate–mediated protection against tumor necrosis factor-α–induced monocyte chemoattractant protein–1 expression is heme oxygenase–1 dependent. *Metabolism* 2010, *59* (10), 1528-1535.

192. Li, W.; Wang, C.; Peng, J.; Liang, J.; Jin, Y.; Liu, Q.; Meng, Q.; Liu, K.; Sun, H., Naringin inhibits TNF-α induced oxidative stress and inflammatory response in HUVECs via Nox4/NF-κ B and PI3K/Akt pathways. *Current pharmaceutical biotechnology* 2014, *15* (12), 1173-1182.

193. Choi, J.-S.; Choi, Y.-J.; Park, S.-H.; Kang, J.-S.; Kang, Y.-H., Flavones mitigate tumor necrosis factor-α-induced adhesion molecule upregulation in cultured human endothelial cells: role of nuclear factor-κB. *The Journal of nutrition* 2004, *134* (5), 1013-1019.

194. Liang, C.-J.; Wang, S.-H.; Chen, Y.-H.; Chang, S.-S.; Hwang, T.-L.; Leu, Y.-L.; Tseng, Y.-C.; Li, C.-Y.; Chen, Y.-L., Viscolin reduces VCAM-1 expression in TNF-α-

treated endothelial cells via the JNK/NF-κB and ROS pathway. *Free Radical Biology and Medicine* 2011, *51* (7), 1337-1346.

195. Hoang, M. H.; Jia, Y.; Jun, H. j.; Lee, J. H.; Hwang, K. Y.; Choi, D. W.; Um, S. J.; Lee, B. Y.; You, S. G.; Lee, S. J., Taurine is a liver X receptor-α ligand and activates transcription of key genes in the reverse cholesterol transport without inducing hepatic lipogenesis. *Molecular nutrition & food research* 2012, *56* (6), 900-911.

196. Vandesompele, J., Accurate normalization of real-time quantitative RT-PCR data by geometric averaging of multiple internal control genes. *Genome biology* 2002, *3* (7).

197. Schmittgen, T. D., Analyzing real-time PCR data by the comparative C-T method. *Nature Protocols* 2008, *3* (6), 1101-1108.

198. Kaur, G.; Dufour, J. M., Cell lines: Valuable tools or useless artifacts. Taylor & Francis: 2012.

199. Arora, M., Cell culture media: A review. *Mater methods* 2013, *3*, 175.